Regulation of malignant B cell migration by PI(3,4)P2-specific phosphatases and binding proteins

By

Hongzhao Li

A Thesis submitted to the Faculty of Graduate Studies of

The University of Manitoba

In partial fulfillment of the requirements of the degree of

Doctor of Philosophy

Department of Immunology

Faculty of Medicine

University of Manitoba

Winnipeg, Manitoba, Canada

Abstract

Cell migration is critical to a wide range of physiological and pathological events and is central to disease progression of B lymphocyte (B cell)-derived leukemia and lymphoma as well as many other types of cancer. Malignant B cells express functional chemokine receptors and are capable of directional migration (chemotaxis) by following gradients of chemokines such as stroma-derived factor 1 (SDF-1, or CXCL12). This facilitates their infiltration and retention in bone marrow and other organs, where they disrupt normal physiological functions, such as hematopoiesis, as well as find supportive niches that promote their survival, expansion and resistance to therapeutic drugs. Cell migration is extensively controlled by phosphoinositide 3-kinase (PI3K), which generates PI(3,4,5)P3 (PIP3) and PI(3,4)P2, lipid messengers that recruit pleckstrin homology (PH)-domain-containing signaling proteins. While PIP3 is known to regulate cell migration, it remains a major unanswered question in the field whether PI(3,4)P2 is also implicated in this cellular function.

As described in this thesis, a series of investigations on PI(3,4)P2-specific lipid phosphatases and binding proteins (collectively referred to as the PI(3,4)P2 pathway for simplicity) in the context of chemotaxing malignant B cells provide the first insights into a previously unappreciated role of PI(3,4)P2 signaling in cell migration. First, I found that PI(3,4)P2 is enriched to the migrating front in human malignant B cells chemotaxing to SDF-1. Second, I used physiological regulators of PI(3,4)P2, the inositol polyphosphate 4-phosphatase (INPP4) enzymes, as tool to manipulate PI(3,4)P2 levels to determine the

function of this lipid second messenger. PI(3,4)P2 depletion by INPP4A or INPP4B relative to phosphatase-dead mutants indicated an essential role of PI(3,4)P2 in mediating both the speed and directionality of chemotaxis.

In the attempts to identify signaling effectors downstream of PI(3,4)P2, knock-down (KD) of the authenticated PI(3,4)P2-specific binding protein TAPP2 leads to reduced migration speed and directionality, similar to PI(3,4)P2 depletion. The impaired migration is underlain by alterations in chemokine-induced rearrangement of the actin cytoskeleton and loss of migratory polarity, characterized by a multi-protrusion morphology. TAPP2 colocalizes with the stable-F-actin-binding protein utrophin, with both molecules reciprocally localizaing against the dynamic F-actin accumulated at the leading edge upon chemokine stimulation. In TAPP2 KD cells, the leading edge activator Rac was overactivated and accumulates in multiple cellular protrusions. These data suggest that TAPP2 acts in complex with utrophin and stable F-actin to control Rac activation and regulate the formation of leading edge protrusions. TAPP2 KD also inhibits malignant B cell migration into co-cultured bone marrow stromal cell layers, microenvironments that confer resistance to a chemotherapy drug, fludarabine. The migration inhibition in this context is associated with reduced drug resistance.

A putative PI(3,4)P2-binding protein, lamellipodin (Lpd), is found to strongly colocalize with PI(3,4)P2 on the plasma membrane depending on the Lpd PH domain, with a local enrichment of both molecules at the front facing the direction of migration. Consistent with this pattern, Lpd knock-down rescue experiments indicated that PI(3,4)P2 controls

directionality through Lpd, while Lpd also promotes motility independently of PH domain binding to PI(3,4)P2.

The PI(3,4)P2-binding protein kinase Akt/PKB (also binds to PIP3), known to have differential impacts on migration of various cell types, is found to play a positive role in the B cell context. Here, PI(3,4)P2 depletion does not inhibit phosphorylation of Akt but seemingly reduces its activity. It is likely that PI(3,4)P2 mediates malignant B cell migration in part through promoting Akt activity.

Taken together, the thesis work establishes the PI(3,4)P2 pathway as a novel branch of the PI3K signaling network controlling cell migration and suggests that PI(3,4)P2 may integrate diverse downstream migratory pathways to impact on cell migration. The present and follow-up studies may also lead to the potential identification of new therapeutic intervention targets for blocking the dissemination, expansion and drug resistance of malignant B cells.

Acknowledgement

First of all, I would like to sincerely thank my supervisor, Dr. Aaron Marshall, for encouraging and guiding me through the challenging but rewarding journey of this PhD study. The excellent research resources and inspiring advices, among many other tremendous supports that he has constantly provided are indispensable to all my progress. I am particularly grateful for so much that I have learnt from him and that I believe will benefit me further into my future career. His great personality of being kind, friendly and patient is unbelievable and will surely be significant part of my fond memories whenever I recall my life as a PhD student.

I would like to extend this deep gratitude to my committee members, Drs. Sam Kung, John Wilkins and Spencer Gibson, for their extremely valuable insights, critiques, comments and suggestions. Not only are these directly essential to the advancement of my projects, but they have greatly helped expand my horizons and ability in research. I especially appreciate their being there the entire time ready to help and their always being kind, considerate and encouraging personally while being critical and enlightening in research. I would also like to express my great gratitude to my external examiner for spending time reviewing the thesis and all the insightful comments, critiques and suggestions that I believe will lead to significant improvement of this work.

I owe my warmest thanks to all my colleagues and friends, current and former, in Marshall Lab and the Open Lab of Immunology. They make this place like a sunny home, full of fun, joy and excitement both in research and personally. I apologize that due to limited space, I could not list all their names here.

Special thanks belong to my collaborators, without whom the accomplishments of my projects would not have been possible. These include the laboratories of Drs. Sam Kung, Francis Lin, Spencer Gibson, James Johnston and John Wilkins, the Manitoba CLL bank and the University of Manitoba flow cytometry and confocal microscopy core facilities. I

owe the most thanks to Sen Hou and Xun Wun, my colleagues and friends as well as constant, helpful and productive teammates throughout my projects. These thanks are extended to my colleagues Nipun Jayachandran, Edward Noh and Kennedy Makondo for also contributing data to these projects and Tingting Zhang, Ivan Landego, Samantha Pauls and Sandrine Lafarge for technical assistance or/and helpful ideas.

The important help from the professors and their laboratories who kindly share their reagents, materials or methods is highly appreciated. I wish to be forgiven for not being able to show here all the details, which are provided in Chapter 2, instead.

I would sincerely thank the funding agencies, NCIC/CCS (National Cancer Institute of Canada/Canadian Cancer Society), CIHR (Canadian Institutes of Health Research) and CFI (Canada Foundation for Innovation) for supporting research as well as CIHR, MHRC (Manitoba Health Research Council) and MICH (Manitoba Institute of Child Health) for studentships and travel awards. I feel particularly grateful for the CIHR Frederick Banting and Charles Best Canada Graduate Scholarships - Doctoral Award, which means recognition and encouragement.

Filled with love in my heart, I cannot thank enough my wife (Hongying), son (Goodspeed), daughter (Athena), parents (Shuwen and Zhenbao), brother (Hongxun) and uncle (Wanjiang) for their love, encouragement and support throughout my PhD study and for making my efforts and my whole life meaningful!

Due to limited space, I am sure that I have not had a chance to express my sincere gratitude to some of those who have been very much helpful, encouraging and supportive to me during my life of being a PhD student. I would like to sincerely thank them all and ask their forgiving.

Table of contents

List of publications (Last five years)

Published

1: Dielschneider RF, Xiao W, Yoon JY, Noh E, Banerji V, **Li H**, Marshall AJ, Johnston JB, Gibson SB. Gefitinib targets ZAP-70-expressing chronic lymphocytic leukemia cells and inhibits B-cell receptor signaling. **Cell Death Dis**. 2014 Oct 2;5:e1439. doi: 10.1038/cddis.2014.391. PubMed PMID: 25275600.

2: Lafarge ST, **Li H**, Pauls SD, Hou S, Johnston JB, Gibson SB, Marshall AJ. ZAP70 expression directly promotes chronic lymphocytic leukaemia cell adhesion to bone marrow stromal cells: Correspondence. **Br J Haematol.** 2014 Aug 4. doi: 10.1111/bjh.13063. [Epub ahead of print] PubMed PMID: 25088442.

3: **Li H**, Hou S, Wu X, Nandagopal S, Lin F, Kung S, Marshall AJ. The tandem PH domain-containing protein 2 (TAPP2) regulates chemokine-induced cytoskeletal reorganization and malignant B cell migration. **PLOS ONE.** 2013;8(2):e57809. doi: 10.1371/journal.pone.0057809. Epub 2013 Feb 27. PubMed PMID: 23460911; PubMed Central PMCID: PMC3583899.

4: Gang H, Hai Y, Dhingra R, Gordon JW, Yurkova N, Aviv Y, **Li H**, Aguilar F, Marshall A, Leygue E, Kirshenbaum LA. A novel hypoxia-inducible spliced variant of mitochondrial death gene Bnip3 promotes survival of ventricular myocytes. **Circ Res.** 2011 Apr 29;108(9):1084-92. doi: 10.1161/CIRCRESAHA.110.238709. Epub 2011 Mar 17. PubMed PMID: 21415393.

5: Costantini JL, Cheung SM, Hou S, **Li H**, Kung SK, Johnston JB, Wilkins JA, Gibson SB, Marshall AJ. TAPP2 links phosphoinositide 3-kinase signaling to B-cell adhesion through interaction with the cytoskeletal protein utrophin: expression of a novel cell adhesion-promoting complex in B-cell leukemia. **Blood.** 2009 Nov 19;114(21):4703-12. doi: 10.1182/blood-2009-03-213058. Epub 2009 Sep 28. PubMed PMID: 19786618.

6: Zhang TT, **Li H**, Cheung SM, Costantini JL, Hou S, Al-Alwan M, Marshall AJ. Phosphoinositide 3-kinase-regulated adapters in lymphocyte activation. **Immunol Rev.** 2009 Nov;232(1):255-72. doi: 10.1111/j.1600-065X.2009.00838.x. Review. PubMed PMID: 19909369.

7: **Li H**, Liu G, Yu J, Cao W, Lobo VG, Xie J. In vivo selection of kinase-responsive RNA elements controlling alternative splicing. **J Biol Chem.** 2009 Jun 12;284(24):16191-201. doi: 10.1074/jbc.M900393200. Epub 2009 Apr 22. PubMed PMID: 19386606; PubMed Central PMCID: PMC2713567.

Submitted

8: **Li H**, Wu X, Hou S, Noh E, Makondo KJ, Du Q, Wilkins JA, Johnston JB, Gibson SB, Lin F and Marshall AJ. Phosphatidylinositol-3,4-bisphosphate and its binding protein lamellipodin regulate chemotaxis of malignant B lymphocytes. **Proc Natl Acad Sci U S A**. Status: Reviewed by Editorial Board on 2014-10-08 and by Editor on 2014-10-10, and being reviewed by reviewers since 2014-10-10.

Prepared

9: **Li H** and Marshall AJ. PI(3,4)P2-specific phosphatases and binding proteins regulate a new branch of PI3K signaling. A review manuscript prepared for publication.

List of figures and tables

List of videos

All videos are “saved as separate files and not embedded within the thesis”, according to the University of Manitoba (MSpace) thesis submission requirements. Video legends are provided as listed below:

List of copy right permissions

Chapter 1.21 The tandem PH domain-containing proteins (TAPP1 and TAPP2)
(Reproduced with permission from Immunol Rev. 2009 Nov;232(1):255-72. Copyright © 1999-2014 John Wiley & Sons, Inc.)

Chapter 2.1 Isolation of primary CLL B cells
(Reprinted with permission from Blood. 2009 Nov 19;114(21):4703-12. Copyright © 2014 by American Society of Hematology)

Chapter 2.4 Lentiviral packaging and transduction
(Partly reproduced with permission from Blood. 2009 Nov 19;114(21):4703-12. Copyright © 2014 by American Society of Hematology)

Chapter 2.6 Neon Transfection of RAJI and primary CLL B cells
(Partly reproduced with permission from Br J Haematol. 2014 Aug 4. doi: 10.1111/bjh.13063. Copyright © 1999-2014 John Wiley & Sons, Inc.)

Chapter 4 TAPP2 mediates malignant B cell migration
(Reprinted from PLOS ONE. 2013;8(2):e57809. PLOS: “Open-Access License No Permission Required”)

Apendix The original QIAGEN® Plasmid Quick-Start Protocol
(Reprinted with permission from QIAGEN. Copyright © 2011 QIAGEN)

List of Abbreviations

4E-BP1	eIF4E-binding protein 1
ACAP1	ADP-ribosylation factor directed GTPase-activating protein 1
ANTH domain	AP180 N-terminal homology domain
APE	Akt phosphorylation enhancer
Arf	ADP ribosylation factor
ARNO	ADP ribosylation factor nucleotide-binding site opener
Arp2/3	actin-related protein2/3
B cell	B lymphocyte
Bam32	B lymphocyte adapter molecule of 32 kDa
BAR domain	Bin–Amphiphysin–Rvs domain
B-CLL	B cell-derived chronic lymphocytic leukemia
BCR	B cell receptor
BMDC	bone marrow-derived dendritic cells
BSA	bovine serum albumin
Btk	Bruton's tyrosine kinase
cAMP	cyclic adenosine monophosphate
CCP	clathrin-coated pits
cdc42	cell division cycle 42
CDS	coding sequence
CI	chemotactic index

CLL	chronic lymphocytic leukemia
CME	clathrin-mediated endocytosis
COX-2	cyclooxygenase 2
DAPI	4', 6-diamidino-2-phenylindole
DAPP1	dual adaptor of phosphotyrosine and 3-phosphoinositides
DGC	dystrophin glycoprotein complex
DMEM	Dulbecco's Modified Eagle's medium
DMSO	dimethyl sulfoxide
DOCK180	Dedicator of cytokinesis 180KDa
ECM	extracellular matrix
EDTA	ethylenediaminetetraacetic acid
EGF	epidermal growth factor
EGFP	enhanced green fluorescent protein
eHSP90α	extracellular heat shock protein 90 alpha
ELISA	enzyme-linked immunosorbent assay
Ena/VASP	Ena, Mena, VASP and EVL
ENTH domain	Epsin N-terminal homology domain
EPEC	enteropathogenic Escherichia coli
ER	endoplasmic reticulum
ERK	extracellular-signal-regulated kinase
EVH1	Ena/VASP homology 1
F-actin	filamentous actin or actin filament

FAK	Focal adhesion kinase
FBS	fetal bovine serum
FERM domain	4.1 protein, ezrin, radixin and moesin homology domain
FilGAP	filamin A-binding GTPase-activating protein
FITC	fluorescein isothiocyanate
FRET	fluorescence resonance energy transfer
FYVE domain	Fab1, YOTB, Vac 1 and EEA1 homology domain
G actin	monomeric globular actin
GAP	GTPase activating protein
GDI	guanine nucleotide dissociation inhibitor
GDP	guanosine diphosphate
GEF	guanine nucleotide exchange factor
Girdin	girders of actin filaments
GPCR	G protein-coupled receptor
Grp1	general receptor of phosphoinositides 1
GSK-3	glycogen synthase kinase-3
GST	glutathione S-transferase
GTP	guanosine triphosphate
HEK293T	human embryonic kidney 293T cell
IMDM	Iscove's Modified Dulbecco's Media
INPP4	Inositol polyphosphate-4-phosphatase
IZ	intermediate zone

KD	knock-down
KI	knock-in
KO	knock-out
MAL	myelin and lymphocyte protein
MAPK	mitogen-activated protein kinase
MDCK cells	Madin-Darby canine kidney cells
MEF	mouse embryonic fibroblasts
MFI	mean fluorescence intensity
ml	milliliter
MLC	myosin light chain
M-LV	measles virus glycoprotein-pseudotyped lentivirus
MRCKα	myotonic dystrophy kinase-related Cdc42-binding kinase α
MRL	MIG-10, RIAM and lamellipodin
ms	millisecond
mTORC2	mammalian target of rapamycin complex 2
MUPP1	multi-PDZ domain protein 1
Mut	muatnt
MVB	multivesicular bodies
NC	neural crest
NFAT	nuclear factor of activated T cells
N-WASP	neural Wiskott-Aldrich syndrome protein
p70SK	70 kDa ribosomal protein S6 kinase

PAK	p21-activated kinase
PAK-PBD	the p21-binding domain of PAK
PBS	phosphate buffered saline
PDGF	platelet-derived growth factor
PDK	3-phosphoinositide-dependent kinase
PDZ domain	PSD-95/discs large/ZO-1 domain
Pen Step	penicillin streptomycin
PEST	proline (P), glutamic acid (E), serine (S) and threonine (T)-rich
PH domain	pleckstrin homology domain
PHLPP	PH domain and leucine rich protein phosphatase
PI	phosphatidylinositol
PI(3,4)P2	phosphatidylinositol-3,4-biphosphate
PI3K	phosphoinositide 3-kinase
PIP3	PI(3,4,5)P3
PIX	PAK-interacting exchange factor
PKB	protein kinase B
PLCγ1	phospholipase Cγ1
POPC	1-palmitoyl-2-oleoylphosphatidylcholine
POPE	1-palmitoyl-2-oleoyl phosphatidylethanolamine
P-Rex1	PIP3-dependent Rac exchange factor 1
PS	phosphatidylserine
PTEN	phosphatase and tensin homolog

PTPL1	protein tyrosine phosphatase L1
PX domain	phox homology domain
RA domain	Ras association domain
RAPH1	Ras association and pleckstrin homology domains 1
RBD	Rho-binding domain
RFP	red fluorescent protein
RIAM	Rap1-GTP-interacting adaptor molecule
ROCK	Rho-associated kinase
ROS	Reactive oxygen species
RPMI-1640	Roswell Park Memorial Institute 1640
S1P	sphingosine 1-phosphate
SD	standard deviation
SDF-1	stroma-derived factor
SEM	standard error of the mean
SH2	Src homology 2
SH3	Src homology 3
SH3BP1	SH3-domain binding protein 1
SHIP	src homology 2-containing inositol phosphatase
SN	supernatant
SNP	single nucleotide polymorphism
SNX9	Sorting nexin 9
Sos	Son of Sevenless

SPR	surface plasmon resonance
SRF	serum response factor
srGAP3	Slit-Robo Rho GTPase activating protein 3
SVZ	subventricular zone
SWAP-70	switch-associated protein-70
Syk	Spleen tyrosine kinase
TAPP	tandem PH domain-containing protein
TRAP	thrombin receptor agonist peptide
TSC2	tuberous sclerosis complex 2
UTR	untranslational region
VSV-G	vesicular stomatitis virus glycoprotein
WASP	Wiskott–Aldrich syndrome protein complex
WAVE	WASP-family verprolin-homologous protein complex
WT	wild type
ZAP-70	Zeta-chain-associated protein kinase 70
∆ PH	PH deletion
µg	microgram
µl	microliter
µM	micro molar

Chapter 1 Introduction

This chapter is partly based on:

(1) Zhang TT, **Li H**, Cheung SM, Costantini JL, Hou S, Al-Alwan M, Marshall AJ. Phosphoinositide 3-kinase-regulated adapters in lymphocyte activation. Immunol Rev. 2009 Nov;232(1):255-72. PMID: 19909369

(2) **Li H** and Marshall AJ. PI(3,4)P2-specific phosphatases and binding proteins regulate a new branch of PI3K signaling. A review manuscript prepared for publication.

1. 1 Cell migration: general implication in physiology and disease

Cell migration, the general process involving the movement of cells from one location to another, plays an important role in many physiological events, such as food searching and socialization of the amoeba Dictyostelium discoideum, and in higher organisms embryonic development (organogenesis and nerve wiring), wound healing and tissue regeneration, and immune cell homing and recruitment. Unfortunately, however, cell migration is also widely involved in pathological situations including allergic inflammation and cancer metastasis [1-7]. With increasingly recognized importance, cell migration is now among the most intensively pursued areas in cell biology. This is well highlighted in the online knowledge database, Cell Migration Gateway (https://www.cellmigration.org/), which also serves as part of reference for some of the information here about cell migration basics [8]. In the case of metastasis, cancer cells spread from the original site of tumor formation and growth. They are often characterized

by invasive phenotypes such as the loss of cell-cell interactions (for example, in epithelial cell cancers), increased migratory activity and ability to migrate directionally towards locations that support their survival and proliferation. Cancer cells can migrate through vessel walls into blood or lymph circulation, in a process termed intravasation, or out of the circulation in the so called extravasation process to reach distal organs as secondary sites of cancer cell proliferation [7, 8].

1.2 The migration of malignant B lymphocytes (B cells)

The critical impact of cell migration on cancer progression may be well illustrated in B cell-derived leukemia and lymphoma, a diverse group of diseases including chronic lymphocytic leukemia (CLL) [9], acute lymphoblastic leukemia (ALL) [10], diffuse large B cell lymphoma (DLBCL) [11], follicular lymphoma (FL) [12], mucosa-associated lymphoid tissue (MALT) lymphoma [13, 14], mantle cell lymphoma (MCL) [15], Burkitt lymphoma [16], and multiple myeloma (MM) [17]. Clinical course varies among types or stages of disease, which can be indolent or aggressive. Traditional treatment includes radiation, chemotherapy and stem cell transplantation. The clinical course and effectiveness of treatment are often affected by the migration and localization of malignant B cells as illustrated below, which raises the need to develop new therapeutic strategies targeting these processes.

Malignant B cells are characterized by their infiltration and retention in bone marrow and other organs, where they disrupt normal physiological functions, such as hematopoiesis. Leukemia and lymphoma B cells express functional chemokine receptors including

CXCR4 and are capable of directional migration (chemotaxis) by following gradients of chemokines such as SDF-1 (CXCL12), the ligand of CXCR4 [18, 19]. Strongly expressed by tissues such as bone marrow, lymph nodes, spleen, lung and liver, SDF-1 is widely known to be an important driving force for the dissemination of cancer cells into these potential destinations [18, 20, 21], while normally it is essential for physiological functions such as hematopoiesis, organogenesis, vascularization, tissue regeneration and immune cell trafficking [22, 23].

Within destination tissues, SDF-1 attracts malignant B cells into stromal niches that provide survival and proliferation signals and confer resistance to therapy [19, 24]. The interaction of malignant B cells with stromal cells is believed to be a key mechanism accounting for minimal residual disease and relapses after traditional chemotherapy [18, 19]. Therefore, blocking malignant B cell access to and interaction with stromal cells may represent a promising strategy for developing improved therapy.

1.3 Modes of cell migration

Different modes of cell migration exist depending on cell types and contexts, which integrate the intrinsic properties of the cells and their interaction with environmental factors such as adhesion strength to extracellular matrix. For example, immune cells are fast moving and turning, adhere relatively weakly to substrata, do not show highly organized segmentation of the cytoskeleton and display an “amoeboid” moving morphology. In contrast, fibroblasts and epithelial cells are generally slower migrating cells and display highly organized, differential cytoskeleton and adhesion structures [8].

It is particularly noteworthy that cell migration modes can be divided into two groups according to the dependence of migration on a directional environmental cue or not. It is often observed that cells have the intrinsic capacity to be motile in an autonomous manner. The migration mode is called basal or random motility. “Motility” is a term used to describe how actively cells move, but sometimes also used as alternative to “migration speed” in directional migration. Cell motility can also be activated or enhanced by uniform stimuli in the process called chemokinesis. Directional cues can be chemotactic (conferred by chemoattractants such as chemokines), mechanotactic (arising from breakdown of cell-cell contacts such as during wound healing), or electrotactic (provided by electric fields) [8]. Among these, chemotaxis, the process in which cells actively migrate towards a chemical attractant, is the most extensively studied type of directional migration, a major driving force of cancer cell dissemination and the focus of this thesis. On the whole cell level, directional migration such as chemotaxis, can be dissected and quantified as two major components: speed (how fast cells move) and directionality (how efficient cells migrate in the direction of chemoattractant gradient). The definitions of these parameters are detailed in Material and Methods chapter. Furthermore, on the subcellular level, chemotaxis can be arbitrarily divided into the following several component processes, although these are all interconnected, overlapping and dynamically integrated during an intact process of cell movement [8, 25, 26].

1.4 Component processes of cell migration

1.4.1 Directional sensing

Chemoattractants include chemokines, complement fragments, lipids, microbial components, and small molecules such as cAMP [27-29]. Chemokines are small proteins with special N-terminal cysteine- containing motifs [30]. Chemoattractant gradients are believed to form and guide cell migration in vivo. Despite significant progress in visualizing cell migration in live animals or tissues based on advances in fluorescent labelling and microscopy techniques, monitoring chemoattractant gradients in vivo remains a challenging task. So far as I know, one study used intravital immunofluorescence imaging in mice to detect an intravascular gradient of chemokine CXCL2, which guides neutrophil migration towards sites of tissue damage [31]. Nevertheless, much has been learnt about chemotaxis using in vitro systems that generate chemokine gradients, including those with well-controlled profiles based on microfluidic technology.

Directional sensing is the ability of a cell to detect an extracellular chemoattractant field around its perimeter, identify the direction of the concentration gradient and initiate asymmetric intracellular signaling accordingly. Chemoattractants are often detected by G protein-coupled receptors (GPCRs). Receptor activation leads to the dissociation of the heterotrimeric G proteins into Gα and Gβγ subunits [32-34]. Gα is known to mediate the control of ion channels, and Gβγ regulates effector enzymes such as PI3K [35, 36]. Chemoattractant GPCRs are uniformly distributed along the cell periphery in chemotaxing cells, allowing cells to detect chemoattractant at all directions [37-39]. The associated G proteins are also generally found to be uniform. At any point along the cell

surface, the local chemoattractant concentration is directly reflected by the extent of GPCR activation and there is no signal adaptation or amplification [34, 40]. The cell can read tiny difference in GPCR occupancy across its length that results from difference in chemoattractant concentration as little as 5% [41]. Therefore, the GPCR sensory machinery provides a simple, accurate and sensitive readout of the chemoattractant gradient [27, 34, 40]. The sensing, however, leads to highly amplified responses, with sharply polarized accumulation of intracellular signaling molecules to the front or back of the cell, such as pleckstrin homology (PH) domain-containing proteins to the leading edge [32]. Directional sensing does not depend on polarization or motility. Treatment of Dictyostelium or neutrophils with latrunculin, which inhibits actin polymerization, disrupts the cellular polarity and motility. Under this condition, cells can still sense chemoattractant gradients, as evidenced by sharp enrichment of fluorescently labelled PH domain probes towards the direction facing higher concentration of chemoattractants [41-43]. GPCR-mediated directional sensing is evolutionarily conserved from Dictyostelium to human. However, the mechanisms linking GPCR activation and the resulting signal amplification are poorly understood [43].

1.4.2 Polarization

This refers to the asymmetry of a migrating cell along the moving direction with a defined front and rear. The leading edge is characterized by high content of actin filaments (F-actin) that generate the primary driving force of cell movement and by adhesion to the substratum. F-actin at the leading edge is highly dynamic in nature with fast polymeriazation and depolymerization, hence termed dynamic F-actin [44]. Actin

dynamics are controlled by a variety of actin-binding proteins and their regulators. The cell rear contains a stable F-actin population with slow kinetics of formation and turnover [44]. This region also undergoes the disassembly and release of adhesion. The cell body at the central part contains the nucleus and microtubules [8]. Polarization can be induced in response to a chemoattractant gradient. However, it can also form in the absence of a directional cue, in the cases of random motility or chemokinesis. The mechanism is not well understood, whereas it was proposed that polarization may be a stochastic process that originates from fluctuations in receptor occupancy or the microenvironments outside or inside the cell [25, 45].

1.4.3 Protrusion

Protrusion is the cellular extension typically seen at the front of most migrating cells, pushed outward by the underlying F-actin backbone. It adheres to the substratum and provides traction for the movement of the cell. Different types of protrusive structures can be generated depending on cell types and contexts, including filopodia, lamellipodia and pseudopodia [8, 46]. Although all these structures are based on a dense core of F-actin, they have different spatial organization of F-actin. Filopodia are one dimensional, spike-like structures, formed in neuronal growth cones and fibroblasts. They comprise long parallel F-actin bundles. Filopodia are considered exploratory devices for such cellular functions as mechanosensing, while the other two types of protrusions drive cell migration. Lamellipodia are two dimensional sheet-like structures, formed in fibroblasts, epithelial cells and neurons. They contain a dense mesh of highly cross-linked and branched F-actin. Pseudopodia are three dimensional, filled with a F-actin gel and formed

in amoeba and neutrophils. The two dimensional geometry of lamellipodia has made them traditionally most convenient for studies with light microscope. Therefore, lamellipodia are the best studied and understood among all the three types of protrusions. In many cases, the term lamellipodia is generalized to simply represent any type of protrusion of migrating cells [8, 46].

Actin polymerization is carried out by a wide array of actin-binding proteins and regular proteins. Formins nucleate unbranched filaments. Arp2/3, a heptamer protein complex, generates new branches from a pre-existing filament, which is essential to the formation of highly branched type of F-actin network typical of lamellipodia of migrating cells. Arp2/3 is activated by binding of adaptor protein complexes, Wiskott-Aldrich Syndrome protein complex (WASP) and WASP-family verprolin-homologous protein complex WAVE [25, 47].

1.4.4 Adhesion

Adhesion to extracellular matrix or other cells is essential for cell migration, which stabilizes protrusions and provides traction force for movement. Adhesion is mediated by integrins and other cell surface receptors that bind to matrix or ligands on other cells. The receptors link the cytoskeleton to the substratum and trigger signaling pathways that regulate protrusion. The size, shape and function of adhesion structures can be variable depending on subcellular localization and cell types. Adhesions in lamellipodia are small and dot-like structures, also called nascent adhesions or focal complexes. In fast migrating amoeboid cells adhesion structures are overall small, actively assembled and

disassembled. Adhesions away from the front in fibroblasts are large and elongated, called focal adhesions, which are more stable and anchor large F-actin bundles [8].

1.4.5 Cell body translocation, rear retraction and adhesion disassembly

These aspects are much less understood. Cell body translocation is promoted by the contraction of the actomyosin (contractile complex of actin and myosin II). Rear retraction is coordinated by actomyosin contraction and adhesion assembly. Adhesion disassembly may be controlled by several proposed mechanisms: pulling force exerted by actomyosin contraction, microtubule-induced disassembly, integrin endocytosis and proteolytic degradation of adhesion proteins [8].

1.5 PI3K is a general regulator of cell migration

A series of pioneering work identified phosphoinositide 3-kinase (PI3K, to be introduced in detail below) as a central regulator, the “chemotactic compass”, in chemotaxis of the social amoeba Dictyostelium discoideum and neutrophils [48-53], which represents a milestone in deciphering cell migration mechanisms. This paradigm was challenged later by observations that the PI3K dependence seemed to be bypassed in the contexts of a few in vitro cell migration systems in the presence of specific chemoattractants or gradient profile settings [54]. However, with the ever-increasing literature on the regulation of cell migration, it now turns out merely isolated reports that under specific conditions some cell types can use alternative pathways to migrate. A general role of PI3K is dominant in

the vast majority of cell types and settings. The PI3K pathway was established as essential for in vivo cell migration in intact tissues [44, 55], and in diverse cellular contexts beyond Dd and neutrophils [25, 27, 29, 56, 57]. PI3K is now known to control migration function at multiple levels depending on cellular contexts, including gradient sensing of chemotactic factors, cell priming to enhance motility, establishing cell polarity, mediating adhesion and probably promoting rear retraction [25, 27, 29, 56, 57]. The currently major known effector pathways of PI3K in mediating cell migration involve the Rho family small GTPases and protein kinase Akt/PKB.

1.6 Introduction to PI3K and 3-phosphoinositide messengers

The ubiquitously expressed phosphoinositide 3-kinase (PI3K) family of lipid kinases regulates diverse cellular functions including cell survival, proliferation, metabolism and migration, among many others. PI3K catalyzes the production of membrane-bound lipid messengers by selectively phosphorylating the hydroxyl group at position 3 of the inositol ring of phosphoinositides [58] (Figure 1.1).

Three classes of PI3K enzymes have been known, mostly based on their molecular structures and substrate specificities. Class I PI3Ks are heterodimers of a catalytic subunit and a regulatory subunit. These are further divided into two sub-classes. Class IA is composed of one of three isoforms of catalytic subunits, p110α, β, or δ, associated with one of five isoforms of regulatory subunits, p85α or β, p55α or γ or p50 α. Class IB is based on a p110 γ catalytic subunit bound with one the regulatory subunits, p101 or

p84/p87 [59]. Class I PI3Ks phosphorylate PI(4,5)P2 and PI(4)P to produce PI(3,4,5)P3 (PIP3) and PI(3,4)P2, respectively [58]. It is traditionally believed that class IA PI3Ks are activated by receptor tyrosine kinases and Class IB by G protein-coupled receptors (GPCRs) [60], however emerging evidences suggest that class IA are also involved in signaling downstream of GPCRs [58, 61]. Class II PI3Ks, including PI3K-C2α, PI3K-C2β and PI3K-C2γ, which are not associated with a regulatory subunit [59], phosphorylate PI4P and PI into PI(3,4)P2 and PI(3)P, respectively [58, 59, 62, 63]. The only known class III PI3K, composed of a 34 KDa catalytic subunit, associated with a p150 regulatory subunit, phosphorylate PI to PI(3)P [29, 59, 64]. Among all classes, class I PI3Ks are the best understood, found to regulate a wide range of key cellular functions as mentioned before, whereas class II and III PI3Ks are less studied.

1.7 Phosphoinositide Phosphatases provide independent control of PIP3 and PI(3,4)P2

Several lipid phosphatases control the levels of various PI species produced by PI 3-kinases (Figure 1.1). Among these, INPP4 is highly specific for PI(3,4)P2, dephosphorylating it into PI(3)P. The cellular level of PI(3)P is much higher than PI(3,4)P2 and the synthesis of PI(3)P is believed to be predominantly contributed by class II and III PI3Ks [63, 65, 66]. The impact of INPP4 on cellular PI(3)P level appears to be negligible [62, 66]. Therefore, the function of INPP4 is considered to be essentially through regulating PI(3,4)P2 [62, 66]. In contrast PTEN regulates both PIP3 and PI(3,4)P2, while SHIP hydrolyzes PIP3 to produce PI(3,4)P2 [58]. As discussed below,

PTEN and SHIP have established functions in cell migration; however, much less is known regarding the functions of INPP4.

Figure 1.1

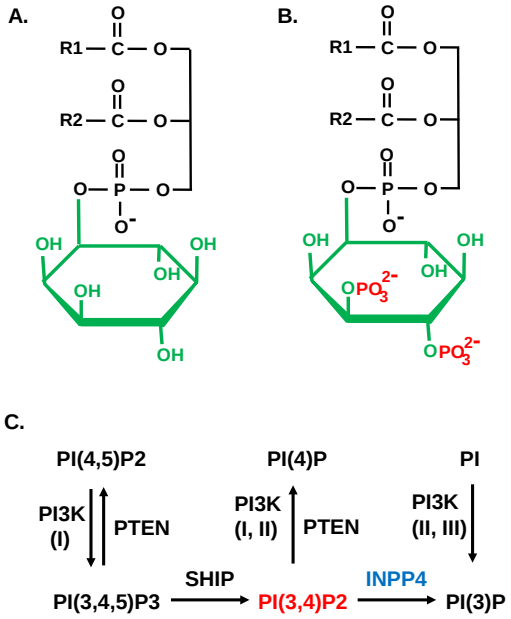

Figure 1.1 3-phosphoinositides are generated by the PI3K signaling network

A. Chemical structures of phosphoinositides. Phosphatidylinositol (PI) consists of a phosphatidic acid backbone, linked via a phosphate group to an inositol ring head group (green). R1 and R2: fatty acid groups. **B.** PI can be phosphorylated at various hydroxyl groups of the inositol ring, producing phosphatidylinositol phosphates, also termed polyphosphoinositides or simplified as phosphoinositides. One such molecule, phosphatidylinositol-3,4-biphosphate, or PI(3,4)P2, is illustrated here. **C.** PI3K generates 3-phosphoinositides. Three classes of PI3Ks (I, II and III) in combination with lipid phosphatases PTEN, SHIP and INPP4 orchestrate a signaling network that regulates diverse cellular functions. INPP4 selectively degrades PI(3,4)P2, converting it to PI(3)P. Since cellular level of PI(3)P is constitutively much higher than PI(3,4)P2, INPP4 is considered to act through inhibiting PI(3,4)P2 and thus its effect can be used to read out PI(3,4)P2 function.

1.8 Binding proteins can have specificity for PIP3 versus PI(3,4)P2

As a major defined cell signaling mechanism, 3-phosphoinositides recruit their specific binding proteins. These are signaling enzymes or adaptors containing protein domains that specifically recognize the 3-phosphoinositides, including PH, PX, FYVE, ANTH, ENTH and FERM domains [58, 66, 67]. Among these, PH domains are the most frequently found in 3-phosphoinositide-binding proteins and best studied. Classically, the function of PI3K has most often been attributed to PIP3, while the role of PI(3,4)P2, initially considered a by-product resulting from the termination of PI3K signaling through PIP3 degradation by the inhibitory phosphatase SHIP [68], has largely been neglected or underestimated. However, emerging evidence now suggests that PI(3,4)P2 may take important part in PI3K-mediated cellular functions. Among 3-phosphoinositide-binding proteins, although some selectively bind to PIP3, such as Btk and Grp1, many others have dual specificities for both PIP3 and PI(3,4)P2, such as Akt, PDK and Bam32/DAPP1 [66]. Most studies have not distinguished the functional contributions between PIP3 and PI(3,4)P2 in specific signaling contexts. Furthermore, novel PH domain proteins have been confirmed (TAPP1 and TAPP2) [69, 70] or proposed (lamellipodin/RAPH1) [71] to be specific for only PI(3,4)P2.

PH domains typically form two orthogonally arranged β sheets containing three (β1 through β3) and four (β4 through β7) strands, respectively. These are followed by a C-terminal α helix [72]. Although basic amino acids in the connecting loops between β1

and β2 and in some cases between β3 and β4 or β6 and β7 participate in binding to the inositol phosphate groups [72, 73], these loops are hyper variable in sequence and length among different PH domains, leading to no unified sequence or structure patterns that predict lipid binding specificities [72, 73]. Lipd binding specificity and corresponding structural mechanism are largely determined on the basis of individual PH domains. Compared to PH domains that bind to both PIP3 and PI(3,4)P2, such as that of Bam32, the PH domain of Btk has a larger β1/β2 loop that interacts extensively with 5-phosphate of the inositol head group, thereby determining high specificity binding to PIP3 [74]. The structure of TAPP1 PH domain is similar to that of Bam32 around the 3- and 4-phosphate binding sites, but binding of TAPP1 PH domain to 5-phosphate is excluded due to the steric hindrance and conformation change caused by a larger alanine residue that substitutes its smaller counterpart, glycine, in the PH domain of Bam32. Mutation of the residue at this position can reciprocally switch the PI(3,4)P2 versus PIP3 binding specificities between the PH domains of TAPP1 and Bam32 [72].

Recent insights into (potentially) PI(3,4)P2-mediated cellular functions are summarized below from studies on PI(3,4)P2-specific phosphatases INPP4A and INPP4B and PI(3,4)P2-binding proteins TAPP1 and TAPP2, lamellipodin and Akt (Figure 1.2).

Figure 1.2

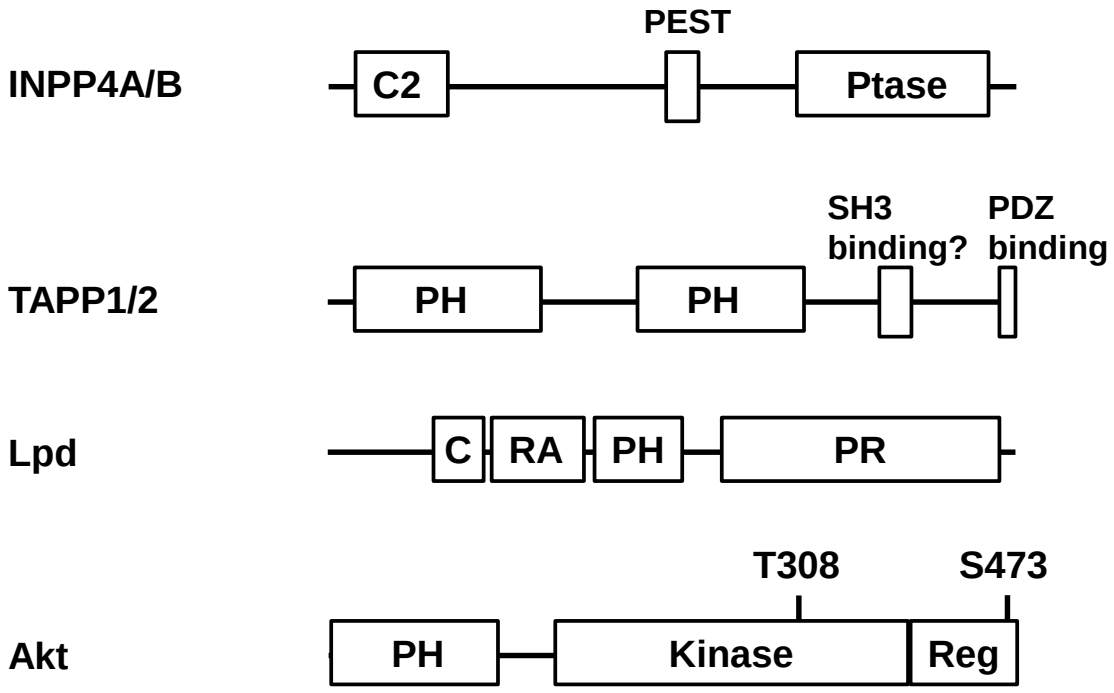

Figure 1.2 The PI(3,4)P2-specific lipid phosphatases and binding proteins

The molecular structures of INPP4, TAPP, lamellipodin (Lpd) and Akt are diagrammed. In INPP4, the C2 domain binds to cell membrane lipids. The PEST sequence is known to mediate the degradation of INPP4A by protease calpain, which has not been reported for INPP4B. The phosphatase (Ptase) activity of INPP4 is specifically against PI(3,4)P2. TAPP1 and TAPP2 are authenticated specific PI(3,4)P2 binding proteins via the C-terminal PH domain, while the function of the N-terminal PH domain remains to be determined. Both TAPPs contain the binding site for PDZ domain-containing proteins. A potential binding site for SH3 domain proteins is present only in TAPP2. Lpd is believed to be another specific PI(3,4)P2 binding protein based on the high specificity binding of its PH domain to PI(3,4)P2 in vitro. Upstream of the PH domain are a putative coiled-coil

(C) motif and a putative Ras association (RA) domain. The C-terminal half of Lpd is characterized by proline-rich (PR) sequences with potential or confirmed binding sites for profilin, SH3 domain-containing proteins or Ena/VASP proteins. Three isoforms of Akt share the same domain structure consisting of an N-terminal PH domain that binds to both PI(3,4)P2 and PIP3, a linker region, a central serine/threonine kinase domain and a C-terminal regulatory (Reg) domain. Phosphorylation of threonine 308 and serine 473 (positions according to Akt1) is key to Akt activation.

1.9 Introduction to Rho GTPases

Rho GTPases [29, 35, 75-77], including Rac, Cdc42, Rho and their related homologues, switch between inactive (GDP-bound) and active (GTP-bound) conformations. The majority of cellular Rho GTPases are in the inactive state, and their activation occurs through the exchange of GDP for GTP, catalyzed by guanine nucleotide exchange factors (GEFs). For inactivation, Rho GTPases have an intrinsic GTPase activity that hydrolyzes their bound GTP to GDP. This activity is facilitated by GTPase activating proteins (GAPs). In addition, guanine nucleotide dissociation inhibitors (GDIs) inhibit GDP/GTP exchange and GTP hydrolysis, and block the cell membrane recruitment of Rho GTPases by masking their hydrophobic regions [76, 78, 79].

Rho GTPases are typically known to regulate cell migration via the actin-remodeling protein complex, Arp2/3, which generates highly branched F-actin network to drive lamellipodia [29, 47, 80]. Arp2/3 is activated by upstream regulators, including adaptor protein complexes WASP, N-WASP and WAVE. WASPs and WAVE are known to be

activated by Cdc42 and Rac, respectively, to promote F-actin and lamellipodia formation [29, 81-84]. On the other hand, Rho, through its downstream effector, Rho-associated kinase (ROCK), promotes stress fiber formation, actomyosin contraction, and the assembly of focal adhesion and myosin II filaments [29, 85, 86].

1.10 Rho GTPases are regulated by PI3K

Many GEFs of Rho GTPases, via their PH domains, are found to be localized and activated by PIP3, and in turn activate their specific Rho GTPases [29, 76]. Examples of these include Vav, DOCK180 and P-Rex1 (GEFs for Rac), Sos (GEF for Rac and Ras) and α and β isoforms of PIX (GEFs for Rac and Cdc42). Not only acting downstream of PI3K, Rac GEFs and Rac seem to promote PI3K activity, leading to a positive feedback loop for signal amplification [29, 76, 87-92]. On the other hand, negative regulation of Rac through the activation of a Rac GAP by PI3K was suggested to balance the signal amplification at the front [29, 93, 94]. Regarding another Rho GTPase, Rho, it was found to be inhibited by PI3K activity [29, 95].

1.11 PI3K and Rho GTPases regulate multiple components of cell migration

1.11.1 Directional sensing with PIP3: the chemotaxis compass?

In Dictyostelium, neutrophils or fibroblasts migrating to a chemoattractant gradient, Akt PH domain probes are enriched towards the leading edge facing higher chemoattractant

concentrations [25, 96]. This localization pattern is abolished by treatment with PI3K inhibitor Wortmannin or PI3K gene deletions, but not dependent on actin polymerization [25, 42, 97]. These initial observations, together with the knowledge that PIP3 interacts with many PH domain-containing proteins that have functions in cytoskeletal regulation, led to the paradigm that PIP3 serves as a “chemotaxis compass” that guides the cell to polarize and migrate towards the direction of chemoattractants. It is noteworthy here that PI(3,4)P2, defined and introduced above, is also generated by PI3K and bound by Akt. As part of this paradigm, the phosphatase PTEN, which switches PIP3 back to PI(4,5)P2, is found to be enriched at the back and sides of chemotaxing cells to restrict PIP3 localization in Dictyostelium [48, 49]. It is believed that mutually exclusive localization of PI3K and PTEN ensures the enrichment of PIP3 to the leading edge and the translation of extracellular chemical gradient into strong intracellular signal amplification response [29]. The low abundance under basal conditions and slow diffusion of PIP3 makes it an ideal messenger and signal amplifier for gradient sensing [1, 29, 98, 99]. The formation of PIP3 gradient as a result of directional sensing then serves as the basis to recruit specific effectors leading to polarized cytoskeletal reorganization and directional migration. This paradigm is now being updated by the fast expanding literature, which dominantly indicate that as a general regulator of cell migration, PI3K may be involved in any of the major component processes, including directional sensing, motility, polarization, adhesion, cell body translocation and rear retraction. The component processes targeted by PI3K and variations in the composition of the PI3K-based regulatory machinery seemingly depend on cellular contexts. In neutrophils and T cells, instead of PTEN, the phosphatase SHIP, which converts PIP3 to PI(3,4)P2, is required to

promote migration [100, 101].

1.11.2 Polarization

As above mentioned, PIP3 regulates the localization and activity of GEFs (or GAPs) of Rho GTPases, which in turn transduce the signal down to their target Rho GTPases. The classical paradigm is that Rac and Cdc42 promote F-actin dynamics and protrusions at the front via the activation of actin regulatory proteins such as WASP, WAVE and Arp2/3 complexes, and Rho promotes rear retraction via functions such as stimulating actomyosin contractility. Rac and Rho have antagonistic relationship, inhibiting each other's activity in promoting "frontness" versus "backness" signaling [25, 29, 102]. However, these simple defined roles are later being updated as evidence indicates more complex crosstalk and versatility of the signaling molecules [25, 29, 76, 103, 104]. Contrary to their normally expected localization, Rac and Rho activity have also been observed at the back and front, respectively [105]. The differential localization patterns seem to be possibly related to cellular contexts [102]. In migrating leukocytes, the distribution of Rho activity, low at the front and high at the sides and back [106], represents a typical example that fits the traditional model. This is also true in PDGF-stimulated fibroblasts. However, in randomly migrating fibroblasts, high Rho activity is found at both the front and back [105, 107]. Functionally, cooperative relationships have been observed between traditional front and back activators in a few cases. PIP3-induced activation of Cdc42 at the front may be linked to Rho activation at the back [108]. RhoA and Cdc42 both control the localization and activation of PTEN [109]. RhoA can cooperate with Rac and Cdc42 at the front to regulate F-actin [110].

1.11.3 Adhesion

Protrusions extended at the front of migrating cells are stabilized by adhesion to the ECM, which also provides traction force to drive cell movement forward. Among cell surface receptors for adhesion, the best studied are integrins. PI3K and Rho GTPases are part of the feedback signaling involving the so-called “outside-in” and “inside-out” integrin activation pathways [25, 111]. Outside-in means that the interaction of the extracellular domains of integrin with a ligand leads to conformational changes of the cytoplasmic domains, which then recruit and activate downstream signaling molecules, such as focal adhesion kinase (FAK). Active FAK in turn activates PI3K and Rac through DOCK180 [112]. Inside-out activation of integrins is induced by the interaction of their cytoplasmic domains with signaling molecules of activated intracellular pathways, which enhances the binding of extracellular domains to ligands. PI3K mediates integrin-dependent migration by modulating integrin inside-out signaling [113, 114]. Active Rac promotes integrin clustering and thus integrin avidity [115].

1.11.4 Cell body contraction and tail retraction

As the cell moves, Rho promotes the maturation of nascent adhesion/focal complexes into more stable adhesions (focal adhesions in fibroblasts), which are thought to contribute to cell body contraction by providing anchorage and mechanical strength [76]. However, increasing Rho activation can over-stabilize focal adhesion to ECM, thereby inhibiting cell migration [116-118]. The main driving force of cell body contraction and

rear retraction is actomyosin contractility controlled by Rho signaling. A major downstream target of Rho, the serine/threonine kinase ROCK phosphorylates myosin light chain (MLC) to activate actomyosin contractility. On the other hand, ROCK inhibits MLC phosphatases from dephosphorylating MLC [119]. In addition, Rho-ROCK signaling defines the back of the cell by inhibiting pathways that promote protrusions. Although Rac may also be implicated in rear retraction in some cases [120], it in general acts as an activator of protrusions and suppressor of backness. Rho and ROCK regulates a Rac GAP, FilGAP, which inhibits Rac [102, 121]. The switch between a dynamic (at the front) and static (at the back) state of F-actin is controlled by cofilin, which severs and depolymerizes F-actin and promotes protrusions [122]. Cofilin is phosphorylated and inhibited by LIM kinase, a downstream target of ROCK [102, 123].

Interestingly, although PI3K is generally believed to function at the front, PI3K activity is also found at the rear of randomly migrating neutrophils, as indicated with PH domain probes from Akt (for PIP3 and PI(3,4)P2) or from TAPP1 (for PI(3,4)P2) [44, 55]. Consistent with these localization patterns, PI3K activity promotes RhoA activation and tail retraction in endothelial cells, as well as myosin contraction through regulating PAK (p21-activated kinase) homologue in Dictyostelium [25, 124]. To maintain properly controlled PI3K activity at the rear, a Rho GTPase analog of mammalian RhoA called RacE and its potential GEF, GxcT, restrict PI3K activity during the chemotaxis of Dictyostelium cells to cAMP. Cells deficient in these molecules extended abnormal pseudopods at the lateral sides and showed reduced chemotactic efficiency [43, 125].

Rear retraction requires the disassembly of adhesions. Integrins are recycled by endocytosis and transported to the front, which involves the regulation by Akt, a major signaling protein downstream of PI3K [126].

1.12 Introduction to Akt

The ubiquitously expressed serine/threonine protein kinase Akt (or protein kinase B, PKB) is a key regulator of a wide range of cellular functions such as survival, proliferation, metabolism and migration. Its three human isoforms Akt1 (PKBα), Akt2 (PKBβ) and Akt3 (PKBγ), comprising 480, 481 and 479 amino acid residues respectively (UniProtKB database), share about 80% amino acid sequence homology and a common domain structure, with an N-terminal PH domain, central kinase domain and C-terminal regulatory domain (Figure 1.2) [127]. The intramolecular interaction between the PH and catalytic domains is believed to keep Akt in an inactive conformation. According to the current dogma of Akt activation, cellular stimuli activate PI3K to produce PIP3, which in turn recruits Akt to the cell membrane by binding to the PH domain and unlock the inactive conformation. This facilitates the phosphorylation of Akt by upstream kinases at two critical residues: Thr308 and Ser473 (positions according to isoform Akt1), located in the kinase domain and regulatory domain, respectively, leading to full activation of Akt. The fully activated Akt can translocate to other subcellular locations such as the cytoplasm and nucleus to phosphorylate its substrates [127].

1.13 Akt regulates cell migration

A number of studies indicated that Akt plays a positive role in cell migration in fibroblasts, fibrosarcoma, endothelial cells and Dictyostelium [126, 128-138]. Several direct or indirect targets of Akt have been identified in the context of cell migration [130]. Akt directly binds to and phosphorylates actin [139-141]. The girders of actin filaments (girdin), also known as Akt phosphorylation enhancer (APE), is an actin-binding protein that maintains the integrity of actin structures at the leading edge and promotes lamellipodia and migration of the Vero fibroblast cell line, depending on its phosphorylation by Akt [129]. Akt promotes integrin recycling by phosphorylating its substrates ADP-ribosylation factor directed GTPase-activating protein 1 (ACAP1) [131] and glycogen synthase kinase-3 (GSK-3) [126]. Akt also regulates myosin II assembly through PAKa, the slime mold structural homolog of the mammalian p21- activated kinase [134].

1.14 Differential roles of Akt isoforms in cell migration

Functional redundancy was initially assumed for the three highly homologous Akt isoforms (more than 80% protein sequence homology) [142]. However, studies with single isoform knockout (KO) mice have revealed non-overlapping functions among Akt isoforms [127, 143-149]. Akt1 KO affects body size and adipogenesis, Akt2 KO results in severe insulin resistant diabetes, and Akt3 KO leads to decreased brain size. Furthermore, using Xenograft or transgenic mouse models and cultured cells, a series of studies indicated that, in the context of breast cancer cell metastasis and migration, Akt2

promotes migration while Akt1 suppresses it [127, 150-152].

Akt1 inhibits the pro-migratory MAPK/ERK signaling [150]. It also promotes the ubiquitination and proteosomal degradation of the Nuclear Factor of Activated T cells (NFAT), a pro-migratory transcription factor [152]. One of NFAT's transcriptional targets, cyclooxygenase 2 (COX-2) [153], is implicated in the regulation of integrin expression [154] and the activation of Rac and Cdc42 [155, 156]. Akt1 may limit the intracellular level of RhoGTP through the effect on the phosphorylation and stability of tuberous sclerosis complex 2 (TSC2) [151]. The actin bundling protein palladin is a specific substrate of Akt1. Phosphorylation of palladin promotes its actin-bundling activity, thereby inhibiting cell migration [157]. No specific substrate of Akt2 has been identified yet that mediates its enhancing effect on breast cancer cell migration. Akt2 up-regulates β1 integrins, which has been proposed to account for the Akt2 effect [158]. The less studied isoform, Akt3, was found to play an inhibitory role [159, 160].

1.15 The isoform-specific function of Akt in cell migration is variable depending on cellular contexts

The differential regulation of cell migration by Akt at the level of isoform specificity is itself further regulated according to specific cellular contexts. In sharp contrast to the roles of Akt1 and Akt2 in breast cancer cells, the exact opposite is observed that in mouse embryo fibroblasts and a prostate cancer cell line PC-3, Akt 1 promotes whereas Akt2 inhibits migration [161, 162]. In human placental trophoblasts, Akt1 and Akt3 promote

basal and EGF-induced migration, whereas Akt2 has no effect [163]. In neutrophils, Akt1 negatively regulate migration in acute inflammatory response [164]. In human dermal fibroblasts, migration stimulated by extracellular heat shock protein 90 alpha (eHSP90α) requires Akt1 and Akt2 working in concert, but does not involve Akt3 [165].

1.16 Potential mechanisms of context-dependent isoform-specific function of Akt

The differential effects conferred by Akt isoforms must primarily come from the sequence divergence among these molecules. A few studies have been elegantly performed using Akt isoform chimera molecules to identify specificity determinant regions [127, 157, 161, 166]. The PH and linker regions have been shown to be implicated in phenotypic specificity and substrate selectivity. Expanding from these findings, it can be arguably expected that specific sequences/regions of Akt isoforms determine the specificities of their recognition by upstream regulators, interaction with binding partners or activity on substrates. Akt activity is negatively regulated by isoforms of PHLPP (PH domain and leucine rich protein phosphatase), a phosphatase that dephosphorylate Akt isoforms at Serine 473. PHLPP1 selectively acts on Akt2 and Akt3 and PHLPP2 on Akt1 and Akt3 [127, 167]. Differential interaction with other cellular molecules may lead to distinct localizations. Total Akt has been found at various cellular locations [127]. In the study of placental trophoblast migration [163], Akt2 and Akt3 localizes in the cytoplasm and nucleus, respectively, while Akt1 in both compartments. However, in the prostate cancer cell line PC-3, Akt1 and Akt2 mainly localize in the

cytoplasm and nucleus, respectively [162]. As far as Akt substrates are concerned, only a few out of more than 100 of them identified so far show isoform specificity, including palladin, specific for Akt1 [142, 168, 169]. Notably, the intrinsic determinants embedded in the sequences of different Akt isoforms do not seem to fully explain the differential behaviors and functions of Akt isoforms. Intracellular environments, the signaling contexts, are expected to contribute to the phenotypic outcomes. The presence, amount, spatiotemporal distribution of the regulators, substrates, binding partners and scaffolding proteins may integrate to determine the effect of an individual Akt isoform on cell migration in a specific cellular context. However, context-dependent isoform specificity of Akt remains poorly understood and represents an interesting but challenging topic of exploration.

1.17 Potential role of PI(3,4)P2 signaling in cell migration

The function of PI3K in regulating cell migration has traditionally been attributed to PIP3. PI(3,4)P2 is often considered merely a by-product resulting from the termination of PI3K signaling through PIP3 degradation by the inhibitory phosphatase SHIP [68]. While it remains to be determined whether PI(3,4)P2 contributes to this cellular function, emerging evidence suggests that a potential role of PI(3,4)P2 may have been neglected or underestimated. As my thesis research addresses the role of PI(3,4)P2 and its binding proteins in B cell migration, the next sections will review the phosphoinositide 4-phosphatase enzymes that control PI(3,4)P2 levels and major known PI(3,4)P2 binding proteins.

1.18 Inositol polyphosphate-4-phosphatase (INPP4)

1.18.1 Molecular characteristics

Two highly related PI(3,4)P2-specific lipid phosphatases have been identified, type I and II inositol polyphosphate-4-phosphatases (INPP4A and B). These are Mg^{2+}-independent enzymes that selectively hydrolyze the phosphate group at position 4 of the inositol ring from PI(3,4)P2, with weak activities against inositol (3,4)P2 and inositol (1,3,4)P3 incomparable to that against PI(3,4)P2 in vitro [170-174]. More recent work determined the in vivo substrate specificity of INPP4 and performed detailed characterization of INPP4 overexpression intended as a genetic tool to specifically turn off PI(3,4)P2 signaling. Consistently with previous in vitro data, INPP4 selectively degraded cellular PI(3,4)P2 but not other phosphoinositides including PI(3)P, PI(4,5)P2 and PI(3,4,5)P3, confirming that PI(3,4)P2 is the preferred substrate of INPP4 in vivo [62, 174-177].

INPP4A (107 KDa) and INPP4B (105 KDa) proteins share 37% sequence homology and similar domain structures, including N-terminal C2, central uncharacterized and C-terminal phosphatase domains (Figure 1.2) [172, 173, 176, 178]. INPP4A was proposed to contain two C2 domains in tandem, which bind PI(3,4)P2 and to a lesser extent PI(4)P and phosphatidylserine (PS) and are required for PI(3,4)P2 4-phosphatase activity [176]. The INPP4B C2 domain binds phosphatidic acid and PIP3 [178]. The central domain of INPP4A contains a PEST (proline, glutamate/aspartate, serine/threonine rich) motif, commonly shared by substrates of the calcium-dependent

protease, calpain [173, 179, 180]. INPP4A was degraded by Calpain in vitro and in platelets treated with calcium ionophore or stimulated with thrombin and preincubation of platelets with calpeptin, a calpain inhibitor, suppressed thrombin-stimulated PI(3,4)P2 accumulation [173]**.** The PEST-mediated degradation of INPP4B by calpain has not been reported. The C-terminal phosphatase domains share the highest sequence homology between INPP4A and INPP4B. They both contain a conserved CX5R catalytic motif (CKSAKDR) and mutation of the cysteine residue abolishes the phosphatase activity [174, 176].

INPP4A and INPP4B transcripts both showed wide tissue distribution pattern, in such as brain, lung, spleen and testis with high expression found in brain, and similar expression pattern at protein level has been confirmed in INPP4B [178]. Differential expression was observed in hematopoietic cell types with the transcripts of INPP4B but not INPP4A detected in B cells, NK cells and macrophages [178].

1.18.2 INPP4A deficiency leads to neurodegeneration

Two mouse models of INPP4A loss have been available to study its physiological role. The weeble mutant mouse has a single basepair deletion in the INPP4A gene leading to the coding of a truncated protein lacking the phosphatase domain [181, 182]. The other mouse model is based on targeted INPP4A knockout (KO) [182]. Both models indicated a critical role of INPP4A in the development and function of the brain. INPP4A

deficiency led to neuronal loss in the cerebellum and hippocampus of weeble mice [181, 183] and the striatum of KO mice [182]. Mechanistic studies using cultured primary striatal neurons indicated that INPP4A knockdown with shRNA or adding PI(3,4)P2, but not PIP3, enhanced the neuronal susceptibility to glutamate-induced excitotoxicity [182], suggesting a neuroprotective role of INPP4A through preventing hyperactivation of PI(3,4)P2 signaling.

1.18.3 INPP4A is a suppressor of Asthma

Asthma is a common chronic inflammatory disease of the airways characterized by airway obstruction, hyperresponsiveness and inflammation. In an initial work to screen candidate genes involved in asthma, a single nucleotide polymorphism (SNP), +110832A/G (Thr/Ala), in the PEST motif of INPP4A, was identified as a correlation marker with asthma susceptibility [184]. INPP4A proteins from individuals with A/A genotype was found to be less stable than A/G or G/G genotypes, presumably due to reduced stability against degradation by calpain. In subsequent work, reduced expression of INPP4A was found in asthma mouse models by calpain-mediated degradation. Further knockdown of INPP4A worsened the asthma phenotype. Loss of INPP4A also induced asthma-like condition in naive mice [185]. Conversely, calpain inhibition or overexpression of INPP4A limited asthma phenotype. These data provide direct evidence that INPP4A is a suppressor of airway inflammation.

The function of INPP4A to suppress asthma may be (partly) through restricting oxidative stress-induced accumulation of PI(3,4)P2. Reactive oxygen species (ROS) produced by

inflammatory cells play a prominent role in asthma [186]. Oxidative stress is known to stimulate the accumulation of PI(3,4)P2 in platelets [187] and PI(3,4)P2 has been proposed to promote platelet activation [188], key component in asthma pathogenesis [189].Treatment of asthmatic mice with a natural dietary antioxidant, Resveratrol, alleviated asthmatic features, associated with inhibited calpain activation and restored expression of INPP4A in bronchial epithelia [190].

1.18.4 INPP4B is a negative modulator of osteoclast differentiation

In vivo insights into the function of INPP4B were available using INPP4B deficient mice [191] with similar mutation to the weeble INPP4A deficient mice [181]. INPP4B deficiency did not lead to major defects in development or life span but defect in bone homeostasis. The bone is controlled by bone-forming osteoblasts and bone resorbing osteoclasts. INPP4B deficient mice demonstrated increased osteoclast differentiation, decreased bone mass and osteoporosis. In human INPP4B was found to be a susceptibility locus for osteoporosis [191].

1.18.5 INPP4B is a putative tumor suppressor

Uncontrolled amplification of PI3K signaling is a common feature of a variety of cancers. It has been widely believed that it is the enhanced PIP3 signaling that leads to cancer. However, a potential role of PI(3,4)P2 dysregulation has largely been neglected. Accumulating evidence indicates that loss of INPP4B correlates with cancer incidence, metastatic potential or poor prognosis in multiple cancer types, including breast [174, 192-194], prostate [195] and ovarian [174, 196] cancers, melanoma [197] and leukemia

[198, 199]. In fewer cases, there are also evidences of altered INPP4A expression in prostate cancer [200] and leukemia [201]. Beyond the correlative observations, a functional role of INPP4 has been suggested by several direct loss- or gain-of-function experiments. INPP4B [174, 197] or INPP4A [175] deficiency through knockdown or mutagenesis led to enhanced proliferation of breast cancer cells [174], melanoma cells [197] or transformed mouse embryonic fibroblasts [175], and conversely, INPP4B overexpression inhibited the proliferation of melanoma cells [197]. Furthermore, emerging evidences suggest that INPP4B may function to restrict the migratory capacity of cancer cells. INPP4B knockdown led to reduced wound healing responses in vitro in breast cancer [174] and melanoma cells [197].

Interestingly, based on mouse models, INPP4 deficiency alone (uncontrolled PI(3,4)P2 production), similar to SHIP deficiency (uncontrolled PIP3 production), does not result in spontaneous tumor formation [191, 202, 203], while PTEN deficiency alone (uncontrolled production of both lipids) has long been known to cause high incidence of cancer [204]. This raised the possibility that malignant transformation through PI3K dysregulation may require uncontrolled production of both PIP3 and PI(3,4)P2. Alternatively, INPP4 deficiency may contribute to tumor formation in combination with other factors, or affect later stages of cancer development [205], especially concerning the migratory capacity of breast cancer cells [174] and melanoma cells [197].

1.18.6 PI(3,4)P2-binding proteins as INPP4 targets

So far a number of PI(3,4)P2-binding proteins have been identified or proposed,

including those that specifically bind to PI(3,4)P2, such as the TAPP proteins and lamellipodin, and those that also bind to other lipids such as PIP3, including Akt. While all cellular function of these multi-domain proteins may not necessarily depend on the PI(3,4)P2-binding domains, in some cases, their function have been shown to be regulated by INPP4, or altered by mutation of phosphoinositide-binding domain. The current literature on PI(3,4)P2-binding proteins is reviewed below and the thesis work will further extend this.

1.19 Akt: regulation by PI(3,4)P2

The regulation of Akt mediated by PH domain – phosphoinositide interaction has often been conveniently attributed to PIP3, however, an important role of PI(3,4)P2 needs to be better appreciated based on accumulating evidence as summarized below. Several groups investigated the effects of synthetic phosphoinositide derivatives on purified Akt in vitro cell-free systems [206-210]. Akt was found to bind both PI(3,4)P2 and PIP3, but not other lipids including PI(4,5)P2 [208, 209], which was later further supported by the crystal structure of Akt PH domain [211]. PI(3,4)P2, but not PI(3)P, PI(4,5P)2 or PI stimulated Akt activity [208-210]. PIP3 did not stimulate but even showed some inhibitory effects on Akt activity [208, 209]. The effects of phosphoinositides on Akt activity depended on the Akt PH domain [208, 210]. The effects of adding PI(3,4)P2, PIP3, PI(3)P or PI(4,5)P2 to intact NIH 3T3 cells on Akt activity were consistent with those observed in the cell-free systems [208]. The activation of Akt by adding PI(3,4)P2 to cells was also reported later by two other studies [212, 213]. These initial studies suggested that PI(3,4)P2 may have a major capacity to activate Akt through direct

binding to Akt.

However, additional/alternative regulatory mechanisms was suggested by subsequent findings that both PIP3 and PI(3,4)P2 activated the 3-phosphoinositide-dependent protein kinase, PDK1, an upstream kinase that in turn activates Akt by phosphorylating Thr308 [206, 207]. The upstream kinase(s) that phosphorylate Ser473, the putative “PDK2” [207], has not been clearly determined yet. The mTORC2 protein kinase complex has been accepted by current consensus as the major Ser473 kinase of Akt [127, 214]. Apart from the earlier insights using cell-free systems, emerging complexity in the regulation of Akt activity by PI(3,4)P2 and PIP3 in vivo is being revealed by using stimulated live cells. In human platelets stimulated with TRAP, Akt activity correlates with the kinetics of cellular PI(3,4)P2, but not PIP3 [208]. In Swiss 3T3 mouse fibroblasts, oxidative stress induced increased cellular level of PI(3,4)P2, which correlated with Akt activation. In contrast, however, osmotic stress induced increases in both PI(3,4)P2 and PIP3, neither of which correlated with Akt activity [187]. The phosphatase SHIP, which converts PIP3 to PI(3,4)P2, was found to mediate inactivation of Akt [213, 215, 216]; however it remains unclear whether this is due to the phosphatase activity of SHIP or other inhibitory mechanisms mediated via its multiple protein interaction domains [217]. These data suggest that both PI(3,4)2 and PIP3 can influence Akt activity, depending on experimental systems or cellular contexts.

Cellular PI(3,4)2 and PIP3 levels also show differential correlations with Akt phosphorylation at Thr308 versus Ser473. Two studies found that PI(3,4)P2 stimulated or

correlated with Ser473 phosphorylation [213, 218], while PIP3 correlated with Thr308 phosphorylation [218]. This is in contrast to the in vitro findings that PI(3,4)P2 activates PDK1, a Thr308 kinase [206, 207]. These inconsistent relationships observed between PIP3 or PI(3,4)P2 and Akt activation or phosphorylation are correlative in nature. Cellular stimuli may also activate multiple pathways other than those initiated by PIP3 or PI(3,4)P2, which potentially modulate Akt activation or phosphorylation. Ideally, knockdown or overexpression of INPP4 in cells may serve as a better in vivo tool to specifically address the role of PI(3,4)P2 by directly manipulating cellular levels of PI(3,4)P2 while leaving PIP3 unaffected and the potential effects on other signal pathways minimized. Based on INPP4A deficiency in Weeble mouse embryonic fibroblasts (stimulated with EGF) [175] or INPP4B knockdown in human mammary epithelial cells (stimulated with insulin) [174], increased cellular PI(3,4)P2 levels led to enhanced Akt activity and phosphorylation at both Thr308 and Ser473. These data supported the idea that PI(3,4)P2 can promote Akt activation and INPP4 negatively regulates Akt signaling through restricting PI(3,4)P2.

Collectively, the literature suggested that the phosphorylation and activation of Akt are subject to complex regulation. To the currently over simplified, PIP3-dominating dogma, it should be a clear and essential update that not only PIP3 but PI(3,4)P2 can contribute to the regulation of Akt. It is likely that the relative contribution of these lipids to the regulation of Akt may depend on specific cellular signaling contexts. The work in this thesis will address the effect of PI(3,4)P2 depletion in the context of malignant B cells. Future work is needed to uncover how PI(3,4)P2 and PIP3 mediate the spatiotemporal

assembly of specific signaling complexes to exquisitely fine tune Akt activity in a cellular context-dependent manner.

1.20 Sorting nexin 9 (SNX9)

During clathrin-mediated endocytosis (CME), PI(3,4)P2 is produced through phosphorylation of PI(4)P by class II PI3K, PI3K C2α, and controls maturation of late-stage clathrin-coated pits (CCPs) by recruiting PX-BAR domain protein sorting nexin 9 (SNX9) [62]. SNX9 preferentially binds to PI(3,4)P2 with weaker binding to PI(4,5)P2 and PI(3,4,5)P3. INPP4B-mediated depletion of PI(3,4)P2 prevented SNX9 accumulation at CCPs and PI(3,4)P2-binding deficient PX domain mutants of SNX9 were impaired in controlling CME [62]. SNX9 is known to interact with endocytic machinery proteins clathrin, dynamin and N-WASP, but the exact mechanism downstream of SNX9 remains to be determined in the context of PI(3,4)P2-controlled endocytic pathway [219].

1.21 The tandem PH domain-containing proteins (TAPP1 and TAPP2)

1.21.1 Introduction to the TAPPs

The highly homologous TAPP1 and TAPP2 proteins stand out among phosphoinositide-binding proteins as the first and only known proteins that interact specifically with PI(3,4)P2 both in vitro and in vivo, and thus may serve as major

mediators of the cellular processes controlled by this lipid messenger. Our group identified the TAPPs based on their homology to Bam32 [70], while Alessi laboratory independently discovered these proteins through a screen for putative phosphoinositide binding motif-containing PH domains in the EST database [220]. TAPP1 and TAPP2 are broadly expressed in human tissues including the lymphoid tissues [70, 220]. But TAPP2 seems to be more frequently and more abundantly expressed in cancer cell lines [70, 220].

Sequence analysis revealed the modular structures of TAPPs (Figure 1.2) [220, 221], which are primarily characterized by the possession of two sequential PH domains in each protein. Encompassing the two PH domains, the first 300 or so amino acids are overall well conserved between TAPP1 and TAPP2 and across divergent species. A "TAPP conserved region", consisting of about 30 amino acids preceding the N-terminal PH domain is strongly conserved between the TAPPs and among species. However, no known protein domain homologous to this region can be identified from database searching. Thus, this region may confer a unique function conserved in the TAPPs. Of the two PH domains, only the C-terminal one has a phosphoinositide binding motif and shows amino acid sequence homology to the PH domain of Bam32. The C-terminal about 100 amino acids apparently show much less homology except the last 14 residues. The three residues Ser/Thr-Asp-Val at the very end match with a sequence motif for binding by PDZ domain proteins. Although the remaining C-terminal regions are seemingly more variable, there are indeed sequence stretches conserved among species, among which there is a putative SH3-binding motif for TAPP2. Among the domains/motifs described,

the C-terminal PH domain and PDZ binding motif have been experimentally confirmed, with the C-terminal PH domain being the best characterized component of the TAPPs. It is noteworthy that the TAPPs are now quite often referred to as signaling adaptor proteins in that they seem to contain only domains or motifs known to mediate intermolecular interactions without enzymatic or transcription-regulatory activities. However, this may potentially turn out in the future to be misleading since it is not excluded that the N-terminal TAPP-unique region or the distinct sequences intervening between the C-terminal PH domain and the PDZ-binding motif may serve to function as other than adaptor modules.

1.21.2 Specific interaction of TAPPs with PI(3, 4)P2 in vitro and in vivo

While the N-terminal PH domains of the TAPPs failed to interact with any phosphoinositide tested, their C-terminal PH domains were found to specifically and strongly bind to PI(3,4)P2 as shown by in vitro protein-lipid overlay assay and surface plasmon resonance (SPR) measurement coupled with mutations of key conserved amino acid residues in the domains of recombinant TAPP proteins [220]. In a subsequent study, the three dimensional structure of the C-terminal PH domain of TAPP1 was determined, providing the structural mechanism for its specific binding to PI(3,4)P2 [72]. A more recent study [222] quantitatively characterized the binding of a variety of PH domains to mixed vesicles (POPC/POPE/PI(77:20:3)) containing various phosphoinositides by using equilibrium SPR analysis. In agreement with the above observations, the C-terminal PH

domain of TAPP1 bound to PI(3,4)P2 vesicles specifically, 20 times more tightly than to PIP3-containing vesicles.

To gain insights into the role of the TAPPs in vivo, our lab expressed EGFP-tagged TAPP1 or TAPP2 in transfected B cells and examined their subcellular localization in response to immunoreceptor acivation or oxidant treatment using live cell confocal microscopy [69]. Clear re-localization to the plasma membrane was observed in response to these cellular stimuli. TAPP membrane recruitment required PI3K and the 3-phosphoinositide-binding motif in the C-terminal PH domain; however, the kinetics of recruitment were quite distinct from that observed with PIP3-binding PH domain (Btk-PH). TAPP PH domains showed delayed and sustained membrane recruitment that correlated closely with the kinetics of PI(3, 4)P2 production, whereas membrane association of Btk-PH was more rapid and transient, mirroring PIP3 levels [69]. Consistently, Overexpression of INPP4A, which specifically degrades PI(3,4)P2, inhibited recruitment of GFP-tagged TAPP1 PH domain to the plasma membrane [176]. Taken together, the in vitro and in vivo data support each other and indicate that TAPP proteins are specific binding proteins of PI(3,4)P2.

1.21.3 Localization to subcellular compartments other than the plasma membrane?

Recruitment to the plasma membrane by phosphoinositides is known to be the major mechanism by which PH domain proteins play their role in signal transduction. However,

phosphoinositides inside the cell present beyond the plasma membrane may possibly recruit these proteins as well. The first evidence for PI(3,4)P2 presence in membranes other than the plasma membrane was provided by immunostaining using a PI(3,4)P2 monoclonal antibody, which showed generation of PI(3,4)P2 on the nuclear membrane of cells treated with H2O2 or expressing active PI3K [223]. It is likely that TAPP proteins diffusely distributed in the cell have the chance to bind PI(3,4)P2 in these areas. The study by Lucocq and colleagues [224] using an on-section immunoelectron microscopy labeling method found that in cells treated with PI(3,4)P2 agonists, including H2O2 or PDGF, TAPP1 C-terminal PH domain was re-localized to not only the plasma membrane but also endomembranes including the endoplasmic reticulum (ER) and multivesicular bodies (MVBs). It may be an interesting future direction to investigate whether TAPP recruitment to these locations plays any physiological role.

1.21.4 TAPP interacting proteins

Accumulating evidence has indicated that TAPP1 and TAPP2 are physiological binding partners of PI(3,4)P2 and the recruitment of TAPPs by PI(3,4)P2 upon cellular stimulation is subject to various regulatory mechanisms. The major unanswered question is what biological functions TAPPs will perform, and what the role of PI(3,4)P2 binding in these functions is. In our laboratory, a proteomic approach was used to identify TAPP-associated proteins in B lymphocytes as potential components of signaling complex assembled on TAPPs. We also use TAPP over-expression, mutation or gene silencing methods in animal or cell culture systems to examine the phenotypes influenced by manipulation of TAPPs.

A human TAPP2 antibody was used to immunoprecipitate TAPP2-associated proteins from lysates of BCR-stimulated BJAB lymphoma B cells stably expressing TAPP2. Mass spectrometry analysis of these proteins identified 40 potential interaction partners of TAPP2 with high confidence values, including proteins involved in cytoskeletal rearrangement, signal transduction and endocytic trafficking [225]. The TAPP1 binding proteins, MUPP1 and PTPL1, found in HEK293T cells [226, 227], were not identified in our analysis, possibly due to the difference between TAPP1 and TAPP2 or because MUPP1 and PTPL1 proteins were not present in the B cells as we were unable to verify their expression. Among these candidate interaction partners of TAPP2, utrophin and syntrophin have been confirmed by co-immunoprecipitation and Western blot to complex together with TAPP2, while most of the mass spectrometry results remain to be further validated. Consistent with our results, another study found that TAPP1 bound to the PDZ domains of syntrophins and colocalized to PDGF-induced circular ruffles in NIH-3T3 cells [228].

Utrophin is an F-actin-binding protein and a homologue of dystrophin. These are components of the dystrophin glycoprotein complex (DGC), in which they are known to bind with syntrophin [229, 230]. While DGC is found in numerous tissues, its function is not fully understood. Expression of DGC components in lymphocytes has not been previously reported. It was found that TAPP2, utrophin and syntrophin were coexpressed in all human and mouse B cell lines examined and in primary human and mouse B cells. In B cell-derived chronic lymphocytic leukemia (B-CLL) cells, TAPP2 and syntrophin

expression levels were correlated with ZAP-70 [225], a syk family kinase normally expressed in T cells but a known prognostic marker of the more aggressive B-CLL subtype [231].

Other potential interaction partners of TAPP2 include clathrin heavy chains 1 and 2 and clathrin-associated adaptor subunit (AP-2) [225]. The identification of these potential binding partners suggested that TAPPs may regulate receptor internalization via clathrin-coated pits. In support of this idea, there is a candidate sequence motif near the C-terminus of TAPP sequences resembling the consensus clathrin-box binding sequences. However, alternative possibility might exist that clathrin-coated vesicles may transport DGC components along with microtubule network to the membrane sites [230], where DGC is assembled and these clathrin components were indirectly pulled down as DGC associated proteins by TAPP2 antibody. This possibility is also supported by the identification of tubulin complex components and protein transport proteins Sec23A and Sec24C.

1.21.5 Function of TAPPs in B cell adhesion

One known function of DGC is to link the actin cytoskeleton to the extracellular matrix (ECM) [230]. Our lab was therefore interested to test whether TAPP2 regulates B cell adhesion to ECM proteins [225]. A B cell adhesion model was established where BCR engagement induced increase in the adhesion to fibronectin or laminin, and the effect was largely blocked by PI3K inhibitors. It was found that overexpression of wildtype or membrane-targeted TAPP2 led to increased adhesion while expression of C-terminal PH

domain mutant TAPP2 inhibited adhesion. In addition, siRNA knockdown of TAPP2 resulted in reduced adhesion. Interestingly, an siRNA targeting TAPP1 that showed little effect on adhesion on its own led to stronger reduction of adhesion when combined with the TAPP2 siRNA than TAPP2 siRNA alone. As expected, utrophin knockdown also led to decreased adhesion. Together, these results suggest that the TAPP/syntrophin/utrophin complex mediates the BCR-induced adhesion to ECM proteins [225].

One of the remaining questions of this study is what cell surface receptors for fibronectin or laminin link these ECM proteins to the intracellular TAPP2/syntrophin/utrophin complex. Leukocyte adhesion functions are generally mediated by integrins, including the known fibronectin receptors, α4β1 andα5β1 integrins [232]. As for laminin, two main types of receptors have been known: integrins, such as α6β1 [233] and the non-integrin receptor dystroglycan [234]. Although dystroglycan is expressed in a variety of cell types [228, 230], there is no report whether it is expressed in B cells. Antibody blockade [235] or genetic knockdown of these receptors may be applied to establishing their roles in mediating the effect of TAPP2 on adhesion. In addition, colocalization of TAPP2/DGC/ECM receptor-ECM at sites of adhesion could be visualized by immunofluorescence confocal microscopy to further demonstrate the association of these components.

Given the role of TAPPs in B cell adhesion, and the role of 3-phosphoinositides in cell migration, another important question is whether these molecules have any role in B cell migration. This question will be addressed in Chapter 4 of this Thesis.

1.21.6 TAPP proteins mediate inhibitory signaling of PI(3,4)P2 in vivo

The physiological role of TAPP proteins through transducing the PI(3,4)P2 signal has been recently studied using a knock-in mutant mouse strain, $TAPP^{R211L/R211L}TAPP2^{R218L/R218L}$ (TAPP KI) [236, 237]. Critical mutations in the PI(3,4)P2-binding pocket of the C-terminal domains of TAPP proteins abolish their ability to bind PI(3,4)P2 without affecting their normal expression levels [237]. These mice are viable, but show increased whole body insulin sensitivity and glucose uptake into muscle tissues, associated with enhanced insulin-induced Akt activity [237]. Similarly, “overactivation” phenotypes are also seen in B cell development and function [236]. TAPP KI mice display markedly elevated serum antibody levels and in females anti-DNA and anti-nuclear antibodies, associated with IgG deposition in kidneys and glomerulonephritis pathology. Consistent with these phenotypes, B cells from TAPP KI mice are hyperresponsive to antigen receptor stimulation, showing enhanced proliferation, expression of activation marker CD86 and Akt phosphorylation. Together, these recent data suggest an emerging role of the TAPP proteins in negatively regulating cellular activation responses, besides the positive function of TAPP2 in malignant B cell adhesion [225]. A working model of negative signaling through PI(3,4)P2-TAPP coupling was proposed that TAPPs recruit inhibitory signaling molecules such as the phosphatase PTPL1 to sites of PI(3,4)P2 [227, 236]. An alternative mechanism might be that TAPPs restrict the availability of PI(3,4)P2 against other PI(3,4)P2-binding proteins such as Akt. Thus, uncoupling of TAPPs may lead to increased amount of PI(3,4)P2 available to activate Akt.

1.22 Lamellipodin/RAPH1

1.22.1 Molecular structure

Lamellipodin (Lpd), also known as Ras association and pleckstrin homology domains 1 (RAPH1), is a ubiquitously expressed protein that belongs to the MRL family of Ras effector proteins, which includes C. elegans MIG10, mammalian RIAM and Lpd, and Drosophila Pico [71, 238-242]. Lpd was named after its localization at lamellipodia (and filopodia), where it interacts with actin regulatory proteins and controls actin and lamellipodial dynamics [71].

Lpd is a 1250 amino acid protein, with an apparent molecular weight of 200KDa [71]. The first half of the molecule consists of a highly charged N-terminus, followed by a putative coiled-coil motif, a putative Ras association (RA) domain and a PH domain. The second half is characterized by proline-rich sequences with multiple potential binding sites for interacting proteins, including three sites for profilin (actin-binding protein), eight for SH3 domain-containing proteins and six for the N-terminal Ena/VASP homology 1 (EVH1) domain [71] (Figure 1.2).

Lpd was known to recruit the cytoskeletal protein talin and activate integrin [243]. An N-terminal fragment of Lpd (residues 13 – 60) containing an amphipathic helix was found to bind talin, and mutations predicted to disrupt the hydrophobic face of the helix abolished the binding [244]. The binding partner(s) of the RA domain have not been

clearly established in agreement. While direct binding of the Lpd RA domain to Ras (K-Ras) was not detected in yeast two-hybrid or in vitro binding experiments [71], pull-down assays suggested that Lpd binds to activated K-Ras, N-Ras, H-Ras, and R-Ras [245] as well as M-Ras and is required for M-Ras-mediated neuronal dendrite remodeling [246]. The PH domain is proposed to specifically bind to PI(3,4)P2, but not other phosphoinositides (see below). Both the RA and PH domains cooperate to target Lpd to the membrane of growth factor stimulated fibroblasts [71]. Currently, there are no data determining direct binding of Lpd to profilin. The SH3- and EVH1-binding sites are now best known for their functions through interaction with regulators of the actin cytoskeleton.

1.22.2 Lpd is a putative specific PI(3,4)P2-binding protein

The PH domain of Lpd was initially found to bind PI(3,4)P2, but not other phosphoinositides such as PI(3)P and PIP3 in an in vitro lipid overlay assay. The binding was also verified by an ultracentrifugation assay for liposome binding in the same study [71]. Challenging this, another study analyzed the crystal structures of Lpd N-terminal fragments corresponding to the RA-PH domains with or without the coiled-coil region and performed sequence alignments of the Lpd PH domain against known PI-binding PH domains, suggesting that the Lpd PH domain is not highly homologous to the known PI-binding domains [247]. This study also showed that Lpd binds to phosphoinositides with low affinity using an in vitro fluorescence polarization assay. However, studies in live cells are providing further evidence in favor of the idea that Lpd is indeed a PI(3,4)P2-binding protein.

In PDGF-stimulated, profilin1-deficient MDA-MB-231 breast cancer cell line, PI(3,4)P2 (but not PIP3) and Lpd both highly accumulate to the lamellipodial membrane, and treatment with PI3K inhibitor LY294002 or overexpression of GFP-PTEN or GFP-PH-Akt, expected to deplete or sequester 3-phosphoinositides PI(3,4)P2 and PIP3, resulted in dissociation of Lpd from the cell membrane, supporting the possible binding of Lpd to phosphoinositides, probably PI(3,4)P2, in this cellular context [248]. Adhesion of enteropathogenic Escherichia coli (EPEC) to host enteric epithelial cells was found to induce Lpd translocation to F-actin-containing, pedestal-like pseudopod in the host cell beneath the attachment site. The vast majority of enriched phosphoinositide species in the pedestal was found to be PI(3,4)P2 while PI(3,4,5)P3 was rarely seen [249]. Similar correlation between the localization of PI(3,4)P2 and Lpd was seen during the activation of the Slit diaphragm junctional protein Nephrin in podocytes (renal epithelial cells). Nephrin clustering activates PI3K [250-252] and generates PI(3,4)P2 proximal to the Nephrin clusters at the membrane [253]. The Nephrin clusters recruit Lpd in a signaling complex containing SHIP2 and the recruitment of Lpd depends on SHIP2 activity. In these previous studies, PI(3,4)P2 and Lpd both localized to a common location or target (lamellipodial membrane, F-actin pedestal or Nephrin cluster), strongly implying potential interaction.

Taken together, the currently available data dominantly supports the specific binding of Lpd to PI(3,4)P2. The lack of strong homology of Lpd PH domain to known PH domains may instead suggest a new class of phosphoinositide-binding domain. The in vitro

binding assay that failed to find significant binding of Lpd PH domain to phosphoinositides, without showing control experiments based on known PH domain-phosphoinositide interactions, may not have provided favorable conditions that allow the binding of interest to occur. My thesis work will further assess the colocalization of Lpd with PI(3,4)P2 using stringent confocal microscopy analysis in B cell migration context.

1.22.3 Lpd binds to Ena/VASP proteins

The Ena/VASP family of actin-binding proteins (Ena, Mena, VASP and EVL) promote the elongation of F-actin [254]. Lpd uses all its six EVH1 binding sites to interact with the EVH1 domain of Ena/VASP. The interaction between Lpd and Ena/VASP is positively regulated by the tyrosine kinase c-Abl, which phosphorylates Lpd at Y426, Y456 and Y1226 [255]. Lpd-Ena/VASP interaction regulates PDGF-induced dorsal ruffling [255], neuronal morphogenesis [246, 255, 256] and F-actin-dependent EGFR endocytosis [257].

1.22.4 Lpd regulates cell migration via the WAVE complex

Cell migration is primarily driven by F-actin dynamics at the front of the cell, which often displays as a protruding lamellipodium. Among actin regulatory proteins known to regulate cell migration, the WAVE complex is activated by Rac and in turn activates the Arp2/3 complex to generate branched F-actin networks [83, 255, 258-263]. Lpd interacts with the WAVE complex by directly binding to Abi, one of the five protein units of the

complex. This interaction is mediated by the SH3 domain of Abi and three of the SH3 binding sites of Lpd [260]. Lpd was found to be in complex with active Rac [260, 264, 265], which positively regulates the interaction between Lpd and WAVE [260]. Consistent with its interaction with these cell migration regulators, Lpd was found to mediate cell migration in multiple cellular contexts.

Lpd knock-down reversed the increase of migration speed due to loss of profilin1 in the MDA-MB-231 breast cancer cell line [248]. In Lpd KO mouse embryonic fibroblasts (MEFs), the speed and persistence of random migration were reduced [260]. The directional migration of these cells as well as Rat2, a fibroblast cell line, was also impaired in a wound healing assay. In MDA-MB-231 cells, while overexpression of intact Lpd led to enhanced wound healing response, Lpd mutant in all three Abi binding sites inhibited the response. Interestingly, mutations in all Ena/VASP binding sites did not reduce the promoting effect of Lpd on migration, suggesting that the function of Lpd in cell migration depend on its interaction with WAVE but not Ena/VASP. In agreement with this, both Lpd and WAVE promote highly branched F-actin networks characteristic of lamellipodial protrusions in migrating cells. Loss of Lpd disrupts lamellipodia formation, similarly to WAVE knockdown [71, 260, 266-268]. Lpd KD cells display uncondensed disordered F-actin structures devoid of dense meshwork [71, 249]. In contrast, Ena/VASP promotes longer, less branched F-actin structures associated with less stable lamellipodia and its knockdown does not severely impair lamellipodia formation as in Lpd or WAVE knockdown [71, 269].

The in vivo function of Lpd was investigated using knockout (KO) mice. These mice mostly die shortly after birth and surviving mice show reduced body size and no ingestion of milk. Lpd KO mice are especially characterized by missing pigmentation on their ventral side due to defective migration of neural crest (NC)-derived melanoblasts during development. An evolutionarily conserved role of Lpd-WAVE signaling in cell migration was confirmed using cells other than mammalian cells as described above, including Xenopus laevis embryonic NC cells and Drosophila melanogaster ovarian epithelial border cells (The Drosophila orthologue of Lpd is called Pico) [71].

1.22.5 Lpd controls neuronal migration modes through modulating G:F actin ratio

In developing cortex, pyramidal neurons (major type of cortical neurons) originate from the ventricular zone and migrate to superficial layers of the cortex. While they pass through subventricular (SVZ) and intermediate (IZ) zones, regions characterized by tangentially migrating interneurons and axon fiber tracts, pyramidal neurons migrate radially along glial substrate. Lpd depletion casuses failure of pyramidal neurons to reach their proper positions but instead retention in the SVZ and IZ zones. The defect is not underlain by decreased migration speed or increased cell death, but by a switch of migration mode from radial to tangential [270].

In agreement with the role of Lpd in promoting F-actin formation as described above, Lpd depletion in Drosophila, human Hela cell line or mouse cortical neurons leads to

increased ratio of monomeric globular (G) actin to filamentous (F) actin [71, 241, 242, 270]. Elevated level of cellular G actin binds to and inhibit the nuclear import of MAL, the coactivator of serum response factor (SRF), a transcription factor that regulates the expression of cytoskeleton-regulatory genes [270-272]. Consistent with the possibility that Lpd controls the migration mode of pyramidal neurons by maintaining SRF activity through limiting G-actin level, reduction of SRF activity causes shift in neuronal mode as in Lpd depletion, and G-actin sequestering with a G-actin-binding domain of MAL rescues the defects in cell positioning and migration mode resulting from Lpd depletion [270]. In addition to determining neuronal migration path, Lpd also controls cell proliferation through maintaining SRF activity [270]. Future work remains to identify the targets and pathways downstream of SRF that mediate the function of Lpd in these processes.

1.22.6 Negative regulation of the Lpd/WAVE/Rac complex

Lpd is in complex with WAVE [260] and active Rac [260, 264, 265]. Rac enhances the interaction between Lpd and WAVE as well as directly interacts with and stimulates the activity of WAVE [260, 273]. In cooperation with Rac, Lpd regulates cell migration [260] and controls mechanosensing response to extracellular matrix stiffness [274]. A potential negative regulator of the Lpd/WAVE/Rac complex has been identified, known as srGAP3, a Rac-selective GTPase-activating protein (GAP) and member of the Slit-Robo GAP(srGAP) family. It contains an N-terminal F-BAR domain, a central GAP domain and an SH3 domain [264, 275-278]. The F-BAR domain contributes to the localization of srGAP3 to sites of lamellipodia formation [264]. The GAP activity deactivates Rac by

switching it from GTP- to GDP-bound form. The SH3 domain of srGAP3 is known to directly bind the WAVE1 protein (a subunit of the complex WAVE) [277]. Consistent with the interaction between Lpd and WAVE, srGAP3 is in complex with Lpd depending on the SH3 domain of srGAP3 [264]. In PDGF-stimulated NIH3T3 cells, srGAP overexpression abolishes lamellipodia formation and dominantly interferes with the stimulatory effect of Lpd overexpression on actin dynamics at the lamellipodia through both GAP-dependent and -independent mechanisms. Consistently, srGAP3 KO MEFs display increased lamellipodia formation, which can be blocked by Lpd KD. In another cellular context, srGAP3 KD promotes the formation of neurite-like processes in the N1E-115 neuroblastoma cell line, depending on Lpd. The detailed mechanism by which srGAP3 negatively regulates the function of Lpd in promoting lamellipodia has not (yet) been demonstrated. The Lpd effector, WAVE, maybe inhibited through the inactivation of Rac by the GAP activity of srGAP3, whereas active Rac promotes WAVE function both by directly binding to WAVE to release it from an inactive conformation and by enhancing the interaction of Lpd with WAVE. However, srGAP3 may also interfere with the Lpd/WAVE/Rac complex through scaffolding interaction independent of its GAP activity against Rac.

1.23 Rationale, questions, hypotheses and specific aims

1.23.1 Rationale and questions

Apart from the classically dominant role of PIP3, PI(3,4)P2 emerges to lead an important

new branch of the PI3K signaling network. Recent investigations that have started to uncover the involvement of PI(3,4)P2-specific phosphatases and binding proteins in a variety of cellular processes in heath and disease will prompt future efforts in finding new roles of these molecules and mechanisms of their functions. It is also likely to discover additional binding partners specific for PI(3,4)P2. Since a number of classical "PIP3-binding proteins" such as Akt actually bind to PI(3,4)P2 as well, with comparable affinity, it will be particularly interesting to dissect the relative contributions of PI(3,4)P2 versus PIP3 to the functions of these molecules, based on their differential cellular levels, temporal kinetics and spatial distribution in specific cellular processes or contexts. As far as the research interest that prompts this thesis work is concerned, PI3K extensively regulates cell migration, with known involvement of PIP3; however it is a major unanswered question of the field if PI(3,4)P2 is also implicated. Emerging evidence implies that PI(3,4)P2 may contribute to this cellular function as well. Loss of PI(3,4)P2-specific phosphatase INPP4B leads to enhanced wound healing response (a measure of adherent cell migration) in breast cancer cells. The putative PI(3,4)P2-specific binding protein lamellipodin (Lpd) mediates cell migration in multiple cell types. To define the role of PI(3,4)P2 in cell migration, at least a few major questions need to be answered. INPP4B and Lpd are both multi-domain proteins. It is likely that INPP4B may affect migration through potentially scaffolding interaction with other signaling molecules, independently of its phosphatase activity. Similarly, Lpd may possibly mediate migration independently of its PI(3,4)P2-binding domain. Importantly as well, there has been controversial view whether Lpd is indeed a PI(3,4)P2-binding protein. A series of investigations described in this thesis are aimed at answering these questions to

obtain the first clear insights into the role of PI(3,4)P2-related signaling in cell migration. These are performed in the context of malignant B cell migration, with considerations that cell migration plays a central role in the disease progression of B cell cancers, and that no in-depth molecular mechanism has been reported in the field of B cell migration.

1.23.2 Hypotheses

- PI(3,4)P2 leads a new branch of PI3K signaling that regulates malignant B cell migration
- PI(3,4)P2-binding proteins mediate malignant B cell migration

1.23.3 Specific aims

- Set up experimental systems for study of B cell migration mechanisms, an area faced with technical challenges
- Evaluate the effect of net PI(3,4)P2 depletion by its specific phosphatase INPP4A or INPP4B (relative to phosphatase-dead mutants) on malignant B cell migration
- Investigate the roles of (potential) PI(3,4)P2-binding proteins TAPP2, Lpd and Akt in migration

Chapter 2 Materials and Methods

2.1 Cells

Human leukemia or lymphoma B cell lines NALM-6 (DSMZ, Germany), RS4;11 (DSMZ) and RAJI (DSMZ) and bone marrow stromal cell line M2-10B4 (ATCC) were cultured in RPMI1640 (Life Technologies) containing 10% FBS. The bone marrow stromal cell line S17 was obtained from Ken Dorshkind (UCLA) [71] and cultured in Opti-MEM I (Life Technologies) supplemented with 10% FBS. Human embryonic kidney cells (293T) cells were cultured in IMDM with 10% FBS. To isolate primary chronic lymphocytic leukemia (CLL) B cells, peripheral blood samples were obtained from CLL patients or healthy age-matched persons after informed consent in accordance with the Declaration of Helsinki, with approval from the Research Ethics Board at the University of Manitoba. Mononuclear cells were isolated from the buffy coat of CLL patients or healthy donors using a Ficoll-Paque density gradient. For patients with lymphocyte counts of less than 40×10^9cells/L and for control blood donors, B cells were isolated using the RosetteSep B cell enrichment Cocktail (StemCell Technologies) to remove contaminating T cells and monocytes. B-cell purity was determined by staining with fluorescein isothiocyanate–labeled anti-CD20, and was routinely greater than 95% for CLL patients and greater than 85% for controls [225].

2.2 Constructs

Human INPP4A coding sequence was cloned in three different vectors for lentiviral

expression with GFP and/or drug selection reporters: (1) The expression cassette of EGFP-tagged INPP4A, between Ase I and Mlu I sites of the pEGFP-C2-4-phosphatase plasmid (kindly provided by C. Mitchell) [176], was transferred into pCDH-CMV-MCS-EF1-Puro (System Biosciences) between Nhe I and Swa I sites by restriction digestion and ligation. (2) The INPP4A sequence from an Ultimate ORF Gateway donor vector (purchased from Life Technologies) was shuttled into pLenti4/V5-DEST (Life Technologies) by Gateway recombination cloning, following the supplier's protocol. (3) An INPP4A ORF clone based on pLenti-CMV-GFP-2A-Puro vector was made by Applied Biological Materials (Richmond, BC, Canada). To obtain catalytically inactive INPP4A mutants, mutagenesis was performed in these vectors using QuikChange II XL Site-Directed Mutagenesis Kit (Agilent Technologies). The cysteine residue in the conserved catalytic motif CKSAKDR of INPP4A phosphatase domain was mutated into serine. The three pairs of mutant (Mut) versus wild type (WT) INPP4A constructs were all sequencing confirmed. Lentivirus was packaged based on these constructs and used to transduce malignant B cells using methods described below. INPP4A Mut and WT proteins were overexpressed at similar levels in transduced cells. mCherry-tagged membrane-targeted INPP4B WT or catalytically inactive mutant constructs were kindly provided by V. Haucke [62]. In these constructs, INPP4B proteins were fused to a C-terminal CAAX-box prenylation (lipidation) sequence [279]for membrane targeting. These constructs were transfected into cells using the Neon technology (Life Technologies, see below). For TAPP2 knock-down (KD), shRNA specifically targeting human TAPP2 coding sequence (GCUGGAAACGUCGCUUCUUUG) was designed using Block-iT RNAi Designer

(Life Technologies) and cloned into the pSIH1-H1-copGFP vector (Systems Biosciences) using the supplier's protocols. For Lpd KD, a TRC lentiviral (pLKO.1-puro) shRNA clone targeting Lpd coding sequence (GCCAGGACTATCGGAACAAAT) (Thermo Scientific) was used, along with a pLKO.1-puro non-mammalian shRNA control vector (Sigma-Aldrich, SHC002). A second lentiviral shRNA, targeting the 3' UTR region of endogenous Lpd (CAGGTGTCATTAATCTGGTTGTATA) was designed and cloned using the same methods and parental vector as in TAPP2 KD. The empty pSIH1-H1-copGFP was used as control vector for the TAPP2 and Lpd KD constructs. These constructs were packaged into lentivirus for target cell transduction or Neon-transfected into the cells. EGFP-tagged WT or PH domain-deleted human lamellipodin (Lpd-GFP WT or ΔPH), cloned in the expression vector pCAGGS [280], were a kind gift from K. Nakajima [256]. Transfection with these constructs was based on Neon. Plasmids for lentiviral packaging used in this thesis work include: pCMV-dR8.2 dvpr and pCMV-VSV-G [61, 225], kind gifts from Dr. Sam Kung, as well as pCMV-ΔR8.91 and pMD.G [281, 282], kind gifts from Dr. Ferenc Boldizsar. Protein expression or knock-down (KD) based on all the above mentioned constructs was confirmed by Western blot following published procedures [61, 225].

2.3 Antibodies

Table 2.1 List of antibodies

Description	Source	Catalog
Goat anti human INPP4A polyclonal IgG (A-19)	Santa Cruz	sc-12315
Goat anti human INPP4B polyclonal IgG (N-20)	Santa Cruz	sc-12318
Rabbit anti human GAPDH polyclonal IgG	Trevigen	2275-PC-100
Mouse anti PI(3,4)P2 monoclonal IgG3	Echelon Biosciences	Z-P034b
Mouse anti PI(3,4,5)P3 monoclonal IgG1	Echelon Biosciences	Z-P345b
Alexa Fluor 488 Goat Anti-Mouse IgG	Life Technologies	A11029
Alexa Fluor 647 Goat Anti-Mouse IgG	Life Technologies	A21236
PE-labelled monoclonal mouse anti human CXCR4	BD Biosciences	555974
Phospho-Akt (Thr308) polyclonal antibody	Cell Signaling Technology	9275
Phospho-Akt (Ser473) polyclonal antibody	Cell Signaling Technology	9271
Total Akt polyclonal antibody	Cell Signaling Technology	9272
Rabbit anti lamellipodin polyclonal IgG (H-150)	Santa Cruz	sc-68380

2.4 Lentiviral packaging and transduction

Two major factors determine the outcome of a lentiviral packaging experiment. The host 293T cells are required to be at the best viability without any previous adverse culture conditions such as any overgrowth or sign of poor growth. Plasmids are required to be at high concentration (above 1 ug/ul) and free of bacterial endotoxin, salt, or other contaminants such as isopropanol and ethanol, which may result from steps of plasmid preparation.

For lentiviral packaging in 6-well plates, 293T cells are plated at about 25% confluence (around 3-4×10^5 cells) in 2ml 293T complete Media, IMDM (Hyclone SH30228.02) containing 10% FBS and antibiotics) for each well. The confluence of cells is examined every day. When cell growth reaches 90% confluence (around day 3), start transfection as follows:

1) Pre-warm DMEM (Life Technologies 11995) containing 10% FBS **without antibiotic** (transfection media) to 37°C in water bath.
2) Without disturbing cells, gently aspirate old media and carefully add 2 ml/well pre-warmed transfection media. Put plate back to incubator.
3) Dilute DNA as follows and mix well gently:

250 µl	Opti-MEM I reduced serum medium (Life Technologies 31985-062)
3.6 µg	Expression vector (encoding gene or shRNA of interest)
3.6 µg	Packaging vector (pCMV-dR8.2 dvpr or pCMV-ΔR8.91)*
0.48 µg	Envelope vector (pCMV-VSV-G or pMD.G)

* pCMV-ΔR8.91 appears to give slightly higher viral yield than pCMV-dR8.2 dvpr

4) Mix Lipofectamine™ 2000 (Life Technologies 11668-019) before use by gently inverting the tube for 3 times. Dilute 10 µl Lipofectamine™ 2000 in 250 µl of Opti-MEM® I. Incubate for 5 minutes at room temperature. Note: Proceed to Step 6 within 25 minutes.
5) After the 5-minute incubation, combine the diluted DNA with diluted Lipofectamine™ 2000 (total volume = 500 µl). Mix gently and incubate for 20 minutes at room temperature. Note: DNA-lipofectamine complexes are stable for 6 hours at room temperature.
6) Add the 500 µl of complexes to each well containing cells and medium. Mix gently by rocking the plate back and forth.
7) Incubate for 5-6 hours. (Virus will be harvested 48h after the end of this incubation.)
8) Without changing the media, add antibiotic (25ul of 100× Pen Step) and gently mix by rocking the plate back and forth. Put back to incubator. Note: If the DNA-lipid

complex is applied close to the end of the day, antibiotic may be added early next morning.

9) At 48h post-transfection i.e. 48h after the completion of Step 8, collect the culture supernatants into Screw-Cap Microcentrifuge tubes (VWR 89004-306).
10) Spin at 1000 g for 5 minutes at 4°C.
11) Without touching or disturbing pellet, carefully transfer supernatant (lentiviral stock) into new Screw-Cap microcentrifuge tubes at 250 ul/tube.
12) Store the lentiviral stock in - 80°C freezer. Avoid repeated thaw-freeze.

Viral titer is measured according to Kung Lab protocol of Lentiviral titration using 293T cells [283]. Transduction of cells of interest follows the Kung Lab Spin Protocol [284]. Briefly, 5×10^4 B cells were suspended in 250 µl of viral supernatant (or dilutions with IMDM) at multiplicity of infection of 20 in the presence of 8 µg/ml polybrene (Sigma-Aldrich), plated in 24-well plates, and centrifuged at 800 g for 1 hour at room temperature. Viral supernatant was then replaced by B cell culture media. After 1 week, transduced cells were enriched by drug selection or tracked by GFP expression based on the co-reporters encoded in the lentiviral vectors.

Scaling up: The lentiviral packaging experiment can be scaled up to produce a larger volume of lentivirus based on the surface area of different culture vessels. The following example shows the recipe for a 10-cm dish:

1). Transfection is performed on cells placed in 15ml DMEM + 10% FBS without antibiotic.

2). DNA is diluted as follows:

1.5 ml	Opti-MEM I reduced serum medium (Life Technologies 31985-062)
21.6 µg	Expression vector (encoding gene or shRNA of interest)
21.6 µg	Packaging vector (pCMV-dR8.2 dvpr or pCMV-ΔR8.91)
2.88 µg	Envelope vector (pCMV-VSV-G or pMD.G)

3). Lipofectamine 2000 scales up to 60ul, diluted in 1.5 ml Opti-MEM I.

2.5 Plasmid extraction

Plasmid concentration and quality is critical to lentiviral packaging (also to the Neon transfection procedure). Plasmid extraction was performed using QIAGEN plasmid maxi kit (12163) and by largely following the QIAGEN Quick-Start protocol [285]. Some of my modifications that appear to improve plasmid quality were made to the protocol as described below in detail, where the step numbers correspond to those in the supplier's protocol. The original QIAGEN Quick-Start protocol is provided as an appendix in the end of the thesis for quick reference.

Step 1: On day 1 late in the afternoon streak single colonies. On day 2 morning put plate into Fridge (4 °C). On day 2 late afternoon close to 5 pm, pick a fresh single colony and inoculate in 250 ml LB with antibiotic and shake overnight at 37 °C and 250 rpm.

Step 5: Centrifugation was performed at 20,000 g. Try the best to avoid any pellet from contaminating the transferred supernatant (SN). After the first centrifugation, transfer the SN to a new clean tube. Do not repeat centrifugation of the old tube. Try to avoid pellet being transferred (small amount of pellet, if unavoidable on this first transfer, is allowed).

A second spin is always essential. After the second spin and when loading SN onto the equilibrated Qiagen-tip500 at step 7, avoid any pellet from being transferred or included in the Qiagen-tip. If there is pellet into the transferred SN, use 1000 ul tip or plastic Pasteur pipette to remove it while not wasting too much of the SN volume.

Step 6. Install the Quiagen-tip500 (label your plasmid name here) on a clean 50 ml Falcon centrifugation tube in combination with the blue Qiagen ring-like adaptor. Do not install on dirty bacterial culture flasks.

Step 7. Refer to step 5 – avoid any pellet!

Step 8. Use a new 50 ml Falcon tube while discarding the old tube from steps 6 and 7. After the first wash with buffer QC, discard the flow-through and re-use the same tube to do the second wash.

Step 9. Usea new 50 ml tube while discarding the old tube from step 8. Label the plasmid name on the new 50 ml tube, which will receive the eluted DNA!

Step 10. Use room temperature 2-propanol and centrifuge at 20,000 g. Carefully decant SN, keep tube upside down and press (not throw/bump) the tube onto absorbent paper and leave there for 3-5 minutes to remove leftover of SN.

Step 11. Use 50 ml (instead of 5 ml) room temperature 70% ethanol to wash. 5 ml may not be enough to wash away all the isopropanol, salt and other contaminants. Gently add in the 70% ethanol and try to minimize the disturbance on the DNA pellet. Close the cap. Gently tilt and swirl tube to let the wash cover all area of tube including the cap. Spin down at 20,000 g for 15 min. At the end of spin, handle tube gently. Watch where the DNA pellet now is. Carefully and Gently decant the SN while WATCHING the attachment site of the DNA! The DNA may remain where it was, or move slowly with

the flow but will attach somewhere on the tube, either on side wall or bottom. Note sometimes when the DNA pellet remains at bottom careful look is needed to locate it. At the end of decanting SN, still keep tube upside down-tilted, circle label the pellet on outer wall, and then follow the same procedure as in Step 10 to remove leftover of SN. Do not necessarily expect no droplet of SN on tube wall. Seeing few tiny droplets is allowed. These are expected to contain H2O and ethanol, but no/little isopropanol or salt. Air-dry pellet in cell culture hood for 5-10 min with air flow on. Watch the drying process and ensure that the pellet gets dry without visible liquid on, but not over dry with too much extended time of drying. Now add 200 ul sterile deionized H2O to cover the DNA, by adjusting the angle by which the tube is kept the way the H2O stays on and covers the DNA. Leave the H2O on DNA for about 10 minutes. Extremely gently pipette the H2O/DNA solution on spot for 3-5 times to maximize the wash-off of all DNA. Transfer DNA solution to a sterile eppendorf tube.

Additional step: Freeze the DNA at -20 °C freezer overnight or longer time. Thaw and then centrifuge DNA at 12,000 rpm for 5 minutes (benchtop Eppendorf centrifuge). There can be pellet seen at the bottom (perhaps resulting from denatured/insoluble DNA or contaminants?). Transfer DNA SN to a new tube without touching the pellet. The resulting DNA is expected to have minimized contaminants that may affect transfection and lentiviral production.

2.6 Neon Transfection of RAJI and primary CLL B cells

Transfection was performed using the Neon transfection system (Life Technologies) largely based on the supplier’s procedure. We have established optimal transfection

parameters as follows. For RAJI: 2.5 × 10^5 cells, 0.5 µg plasmid, 10 µl R buffer, electroporation of 1100 V, 20 ms and 2 pulses, 0.5 ml plating media in 24 well plates and culture for 36-72 hours. For CLL cells: 1 × 10^6 freshly isolated cells, 2.5 µg plasmid, 10 µl T buffer, electroporation of 2250 V, 20 ms and 1 pulse, 200 µl plating media in 96 well round-bottom plates and culture for 18-24 hours.

2.7 Cell viability assay

Cells were stained with APC-Annexin V antibody (BD Biosciences) and DAPI (Sigma-Aldrich) and analyzed using a BD FACS Canto II flow cytometer, essentially following a previously established protocol [286]. Cell viability was quantified as percentage of DAPI and Annexin V double negative population.

2.8 Analysis of cell proliferation

Cell proliferation was tracked using the Cell Trace™ Violet Cell Proliferation Kit (Life Technologies), according the supplier's protocol. Proliferation was defined as fold dilution of incorporated fluorescent dye resulting from a 3-day culture, and calculated as the starting mean fluorescence intensity (MFI) obtained by flow cytometry divided by the MFI in the end.

2.9 Cell surface CXCR4 staining

Cells were stained with APC mouse anti-human CXCR4 (BD Biosciences). Cell surface

CXCR4 levels were determined by mean fluorescence intensity (MFI) in flow cytometry.

2.10 Transwell chamber chemotaxis assay

Transwell migration assays were performed largely as described [287], based on 24-well Transwell chambers (Corning life Sciences) with polycarbonate inserts with 8 µm pore size for B cell lines RAJI, NALM-6 and RS411 or 5 µm pore size for Neon-transfected primary CLL B cells. 1-2.5×10^5 RAJI cells, 5×10^5 NALM-6 or RS411 cells or 1×10^6 CLL cells were suspended in 100 µl migration media and added to the top chamber. 600 µl of 100 ng/ml SDF-1 (Peprotech) diluted in migration media (RPMI1640 with 0.5% BSA) were used in bottom chambers. After 9-10 hour incubation for RAJI cells or 4-6 hour for the other cell types at 37°C and 5% CO_2, cells that migrated into the bottom chamber as well as input cells were counted by flow cytometry. Cell migration was defined as the percentage of total input cells that migrated. To inhibit PI3K, pan or isoform inhibitors (Selleckchem) GDC-0941 (pan), CAL-101 (Delta), AS-605240 (Gamma) or TGX-221 (Beta) at 2 µM was applied to input cells and both Transwell chambers. Similarly, to inhibit Akt, MK-2206 (100 nM), Triciribine (1 µM) or Perifosine (1 µM) was applied. The drug vehicles are: DMSO for MK-2206 and Triciribine, and H2O for Perifosine. Where indicated, 100 µl of fibronectin (Sigma-Aldrich) or laminin (Sigma-Aldrich), diluted in coating buffer at 10 µg/ml, was used to coat the polycarbonate surface of the Transwell insert at 4°C overnight. The insert was washed twice with RPMI1640 prior to performing migration assay as described above. To quantify random motility, no chemokine was added to the bottom chamber of Transwell.

2.11 Cell Migration in a microfluidic chambers

A previously reported, a “Y” shape microfluidic device design was used for cell migration experiments in this study [288]. The microfluidic channel was coated with fibronectin and blocked with BSA. Cells were loaded into the microfluidic device from the cell loading inlet and allowed to settle in the fibronectin-coated channel. The device was maintained at 37^{o}C by attaching a transparent heater to the back of the coverslide (Thermal-Clear Transparent Heater, Model No. H15227, Minco, MN). After the cells were settled in the channel, medium and chemokine solutions were infused into the device at the total flow rate of 0.2 µl/min to produce a stable chemokine gradient inside the microfluidic channel. The chemokine gradient was confirmed by measuring the fluorescence intensity profile of FITC-Dextran inside the microfluidic channel. Cell migration was recorded by time-lapse microscopy at 6 frames/min for ~45min using a CCD camera (Model No. 370 KL 1044, Optikon, Canada) and a 10X objective. The image acquisition was controlled by NIH ImageJ (v.1.34s). Alternatively, the recording was performed using a CSU-X1M 5000 spinning disc confocal microscope (Carl Zeiss Canada). The cells were imaged at ~3 mm downstream of the “Y” junction where the gradient yields a smooth profile. Movement of individual cells was tracked using ImageJ. Only the cells that migrated within the microscope field were selected and tracked using the “Manual Tracking” plug-in. Following previously established analysis methods, the movement of cells was quantitatively evaluated by (1) the percentage of cells that migrated toward the chemokine gradient; (2) the Chemotactic Index (C.I.), which is the ratio of the displacement of cells toward the chemokine gradient (Δy), to the total migration distance (d) using the equation C.I. = $\Delta y/d$, presented as the average value ±

standard error of the mean (SEM); (3) the average speed (V) calculated as d/Δt and presented as the average value ± SEM of all cells; and (4) statistical analysis of migration angles performed using MATLAB to examine the directionality of the cell movement. Specifically, migration angles (calculated from x-y coordinates at the beginning and the end of the cell tracks) were summarized in a direction plot, which is a rose diagram showing the distribution of angles grouped in defined intervals, with the radius of each wedge indicating cell number.

2.12 Quantification of F-actin or phosphoinositides by flow cytometry

To quantify total cellular F-actin, 10^6 cells were resuspended in 400 µl pre-warmed (37°C) cell migration media (RPMI 1640 + 0.5% BSA) and SDF-1 was added to a final concentration of 100 ng/ml. At the indicated time points post-stimulation, cells were fixed by mixing with 800 ul ice-cold PBS containing 4% paraformaldehyde and incubating on ice for 30 min. After two washes with cold PBS, cells were permeablized with cold PBS containing 1% FBS and 0.1% Trition X-100, and kept on ice for 10 min. Following two washes with cold PBS containing 1% BSA, cells were stained at room temperature with 200 µl of 165 µM Alexa Fluor 647 Phalloidin (Life Technologies) diluted in PBS containing 1% BSA. Cells were washed twice with cold PBS. F-actin level was determined as MFI from flow cytometry analysis. Similar procedures were used to quantify PI(3,4)P2 or PIP3 except the following: Cells were first starved overnight before the assays. Permeabilization was with 0.5% saponin and 1% BSA in PBS (no serum) at

room temperature for 30min. Staining was performed by using a specific PI(3,4)P2 or PIP3 monoclonal antibody (1:200 at room temperature for 1 hour or 4 ^{o}C overnight) and Alexa Fluo 488 or 647-labelled secondary antibody (1:200 at room temperature for 30 minutes) as listed above.

2.13 Intracellular staining for imaging

To visualize the spatial distribution of PI(3,4)P2 and Lpd-GFP WT or Mutant during chemotaxis, RAJI cells migrating up SDF-1 gradient were fixed on the microfluidic device by carefully injecting PBS containing 4% paraformaldehyde into microfluidic channels as soon as detaching the fluidic tubing. Cells were then washed, permeabilized, and stained for PI(3,4)P2 following the above conditions. To image TAPP2, utrophin, F-actin, myosin II and active Rac in NALM-6 cells, Lab-Tek chambered coverglass (Thermo Scientific) were coated with 10 μg/ml fibronectin at 4 °C overnight and washed with RPMI-1640. 1×10^{5} NALM-6 cells were added and incubated for 1-1.5 h to allow adhesion. The supernatant was replaced with 100 ng/ml SDF-1 to stimulate cells for desired time. To fix cells, supernatant was immediately replaced with cold PBS containing 2% paraformaldehyde. Cells were fixed on ice for 30 min on ice. After wash twice with cold PBS, cells were permeabilized with cold PBS containing 1% FBS and 0.1% triton X-100 for 10minutes on ice, followed by wash with cold PBS containing 1% BSA. To examine the localization of utrophin or TAPP2 (relative to F-actin), these proteins were stained largely as previously described [225], using primary antibodies

(rabbit polyclonal IgG) against utrophin (Santa Cruz, H-300) or TAPP2 [225] and Alexa Fluor 647-labelled goat anti-rabbit IgG secondary antibody (Life Technologies). This was followed by F-actin staining with Alexa Fluor 488 phalloidin. To assess the colocalization of utrophin and TAPP2, permeabilized cells were first stained for utrophin using the antibody H-300 and Alexa Fluor 488-labelled goat anti-rabbit IgG (Life Technologies), and then stained for TAPP2 using TAPP2 antibody [289] directly labeled with Alexa Fluor 647. The direct labeling was performed using Alexa Fluor 647 Protein Labeling Kit (Life Technologies) following the supplier's protocol. The localization of myosin II and active Rac was examined in a similar procedure. Myosin II was stained with rabbit anti non-muscle myosin II heavy chain primary antibody (Covance) and Alexa Fluor 488-labelled goat anti-rabbit IgG secondary antibody (Life Technologies). Active Rac was probed with GST-tagged PAK-PBD protein (Cytoskeleton, Inc.) and GST antibody labeled with Alexa Fluor 647 (26H1, Cell signaling Technology) or HiLyte Fluor 647 (AnaSpec). The two GST antibodies showed the same staining patterns, and did not produce nonspecific signal in control staining where GST-tagged PAK-PBD was omitted.

2.14 Confocal microscopy

Z or time series image stacks for PI(3,4)P2 or Lpd-GFPs in RAJI cells were generated by a CSU-X1M 5000 spinning disc confocal microscope (Carl Zeiss Canada). Calculation of Pearson correlation coefficient, 3D image reconstruction and 3D cell anatomy (sectioning) were performed using Zeiss ZEN2012 software. Pseudo color-coding of fluorescent intensity in time series live cell images was done with Image J. Imaging of the subcellular distribution of other molecules was performed using an Olympus IX81/Ultraview LCI

confocal microscope as previously described [225]. Correlation coefficient of subcellular localization was quantified with Ultraview software.

2.15 Rac and Rho activation assays

Active GTPases were pulled down using PAK-PBD-agarose beads (Rac) or Rhotekin-RBD-agarose beads (Rho), according to the manufacturers instructions (EMD Millipore). Western blotting analysis of total and GTP-bound fractions used Rac1 and RhoA/B/C-specific antibodies from EMD Millipore and followed our Lab's previously established protocols [290].

2.16 Leukemic cell migration into bone marrow stromal cell layers (Under-stroma migration)

2×10^5 NALM-6 cells were seeded onto a confluent layer of S17 or M2-10B4 stromal cells cultured in 24-well plates and incubated for 10 hours at 37°C and 5% CO2. The wells were vigorously washed twice with media to remove leukemic cells that had not migrated into the stromal layer. The stromal layer containing migrated B cells was photographed using phase-contrast microscopy. To quantify the migration, the remaining cells after wash were detached with trypsin/EDTA (Life Technologies), immediately washed and resuspended in RPMI1640 with 10% FBS, followed by staining and counting with flow cytometry. NALM-6 cells were distinguished from stromal cells through a combination of size (forward scatter), granularity (side scatter) and CD19 staining with APC mouse anti-human CD19 antibody (BD Biosciences). Under-stroma migration was

defined as the percent of total input cells that migrated. To assess the effect of blocking SDF-1/CXCR4 signaling on this process, NALM-6 cells were pre-incubated for 30 minutes with AMD3100 (Sigma-Aldrich, 10 or 100 μM), SDF-1 (0.1 or 1 μg/ml), pertussis toxin (Sigma-Aldrich, 0.1 or 1 μg/ml) or GDC-0941 (2 μM). This NALM-6 culture was then used to replace the culture supernatant of stromal cells and under-stroma migration was assayed as described above. In lentiviral shRNA transduction experiments, partially transduced NALM6 cell cultures were used and cells recovered from stromal cell layers were further gated as GFP+ or negative. Data were then calculated a percent migration of control or TAPP KD shRNA transduced cells (both GFP+) relative to the GFP negative untransduced NALM-6 population, which provides an internal control.

2.17 Assessment of drug resistance in stromal co-culture

5×10^4 NALM-6 cells were cultured in suspension or cocultured with 50% confluent S17 stromal cells in the presence of 50 μM fludarabine (Sigma-Aldrich) for 3 days. Cells were then collected, stained with APC mouse anti-human CD19 (BD Biosciences) and DAPI and analyzed by flow cytometry. Leukemic cells that survived fludarabine treatment were counted based on DAPI exclusion in combination with their characteristic size and side scatters and expression of human CD19.

2.18 Akt phosphorylation

PI(3,4)P2-depleted cells (INPP4A WT) or control cells (INPP4A Mut) were stimulated with 100 ng/ml SDF-1 for several time points. Akt phosphorylation was quantified in

Western blot as the ratio of the band intensity of Thr308 or Ser473 phospho Akt to that of total Akt [236]. The ratios were all normalized to control cells at “time point 0” (no stimulation). Alternatively, Ser473 phospho Akt was quantified with the InstantOne ELISA kit (eBiosciences) essentially following the supplier’s protocol. An input of 3.75×10^4 RAJI cells/ELISA well was determined to be optimally within the linear range of detection.

Chapter 3 PI(3,4)P2 depletion by INPP4 inhibits malignant B cell migration

This chapter is based on:

(1) Part of a published paper:

Li H, Hou S, Wu X, Nandagopal S, Lin F, Kung S, Marshall AJ. The tandem PH domain-containing protein 2 (TAPP2) regulates chemokine-induced cytoskeletal reorganization and malignant B cell migration. PLOS ONE. 2013;8(2):e57809. PMID: 23460911

(2) Part of a submitted paper:

Li H, Wu X, Hou S, Noh E, Makondo KJ, Du Q, Wilkins JA, Johnston JB, Gibson SB, Lin F and Marshall AJ. Phosphatidylinositol-3,4-bisphosphate and its binding protein lamellipodin regulate chemotaxis of malignant B lymphocytes. Proc Natl Acad Sci U S A. Status: Reviewed by Editorial Board on 2014-10-08 and by Editor on 2014-10-10, and being reviewed by reviewers since 2014-10-10.

3.1 Introduction

Cell migration is central to physiological processes such as amoeba searching for food, embryonic development and immune cell trafficking. However, it also underlies disease processes such as cancer metastasis. Malignant cells, including B lymphocytes (B cells) that form lymphoma or leukemia (among common types of cancer), are generally characterized by their devastating ability of chemotaxis, defined as directional migration towards a chemical attractant. SDF-1 (CXCL12), a chemokine strongly expressed in a variety of organs is a major chemoattractant driving malignant B cell migration into

lymphoid tissues. Despite the increasingly recognized importance of understanding cell migration mechanisms, much remains to be learned about its molecular regulators, especially in cell types where nearly no in-depth signaling mechanism has been revealed, such as B cells.

As reviewed in Chapter 1, the phosphoinositide 3-kinase (PI3K) family of lipid kinases control diverse cellular functions including migration. PI3K generates membrane-bound 3-phosphoinositide lipid messengers, including PI(3,4,5)P3 (PIP3) and PI(3,4)P2, that recruit signaling effectors such as pleckstrin homology (PH) domain-containing proteins. The function of PI3K signaling has most often been attributed to PIP3, with the role of PI(3,4)P2 largely neglected or underestimated. However, emerging evidence is revealing that PI(3,4)P2 directs a new branch of the PI3K pathway that regulates a variety of cellular processes with critical relevance to health and disease. Signaling through PI(3,4)P2 can be negatively regulated by inositol polyphosphate 4-phosphastases (INPP4A and INPP4B), which selectively degrades PI(3,4)P2. While it remains to be determined whether PI(3,4)P2 contributes to cell migration, its potential role has been suggested by the observation, together with some others, that loss of PI(3,4)P2-specific phosphatase INPP4B leads to enhanced wound healing response in breast cancer cells. A major additional question is whether INPP4B may affect migration through scaffolding interactions with other signaling molecules, or through its PI(3,4)P2-phosphatase activity. In this chapter, the net effect of PI(3,4)P2 depletion by wild type INPP4 relative to phosphatase-dead mutant INPP4 is examined, in the context of malignant B cell chemotaxis to SDF-1.

3.2 Results

3.2.1 Malignant B cell migration depends on class I PI3K activity

As a general regulator of cell migration, PI3K was also reported to mediate the migration of malignant B cells from chronic lymphocytic leukemia (CLL) patients [291, 292]. To investigate the potential role of PI(3,4)P2, a PI3K product, in cell migration, the PI3K dependence of malignant B cell migration was first confirmed in this study in order to establish relevant cellular contexts. Several B cell lines including RAJI (derived from human lymphoma) as well as NALM-6 and RS4;11 (derived from human leukemia) migrate to SDF-1 in Transwell assay (Figure 3.1). To test if the migration of these cell lines depends on PI3K, a variety of class I PI3K inhibitors were applied to the migration assay, including GDC-0941 (all isoforms), CAL-101 (delta-selective), AS-605240 (gamma-selective) and TGX-221 (beta-selective). These inhibitors all reduced cell migration to SDF-1 (Figure 3.1), confirming the PI3K-dependence of cell migration in these cells and suggesting that multiple PI3K isoforms are involved.

Figure 3.1

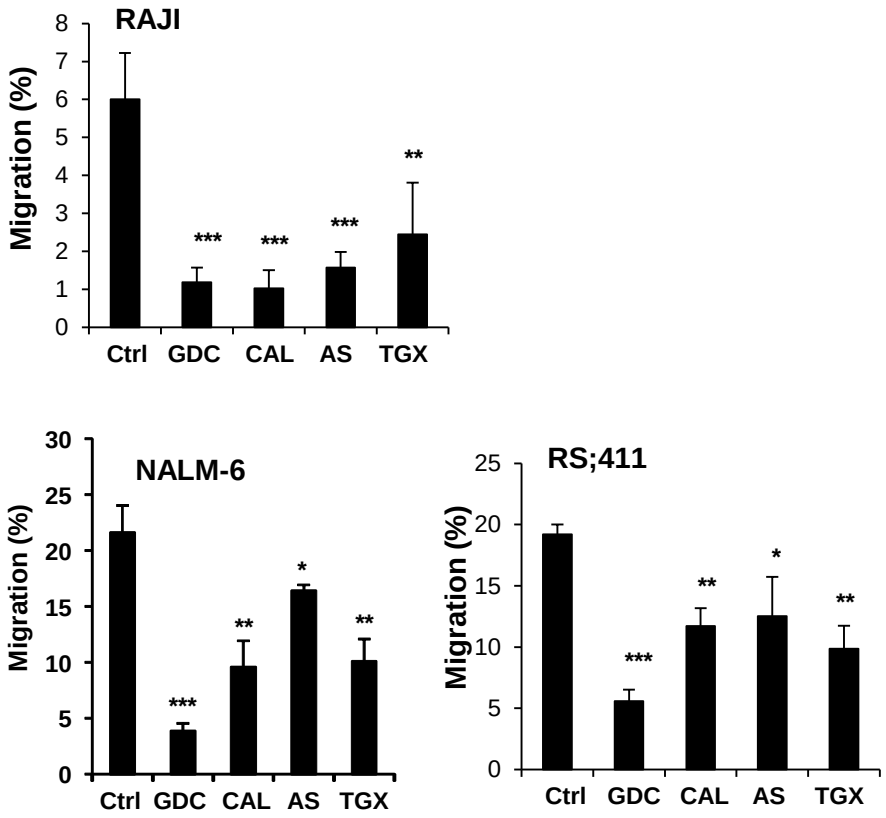

Figure 3.1 Malignant B cell migration depends on PI3K activity

RAJI, NALM-6 or RS4;11 cells were treated with drug vehicle (DMSO) or PI3K inhibitors GDC-0941, CAL-101, AS-605240 or TGX-221 (all 2 μM), and migration to 100 ng/ml SDF-1was assayed in Transwell chambers. Graphs represent the mean ± SD from three independent experiments. All PI3K inhibitors significantly reduced the migration compared to vehicle control according to Student's *t* test: * $p < 0.05$, ** $p < 0.01$ and *** $p < 0.001$.

3.2.2 The presence and distribution of PI(3,4)P2 in malignant B cells during chemotaxis

The presence and distribution of PI(3,4)P2 has not been previously reported in the context of migrating B cells. Here, PI(3,4)P2 was visualized in chemotaxing RAJI cells, a lymphoma B cell line. Cells were allowed to migrate on a fibronectin-coated glass surface in the presence of a stable SDF-1 gradient generated by a microfluidic device [288]. Migrating cells were characterized by a typical migratory morphology with a round cell body followed by a uropod, tail-like structure, and by consistent chemotactic movements up the SDF-1 gradient (Figure 3.2). These cells were fixed during chemotaxis within the microfluidic device and stained using a PI(3,4)P2-specific monoclonal antibody, which has been verified by recent studies [62, 248]. Z-stack images of the stained cells were then taken by confocal microscopy (Figure 3.3). These images were further reconstructed to show the three-dimensional (3D) distribution of PI(3,4)P2 throughout the cell (Video 3.1). PI(3,4)P2 was found to be enriched at the cell membrane in chemotaxing RAJI cells and interestingly, it is not only seen at the front but also on the cell body and at the back. The localization pattern of PI(3,4)P2 appears to be distinct from the classical paradigm that PI3K activity predominantly accumulates at the leading edge, which is generally based on Akt PH probes that recognize both PI(3,4)P2 and PIP3 [293, 294]. However, in further analyses of 3D image reconstructions, “side views”, or vertical cell sections corresponding to the cellular median plane, showed asymmetric distribution of PI(3,4)P2 (Figure 3.4). According to these sections, PI(3,4)P2 was enriched towards the cellular front facing the direction of cell movement. To my

knowledge, this is the first study showing the cellular distribution of a PI3K signal in 3D in a chemotaxing cell, which depends on the major technical advancement made in our lab combining microfluidic migration device and high resolution 3D imaging platforms.

Figure 3.2

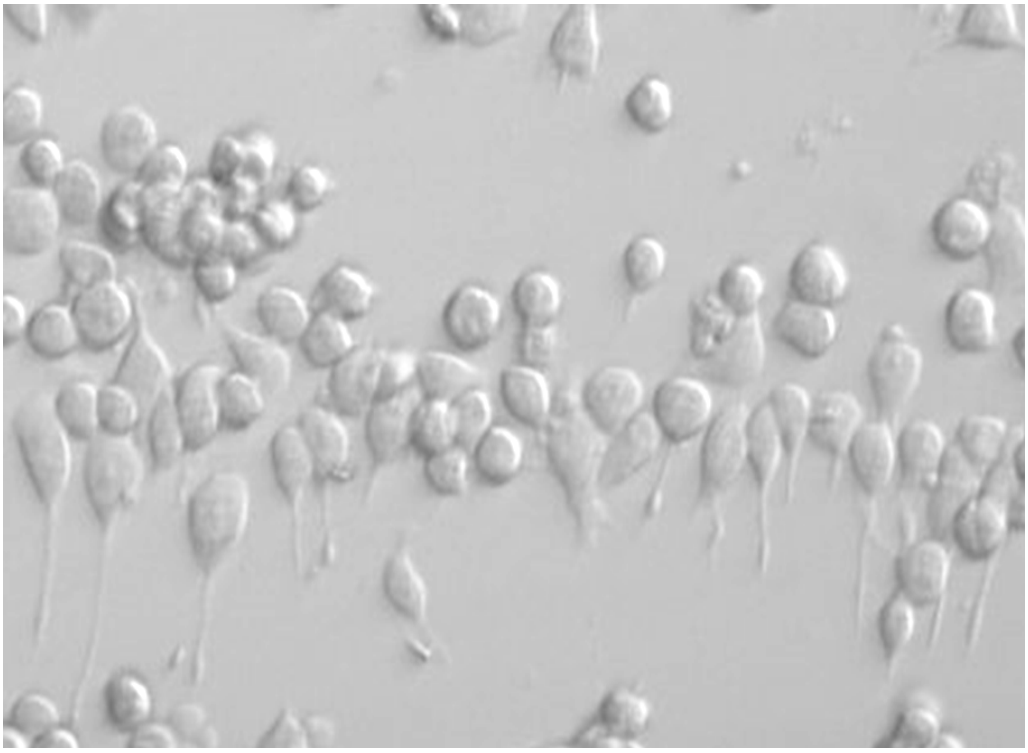

Figure 3.2 Morphology of RAJI malignant B cells during chemotaxis to SDF-1

RAJI cells were allowed to migrate on fibronectin-coated surface in a microfluidic chemotaxis device under a 100 nM SDF-1 gradient (with higher concentration at the top) and visualized by live cell confocal microscopy. Experiments were carried out in collaboration with Xun Wu.

Figure 3.3

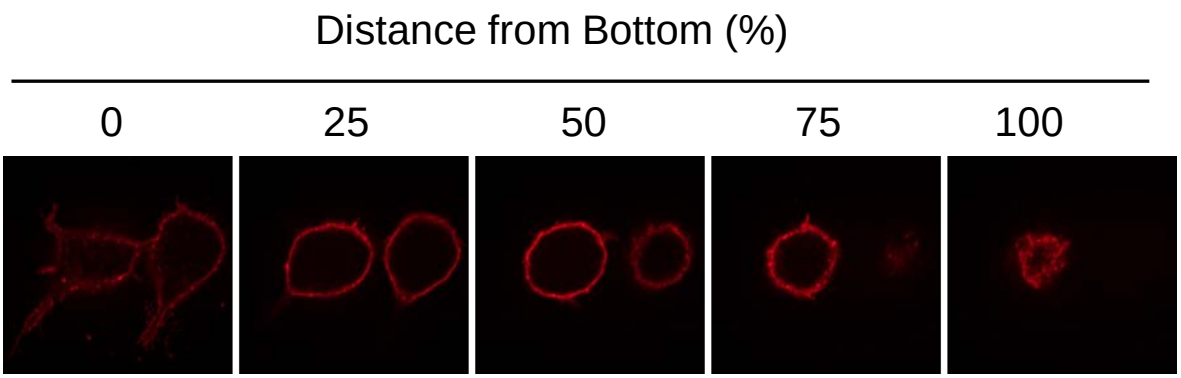

Figure 3.3 The localization of PI(3,4)P2 in chemotaxing cells

Chemotaxing RAJI cells were fixed, intracellularly stained for PI(3,4)P2 and visualized by confocal microscopy (63X). Representative Z stack images are shown. See also Video 3.1 for 3D localization re-constructed based on Z stack images. Experiments were carried out in collaboration with Xun Wu.

Video 3.1 3D distribution of PI(3,4)P2 in chemotaxing RAJI cells

RAJI cells were allowed to migrate on fibronectin coated surface in a microfluidic chemotaxis device that maintains a 100 nM SDF-1 gradient with higher SDF-1 concentration at the top. Cells were fixed, intracellularly stained for PI(3,4)P2 and analyzed by confocal microscopy to acquire Z image stacks. 3D reconstruction of PI(3,4)P2 distribution was performed using ZEN2012 software. Video demonstrates accumulation of PI(3,4)P2 at the cell membrane. Experiments were carried out in collaboration with Xun Wu.

Figure 3.4

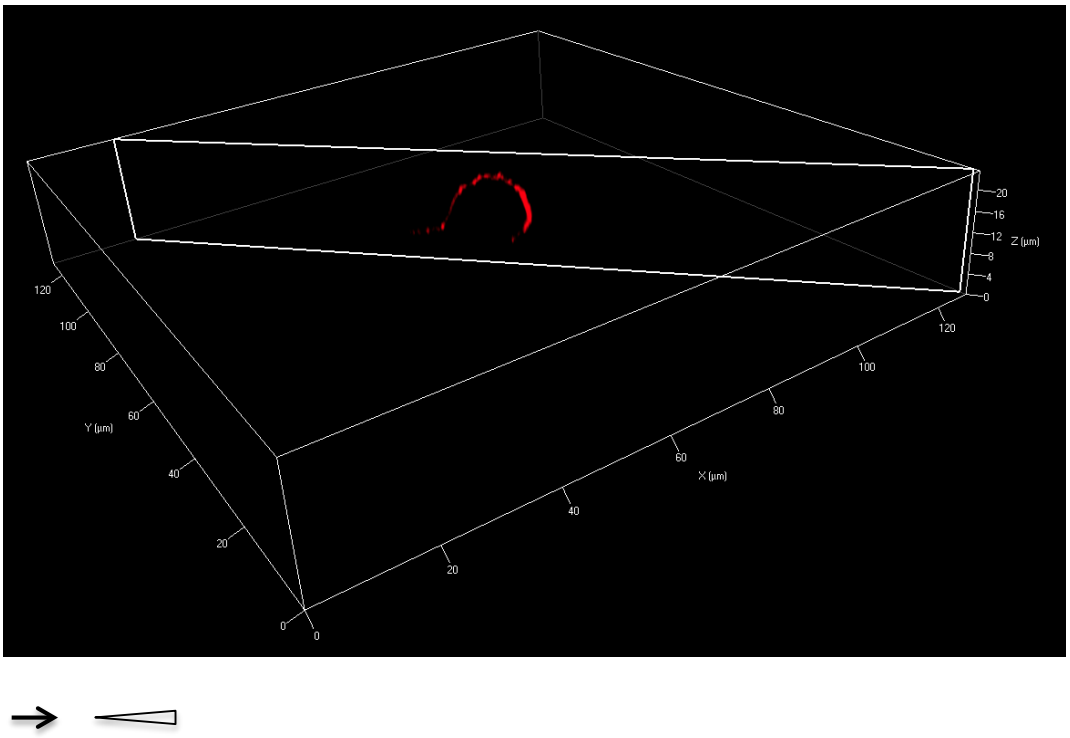

Figure 3.4 Local enrichment of PI(3,4)P2 at the front of chemotaxing cells

3D distribution of PI(3,4)P2 was reconstructed using ZEN2012 software, based on Z stack images of cells migrating under a SDF-1 gradient as in Figure 3.2. Cellular anatomy was then performed using the clipping function of the software. Image shows a cell section corresponding to (or near) the cellular median plane, which runs in the direction of the long axis of the cell and perpendicularly to the matrix surface on which the cell crawls. Arrow and triangle indicate directions of cell movement and SDF-1 gradient, respectively. Localization pattern was consistently observed in 10 out of 10 cells randomly examined. Experiments were carried out in collaboration with Xun Wu.

3.2.3 INPP4 can be stably overexpressed in malignant B cells

As a tool to determine the function of PI(3,4)P2 in malignant B cell migration, I generated or obtained from other labs genetic constructs to overexpress the PI(3,4)P2-specific phosphatases INPP4A or INPP4B. Untagged or GFP-tagged INPP4 genes were cloned in different lentiviral vectors (see Chapter 2 for details) for drug selection or tracking of transduced/transfected cells or microscopic visualization of subcellular localization. These constructs encode either wild-type enzymes or catalytically-inactive versions containing point mutations in the catalytic cysteine in the phosphatase domain. After lentiviral transduction or Neon transfection into RAJI cells, INPP4A and membrane-targeted INPP4B including both wild type (WT) and catalytically inactive mutant (Mut) proteins were expressed at high levels (Figure 3.5).

Figure 3.5

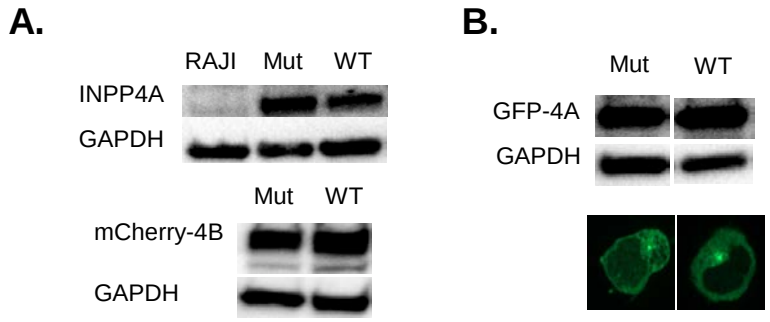

Figure 3.5 Overexpression of INPP4 proteins in RAJI cells

A. Western blots confirming protein overexpression of INPP4A (top) or mCherry-tagged, membrane-targeted INPP4B (bottom) in RAJI cells through lentiviral transduction or Neon transfection. Mut, catalytically inactive mutant; WT, wild type. Note that in the INPP4B blot, lower bands below mCherry-INPP4Bs represent endogenous INPP4B. **B.** Overexpression of EGFP-tagged INPP4A proteins in RAJI cells was shown by Western blot (top) or confocal microscopy (bottom). Western blots were performed in collaboration with Sen Hou.

3.2.4 INPP4 overexpression depletes PI(3,4)P2, but not PIP3 in malignant B cells

PI(3,4)P2 depletion by INPP4 WT relative to Mut control was confirmed by flow cytometry analysis of PI(3,4)P2 staining (Figure 3.6A and B) using the specific PI(3,4)P2 antibody [62, 248]. Similar quantification indicated that cellular PI(3,4,5)P3 levels were not altered along with PI(3,4)P2 depletion (Fig. 3.6C).

Figure 3.6

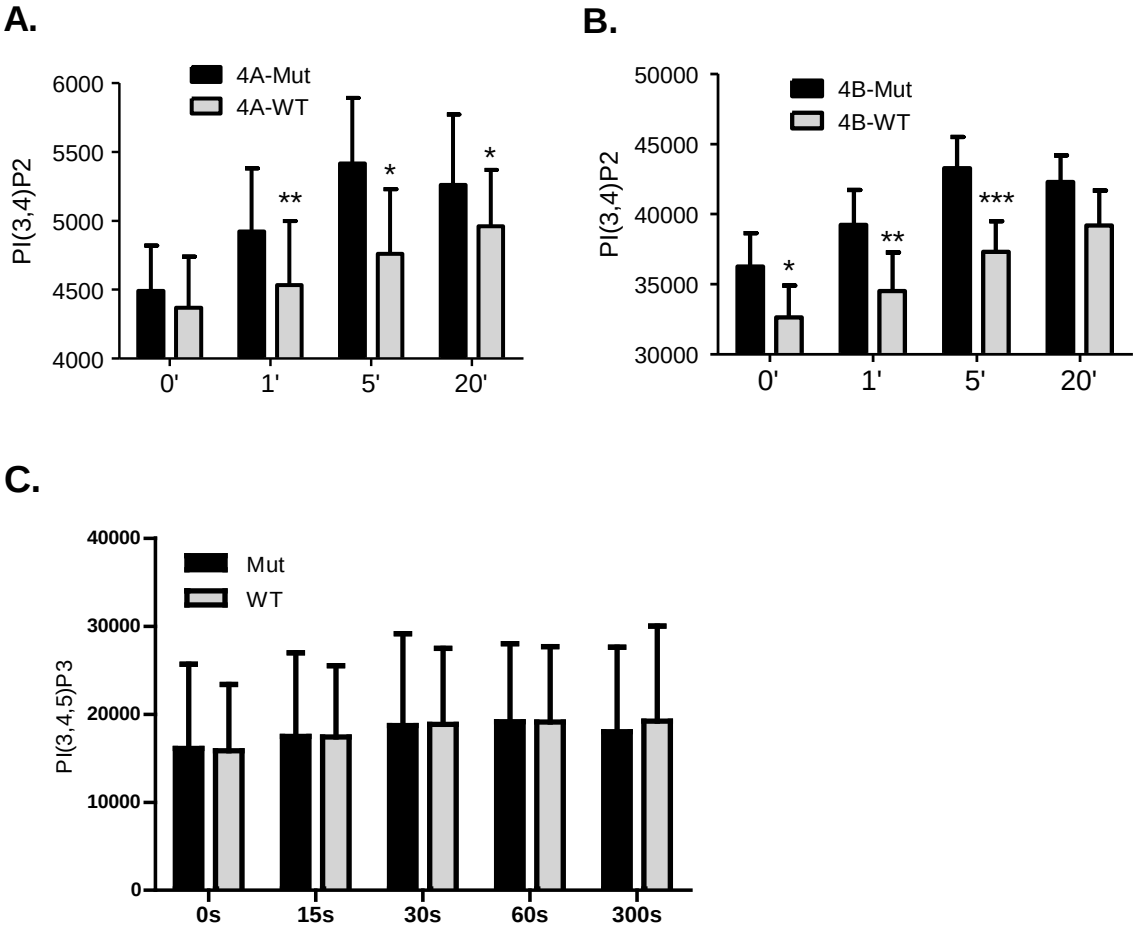

Figure 3.6 INPP4 overexpression depletes PI(3,4)P2, but not PIP3 in malignant B cells

A and B. INPP4 expression inhibits PI(3,4)P2 accumulation. Phosphatase-dead (Mut) or WT INPP4-overexpressing RAJI cells were serum-starved, not stimulated ("time point 0") or stimulated with 100 ng/ml SDF-1 for the indicated time points and intracellularly stained for PI(3,4)P2. Cellular PI(3,4)P2 levels were determined by mean fluorescence intensity (MFI, Alexa Fluo 488 and 647 for INPP4A and B, respectively) using flow cytometry. Graphs represent mean ± SD from four (INPP4A) or five (INPP4B) experiments. Both WT INPP4s significantly reduced PI(3,4)P2 compared to Mut controls according to Student's *t* test (paired): * $p < 0.05$, ** $p < 0.01$ and *** $p < 0.001$. **C.** INPP4 overexpression does not inhibit PI(3,4,5)P3. INPP4A Mut or WT cells were similarly treated as in A and B, and stained by a PI(3,4,5)P3 antibody. Cellular PI(3,4,5)P3 levels were determined by MFI (Alexa Fluo 488) in flow cytometry. Bars represent mean ± SD from four independent experiments. No significant difference in PI(3,4,5)P3 levels were found by Student's paired t test.

3.2.5 PI(3,4)P2 depletion in malignant B cells does not affect cell viability

Cell viability was quantified in RAJI cells overexpressing INPP4A Mut or WT based on staining for Annexin V (apoptotic marker) and with DAPI (dead and permeable cell marker) (Figure 3.7), indicating no difference in cell viability.

Figure 3.7

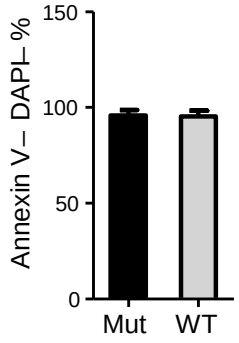

Figure 3.7 PI(3,4)P2 inhibition does not significantly affect cell viability

INPP4A Mut or WT cells were stained for Annexin V and with DAPI and analyzed by flow cytometry. Percentages (mean ± SD) of viable cells (Annexin V and DAPI double negative) from three independent experiments are shown. Student's *t* test found no significant difference in cell viability.

3.2.6 PI(3,4)P2 depletion led to reduced surface expression of CXCR4

I examined expression of the SDF-1 receptor CXCR4 on the surface of transfected RAJI cells using flow cytometry. Cells expressing wild type INPP4A showed a 20% reduction in mean fluorescence intensity after staining with anti-CXCR4, suggesting that PI(3,4)P2 depletion was associated with a reduction in cell surface expression of CXCR4 (Figure 3.8).

Figure 3.8

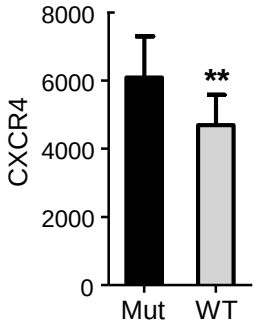

Figure 3.8 PI(3,4)P2 inhibition leads to reduced CXCR4 expression

INPP4A Mut or WT cells were stained for cell surface CXCR4 and analyzed by flow cytometry. MFIs from four independent experiments are shown as mean ± SD. INPP4A WT cells have reduced CXCR4 expression relative to Mut cells, as indicated by Student's *t* test (paired): ** $p < 0.01$. The effect does not arise from any effect of PI(3,4)P2 depletion on cell size, as no significant difference in the mean forward scatters (FSCs, a parameter that indicates cell size) is observed (data not shown).

3.2.7 PI(3,4)P2 depletion inhibits malignant B cell migration

The potential function of PI(3,4)P2 in malignant B cell migration was tested in both RAJI lymphoma B cells and leukemic B cells from chronic lymphocytic leukemia (CLL) patients. Transwell migration assays demonstrated that PI(3,4)P2 depletion by INPP4 inhibited migration to SDF-1 by over 80% in RAJI cells and 20-50% in CLL cells (Figure 3.9), providing the first direct evidence that PI(3,4)P2 is an important regulator of cell migration.

Figure 3.9

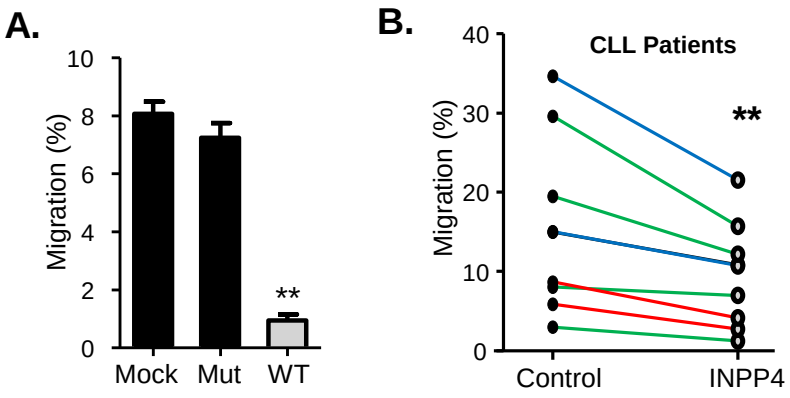

Figure 3.9 PI(3,4)P2 depletion inhibits malignant B cell migration

A. PI(3,4)P2 depletion impairs migration to SDF-1 in RAJI cells. Mock-treated cells or INPP4A Mut or WT cells were assayed for Tranwell migration to 100 ng/ml SDF-1. Data from one experiment performed in replicates were shown as mean ± SD, representing four independent experiments confirming migration inhibition by PI(3,4)P2 depletion. Significant decrease in cell migration was found in WT cells compared to either mock or Mut cells by Student's *t* test: ** $p < 0.01$. **B.** PI(3,4)P2 depletion inhibits the migration of primary leukemic B cells. Chronic lymphocytic leukemia (CLL) B cells freshly isolated from patients were transfected with control (empty vector or INPP4 Mut) or INPP4 WT vectors co-expressing a GFP reporter and assayed for Tranwell migration to SDF-1 based on GFP+ populations. The migration mean values are plotted for each patient. Colors of connecting lines indicate transfection vector types: Blue, empty vector vs INPP4A WT; Green, INPP4A Mut vs WT; Red, INPP4B Mut vs WT. Migration inhibition in INPP4 WT cells relative to control cells were confirmed by Student's *t* test (paired): ** $p < 0.01$. Patient blood samples were obtained through collaborative work with the

Manitoba CLL bank and James Johnston and Spencer Gibson Laboratories, University of Manitoba. CLL B cells were isolated by Sandrine Lafarge.

3.2.8 PI(3,4)P2 controls both the speed and directionality of malignant B cell chemotaxis

To further characterize the role of PI(3,4)P2 in controlling the migratory behaviors of individual cells, real time microscopic tracking was performed in a microfluidic chemotaxis system [61, 288], where control (INPP4A Mut) or PI(3,4)P2-depleted (INPP4A WT) RAJI cells were allowed to migrate on matrix protein fibronectin-coated surface in the presence of a stable SDF-1 gradient (Figure 3.10A, Video 3.2 and Video 3.3). Control cells were characterized by a typical migratory morphology with a round cell body followed by a uropod, tail-like structure, and by consistent chemotactic movements up the SDF-1 gradient (Video 3.2). In contrast, PI(3,4)P2-depleted cells frequently extend protrusions at random directions and their movements appeared less active overall and less chemotactic (Video 3.3). The cell migration paths over time were tracked (Figure 3.10A and B) and quantitative analysis of the cell tracks determined that PI(3,4)P2 depletion led to reduced percentage of migrating cells (with migration of at least one cell length), as well as reduced migration speed and chemotactic index (Figure 3.10B-C). These results indicate that PI(3,4)P2 controls both motility and directionality.

Figure 3.10

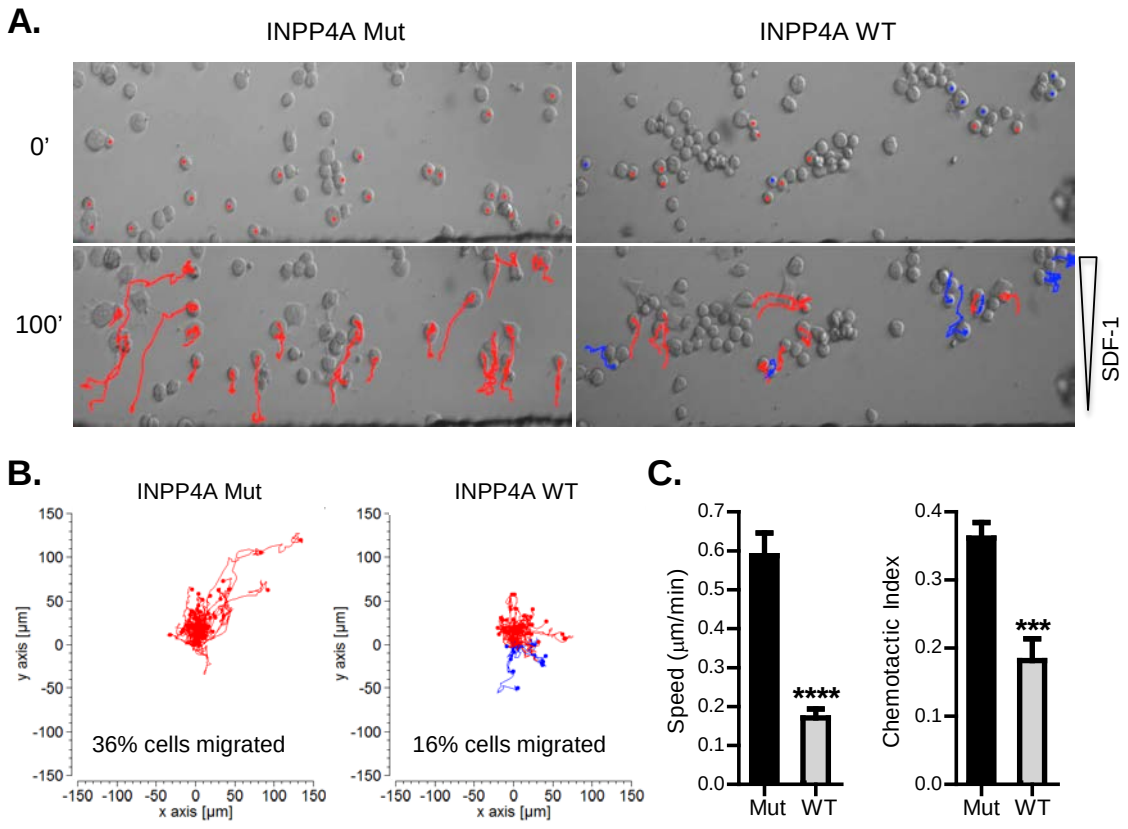

Figure 3.10 Characteristics of migration defects in PI(3,4)P2 depleted cells

A. INPP4A Mut or WT RAJI cells were allowed to migrate in a microfluidic chemotaxis device under a 100 nM SDF-1 gradient (direction of gradient represented with a triangle). Cell movements were recorded using time-lapse imaging and tracked using ImageJ software. The figure shows the first and last images from a representative experiment, with migrating cell tracks marked in red (migration toward SDF-1) or blue (migration away from SDF-1). **B.** Migration tracks were normalized to a common origin (0, 0) in 2D plots. Solid circles label the end of migration tracks. **C.** Migration speed and chemotactic index were calculated as described in Methods. Data represent the mean and

SEM of 204 INPP4A Mut cells and 318 WT cells from two independent experiments. Significant differences in these parameters between Mut and WT were confirmed by Student's *t* test: **** $p < 0.0001$ and *** $p < 0.001$. See also Videos 3.2 and 3.3 for direct view of cells in motion. Experiments were carried out in collaboration with Xun Wu.

Videos 3.2 and 3.3 PI(3,4)P2-depletion leads to impaired speed and directionality

Video 3.2 The chemotaxis of INPP4A Mut cells

Cells were loaded onto a microfluidic chemotaxis device that maintains a 100 nM SDF-1 gradient with higher SDF-1 concentration at the top. Time lapse images were converted to video using Image J.

Video 3.3 The chemotaxis of INPP4A WT cells

Video was generated under the same conditions as Video 3.2. Experiments for Videos 3.2 and 3.3 were performed in collaboration with Xun Wu.

3.3 Discussion

Despite its important role in diverse cellular functions, including cell migration, the PI3K signal pathway has been only partially perceived, with much limited knowledge about the biology of PI(3,4)P2 compared to PIP3. A few recent studies uncoupled the interaction between PI(3,4)P2 and its binding proteins or performed loss-of-function of PI(3,4)P2 using the PI(3,4)P2-specific phosphatase INPP4B [62, 236, 237, 256]. Based on these studies, PI(3,4)P2 was proposed to regulate B cell activation and autoantibody production, insulin sensitivity, neuronal morphology dynamics and endocytosis.

Deciphering how cancer cells migrate is a major challenge but has important potential to guide development of new therapeutics. SDF-1 dependent migration is known to be critical for pathogenesis of many leukemias and lymphomas [18, 19] and drugs targeting the SDF-1 receptor are in development and clinical trials [20, 21]. In the field of cell migration research, it is an interesting unanswered question if PI(3,4)P2 is involved in the regulation of this critical cellular function.

In this study, overexpression of the PI(3,4)P2-specific phosphatases INPP4A or INPP4B was intended as a genetic tool to shut down PI(3,4)P2 signaling. However, since overexpression of INPP4 proteins was not performed in B cells by previous studies, the question is first raised whether INPP4 proteins can be stably overexpressed in B cells considering their potential degradation by the proteinase Calpain via the INPP4 PEST sequence and the possibility that a threshold cellular PI(3,4)P2 level may be critical for cell survival. It was successfully confirmed that INPP4A and membrane-targeted INPP4B

including both wild type (WT) and catalytically inactive mutant (Mut) proteins were able to be overexpressed in RAJI cells, through lentiviral transduction or Neon transfection. Using this tool, PI(3,4)P2 is found to be a critical regulator of migratory pathways in chemotaxing malignant B cells impacting on both migration directionality and motility. Our results, extending previous findings, provide strong direct support that PI(3,4)P2, as a functional messenger, controls a new branch of the PI3K signaling network, impacting on important cellular functions.

Chapter 4 TAPP2 mediates malignant B cell migration

This chapter is in part based on:

Li H, Hou S, Wu X, Nandagopal S, Lin F, Kung S, Marshall AJ. The tandem PH domain-containing protein 2 (TAPP2) regulates chemokine-induced cytoskeletal reorganization and malignant B cell migration. PLOS ONE. 2013;8(2):e57809. PMID: 23460911

4.1 Introduction

The observation as described in Chapter 3 that PI(3,4)P2 signaling is important for malignant B cell migration prompted further steps in identifying downstream effectors of PI(3,4)P2. As a major defined mechanism, phosphoinositides transduce signals through recruiting PH domain-containing proteins [58, 69]. The tandem PH domain-containing proteins (TAPP1 and TAPP2) are best known as the only authenticated specific PI(3,4)P2-binding proteins so far [70, 220, 236]. Several findings imply that TAPP2 may mediate malignant B cell migration as a specific effector of the PI3K-PI(3,4)P2 signaling branch. Previously we found that TAPP2 was predominantly expressed in a more clinically aggressive ZAP-70+ subset of chronic lymphocytic leukemia (CLL) B cells [225, 295], known to be highly migratory in nature [296]. Our study also indicated that in lymphoma and leukemia B cells TAPP2 complexes with components of the dystrophin/utrophin glycoprotein complex (DGC) [225]. Whereas little is known about the functions of the DGC in B cells, it was shown to regulate cell migration in other cell types [234]. Here we provide evidence that TAPP2 controls the migration of leukemia

and lymphoma B cell lines in several distinct models dependent on SDF-1. TAPP2 knock-down (KD) impacted on the organization and polarity of the actin cytoskeleton and the activation of Rac1, a key regulator of the actin cytoskeleton and cell migration [44, 297]. Interestingly, however, TAPP2 co-localizes with utrophin at the sides and rear of migrating cells and functions in migration even under conditions where PI3K signaling is inhibited. Our results provide the first evidence that TAPP proteins function in cell migration and provide initial insights regarding the role of TAPP2 in cytoskeletal reorganization.

4.2 Results

4.2.1 TAPP2 knock-down impairs SDF-1-dependent migration

The potential function of TAPP2 in cell migration was assessed in B cell lines NALM-6, RS4;11 and RAJI (human lymphoma), which migrate to SDF-1 in Transwell assay in a PI3K-dependent manner (Figure 3.1). TAPP2 protein knockdown (KD) significantly inhibited migration in these cells (Figure 4.1A and B), providing the first direct evidence that TAPP2 plays a role in cell migration. TAPP2 KD cells consistently displayed impaired migration on polycarbonate transwell membranes with or without fibronectin or laminin coating (Figure 4.1A).

Figure 4.1

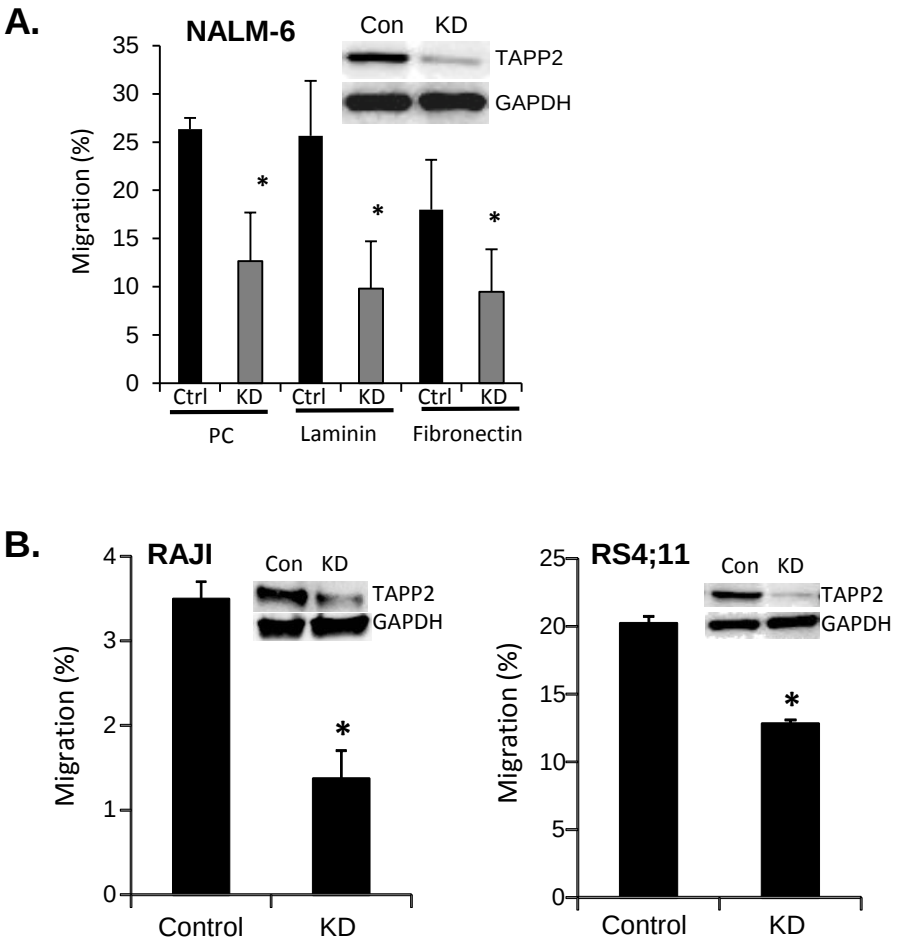

Figure 4.1 TAPP2 knockdown impairs SDF-1-dependent migration

A. TAPP2 knockdown (KD) inhibits NALM-6 migration on a variety of substrata. NALM-6 cells were transduced with control pSIH1-H1-copGFP lentivirus (Con) or virus expressing human TAPP2-targeting shRNA (KD). Western blot represents one of four batches of transduction confirming TAPP2 KD. Transwell assays of migration to 100 ng/ml SDF-1 were performed, where the insert (polycarbonate) was either not coated (-) or coated with 10 μg/ml laminin or fibronectin. Results of three independent experiments are shown as mean ± SD. Significance comparing control versus KD cell migration was

calculated for each coating condition using Student's *t* test: * $p < 0.05$. Note the effect of TAPP2 KD on migration in uncoated transwell chambers has been reproduced in 5 additional experiments. **B.** TAPP2 KD inhibits the migration of RAJI and RS4;11 cells. TAPP2 KD and chemotaxis assay (on bare polycarbonate surface of Transwell inserts) was performed in these cells using the same methods as in A. Western blots are representative of two independent batches of transduction with TAPP2 shRNA expressing lentivirus. Results from one experiment are shown as mean ± SD of replicates, representing three independent experiments confirming migration inhibition by TAPP2 KD. Significance was determined with Student's *t* test: * $p < 0.05$. Western blots are carried out in collaboration with Sen Hou.

4.2.2 The effect of TAPP2 KD on SDF-1-induced migration or random motility in the presence of PI3K inhibitors

Since TAPP2 is considered a PI3K-regulated adaptor protein, it is reasoned that the effect of TAPP2 KD would depend on PI3K activity and thus TAPP2 KD would have no further effect when PI3K activity is inhibited. To test this hypothesis, the effect of combined PI3K inhibition and TAPP2 KD on SDF-1-induced migration was determined. Strikingly, while PI3K inhibitors only partially blocked migration, TAPP2 KD in combination with PI3K inhibitor treatments nearly abolished the migration response (Figure 4.2), suggesting that TAPP2 might contribute some functions independent of the PI3K pathway. Basal migration in the transwell assay, seen without chemokine addition, was also sensitive to PI3K inhibitors and was reduced in TAPP KD cells; however in this case no additional reduction was observed with combined treatment (Figure 4.3). Together these results indicate that TAPP2 functions in malignant B cell migration, potentially via both PI3K dependent and independent mechanisms.

Figure 4.2

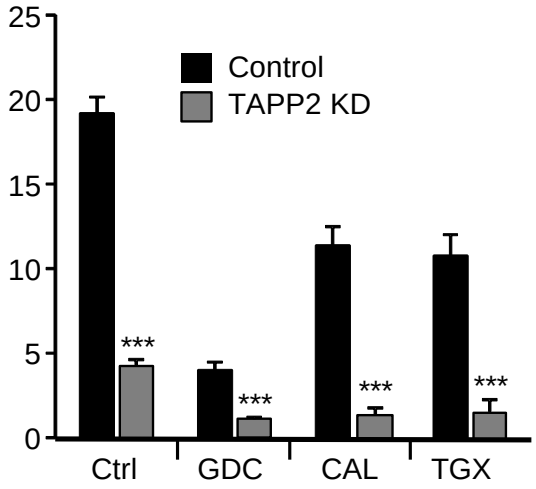

Figure 4.2 TAPP2 KD inhibits SDF-1-induced migration in combination with PI3K inhibitors

Control or TAPP2 KD NALM-6 cells were assayed for migration to SDF-1 in the presence of vehicle (DMSO) or PI3K inhibitors (2 μM) GDC-0941, CAL-101 or TGX-221. Results are mean ± SD of migration % from three independent experiments. Significance of difference in migration was confirmed by Student's t test: *** $p < 0.001$.

Figure 4.3

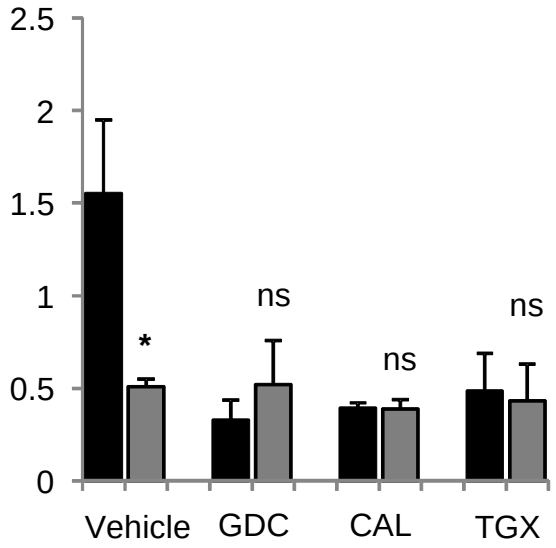

Figure 4.3 PI3K inhibitors and TAPP2 KD reduce basal motility of NALM-6 cells

Control or TAPP2 KD NALM-6 cells were assayed for Transwell migration without chemokine induction in the presence of vehicle (DMSO) or PI3K inhibitors (2 μM) GDC-0941, CAL-101 or TGX-221. Results are mean ± SD of migration % from three independent experiments. Significant difference in migration between control and KD cells under each assay condition using the vehicle or an individual inhibitor was quantified by Student *t* test: * $p < 0.05$; ns, not significant.

4.2.3 The effect of TAPP2 KD on migration does not appear to be indirect through impacting on other cellular functions

I asked whether TAPP2 KD impacts on migration directly through disrupting the cellular migration machineries or indirectly through repressing other major cellular functions. In addressing this question, TAPP2 KD was not found to have significant effect on cell viability, as demonstrated by Annexin V-DAPI staining, or on cell proliferation, as indicated by dilutions of incorporated fluorescent dye during cell divisions. In addition, there was no significant change in the cell surface expression level of CXCR4, receptor for SDF-1, in TAPP2 KD cells, based on flow cytometry analysis of cell surface CXCR4 staining. (Figure 4.4).

Figure 4.4

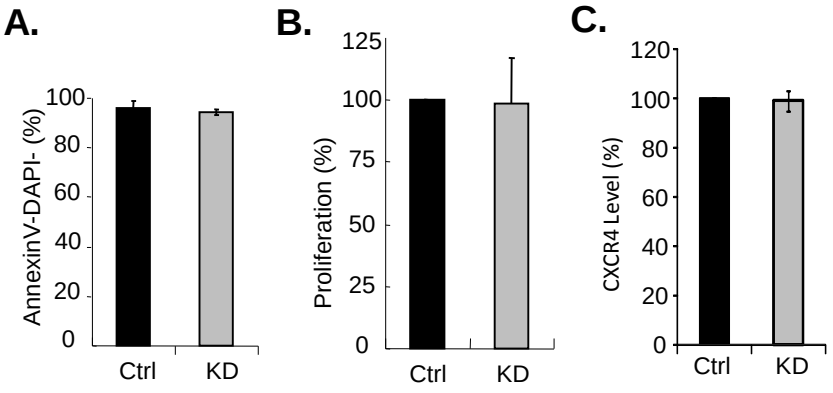

Figure 4.4 Effect of TAPP2 KD on cell survival, proliferation and CXCR4 expression

A. TAPP2 KD does not significantly affect cell viability. Control or TAPP2 KD NALM-6 cells were stained for Annexin V and with DAPI and analyzed by flow

cytometry. Percentages (mean ± SD) of viable cells (Annexin V and DAPI double negative) from four independent experiments are shown. Student *t* test found no significant difference in cell viability. **B.** TAPP2 KD does not significantly affect cell proliferation. Proliferation of Control or TAPP2 KD NALM-6 cells was measured by tracking the dilution of an incorporated fluorescent dye as a result of cell divisions along a 3-day culture. Proliferation, or fold dilution of dye, was calculated as the starting mean fluorescence intensity (MFI) obtained by flow cytometry divided by the MFI in the end, and was expressed as percentage relative to the control. Bars represent mean ± SD of two independent experiments. Student *t* test detected no significant difference in proliferation. **C.** TAPP2 KD does not significantly affect surface expression of CXCR4. Cells were stained for surface CXCR4 and analyzed by flow cytometry. CXCR4 levels were expressed as percentage of mean fluorescence intensity (MFI) relative to control cells. Bars represent mean ± SD of two independent experiments. No significant difference was found by Student's *t* test.

4.2.4 TAPP2 knockdown impairs the speed and directionality of chemotaxis

To further characterize the role of TAPP2 in controlling migratory behavior of malignant B cells, we performed microscopic cell tracking in the presence of a stable chemokine gradient established using microfluidic chambers [288]. TAPP2 KD or control cells were placed in fibronectin-coated chambers and cell movement was recorded for 1-4 hours (Figure 4.5, videos 4.1 and 4.2). Cell tracks were analyzed to determine the percentage of migrating cells, the migration directionality (chemotactic index) and speed. After 1 hour in the chamber, 55% of control cells migrated at least one cell length, whereas only 17% TAPP2 KD cells migrated (Figure 4.5B). By 4 hours, significantly more TAPP KD cells had migrated (30% versus 52% of control cells; Figure 4.5C). However TAPP2 KD cells exhibited significantly reduced migration speed and directionality over this time period (Figure 4.5D and E), indicating that both gradient sensing and motility functions are impaired.

Figure 4.5

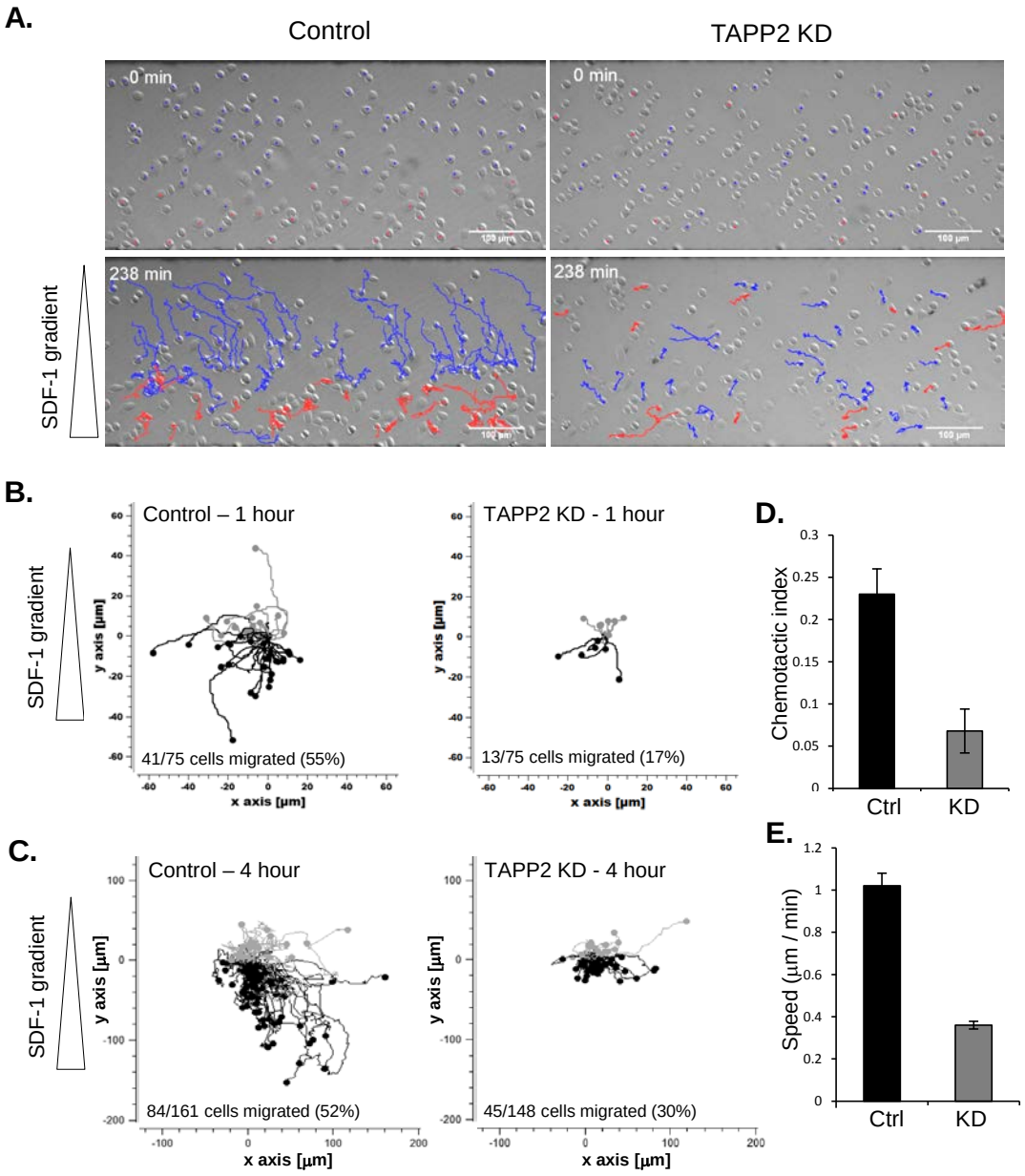
A.
Control
TAPP2 KD
0 min
0 min
238 min
238 min
SDF-1 gradient
B.
Control – 1 hour
TAPP2 KD - 1 hour
SDF-1 gradient
y axis [µm]
x axis [µm]
41/75 cells migrated (55%)
13/75 cells migrated (17%)
D.
Chemotactic index
Ctrl
KD
C.
Control – 4 hour
TAPP2 KD - 4 hour
SDF-1 gradient
y axis [µm]
x axis [µm]
84/161 cells migrated (52%)
45/148 cells migrated (30%)
E.
Speed (µm / min)
Ctrl
KD

Figure 4.5 TAPP2 KD leads to decreased migration speed and directionality in a stable SDF-1 gradient

NALM-6 cells transduced with control or TAPP2 KD lentivirus were loaded onto a microfluidic chemotaxis device and exposed to a 100 nM SDF-1 gradient (represented with triangles). Time-lapse images were taken and cell movement was analyzed using cell-tracking software. **A.** Panels show the first and last image from a representative experiment. Migrating cell tracks are marked in blue (migrating toward higher SDF1 concentration) or red (migrating towards lower SDF1 concentration). **B.** Migration tracks of WT or TAPP2 KD cells in a 1 hour experiment were normalized to a common origin (0, 0) and plotted to visualize patterns of movement in two dimensions (the chemokine gradient is in the y dimension as indicated). Black tracks represent cells migrating toward the gradient and grey tracks are for cells migrating against the gradient. The solid circles indicate the end of the cell tracks. **C.** Migration tracks of control or TAPP2 KD cells in a 4 hour experiment were plotted as in C. **D.** Chemotaxis index of control and TAPP2 KD cells, calculated as described in Methods. **E.** Migration speed of control and TAPP2 KD cells, calculated as described in Methods. Data are representative of four independent experiments. These were performed in collaboration with Xun Wu and Saravanan Nandagopal.

Videos 4.1 and 4.2 TAPP2 KD leads to decreased migration speed and directionality

Video 4.1 Control NALM-6 cells migrating in a microfluidic system

Control NALM-6 cells were loaded onto a microfluidic chemotaxis device and exposed to a 100 nM SDF-1 gradient (higher SDF-1 concentration at the bottom). Images were taken every 1 min for 4 hours and videos were generated from image stacks using ImageJ. Cell tracks are superimposed in the movies with blue tracks representing cells migration toward higher SDF concentration, and red tracks representing cells migrating away from higher SDF concentration. Experiments were performed in collaboration with Xun Wu.

Video 4.2 TAPP2 KD NALM-6 cells migrating in a microfluidic system

TAPP2 KD NALM-6 cell migration was recorded under the same conditions as Video 4.1. Experiments were performed in collaboration with Xun Wu.

4.2.5 TAPP2 regulates chemokine-induced cytoskeletal rearrangement

A prerequisite feature of cell migration is the rearrangement and polarization of the actin cytoskeleton. Given the association of TAPP2 with actin-binding proteins [225, 228, 298] we asked whether TAPP2 KD impacts on migration through disrupting chemoattractant-induced changes in the actin cytoskeleton. SDF-1 stimulation of control cells led to a rapid (within 1 minute) and intense accumulation of filamentous actin (F-actin), as detected by fluorescent phalloidin staining. TAPP2 KD cells also exhibited increase in F-actin after SDF-1 stimulation, however, the intensity of the response was significantly reduced (Figure 4.6A). We next visualized the effect on F-actin distribution patterns using confocal microscopy. SDF-1 stimulated control cells showed intense F-actin staining around the circumference of the cell, with a subpopulation exhibiting asymmetric localization within membrane protrusions formed at one end of the cell (Figure 4.6B). In contrast, a distinct pattern of actin cytoskeleton organization was seen in the TAPP2 KD cells, which often extended numerous protrusions around the cell periphery staining less intensely for F-actin (Figure 4.6B). Scoring of cell morphology indicated a significantly higher frequency of this multi-protrusion morphology in TAPP2 KD cells (Figure 4.6C). These results demonstrated that TAPP2 plays a role in cytoskeletal reorganization in response to chemoattractant stimulation.

Figure 4.6

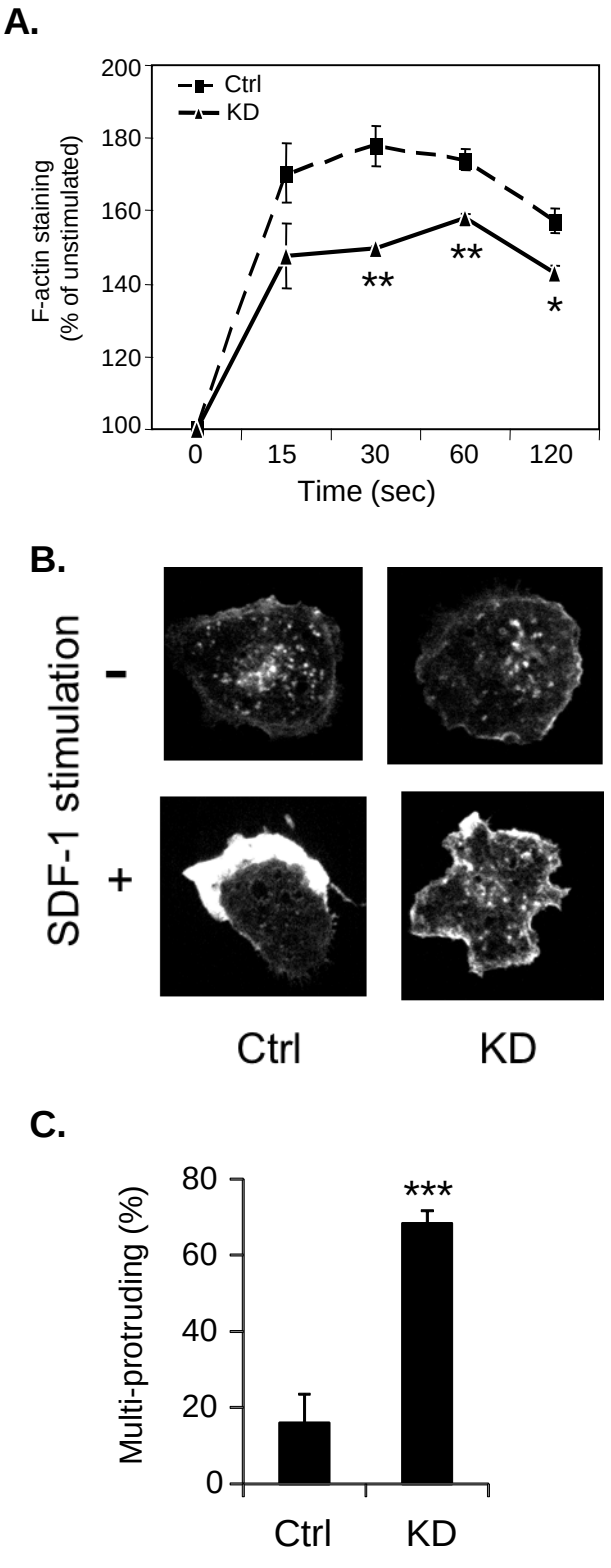
A.
Ctrl
KD
F-actin staining
(% of unstimulated)
200
180
160
140
120
100
0
15
30
60
120
Time (sec)
**
**
*
B.
SDF-1 stimulation
-
+
Ctrl
KD
C.
Multi-protruding (%)
80
60
40
20
0
***
Ctrl
KD

Figure 4.6 TAPP2 KD impairs chemokine-induced rearrangement of the actin cytoskeleton

A. TAPP2 KD cells show impaired accumulation of F-actin in response to SDF-1 stimulation. Control or TAPP2 KD NALM-6 cells were stimulated with 100 ng/ml SDF-1 for a series of time points ranging from 15 – 120 seconds. Control samples without addition of SDF-1 were used for "time point 0". Cells were fixed immediately following stimulation, permeabilized, stained with fluorescent phalloidin and mean fluorescence intensity (MFI) was determined by flow cytometry. Results were normalized relative to the level at time point 0. The values were shown as mean ± SEM for three experiments based on 2 batches of transductions. Significance for KD cells versus control cells at each stimulation time point was confirmed by Student's *t* test: ** $p < 0.01$; * $p < 0.05$. **B.** TAPP2 KD leads to altered organization of the F-actin cytoskeleton. Cells plated on fibronectin-coated chambered coverglass were stimulated with or without 100 ng/ml SDF-1 for 1 minute, fixed, permeabilized and stained for F-actin using Alexa Fluor 647 phalloidin. Confocal microscopy was performed using a 60x objective. Representative images are shown indicating polarized F-actin distribution in SDF-1-stimulated control cells and multiple cellular protrusions with less intense accumulations of F-actin in TAPP2 KD cells. **C.** Frequency of cells having more than 2 protrusions in SDF-1-stimulated control versus TAPP2 KD cells. Results are presented as mean percentage of cells scored as multi-protrusion ± SD from four independent experiments. For each group more than 400 cells were analyzed. The multi-protruding cell frequency is significantly higher in TAPP2 KD cells than in control cells, as indicated by Student's *t* test: *** $p < 0.001$.

4.2.6 Localization of TAPP2 relative to F-actin and utrophin

TAPP2 was previously found to associate with the actin-binding protein utrophin [225, 298]. We investigated the subcellular localization of TAPP2 relative to F-actin and utrophin. Utrophin is reported to selectively bind a stable population of F-actin via its calponin homology domain [44, 298, 299], whereas the F-actin at the leading edge of migrating cells is rapidly polymerized and depolymerized [300, 301] and does not bind to utrophin. Consistent with the literature, we observed a reciprocal distribution between polarized F-actin and utrophin in SDF-1 stimulated cells (Fig. 4.7A). We quantified the relative colocalization between F-actin and utrophin by calculating their colocalization coefficient before and after SDF-1 stimulation. The F-actin/utrophin colocalization coefficient was significantly lower in SDF-1 activated cells (Fig. 4.7A, right panel), consistent with exclusion of utrophin from the dynamic F-actin generated by chemotactic stimulus. We examined the sub-cellular distribution pattern of TAPP2 and found that it also reciprocally localized against the intense dynamic F-actin population and showed a lower coefficient of colocalization with total F-actin in SDF-1-activated cells than in resting cells (Fig. 4.7B). Consistent with these patterns, TAPP2 and utrophin highly colocalized with each other (Fig. 4.7C). In summary, the imaging data indicated that TAPP2 localizes together with utrophin and stable F-actin, but away from dynamic F-actin forming at the leading edge.

Figure 4.7

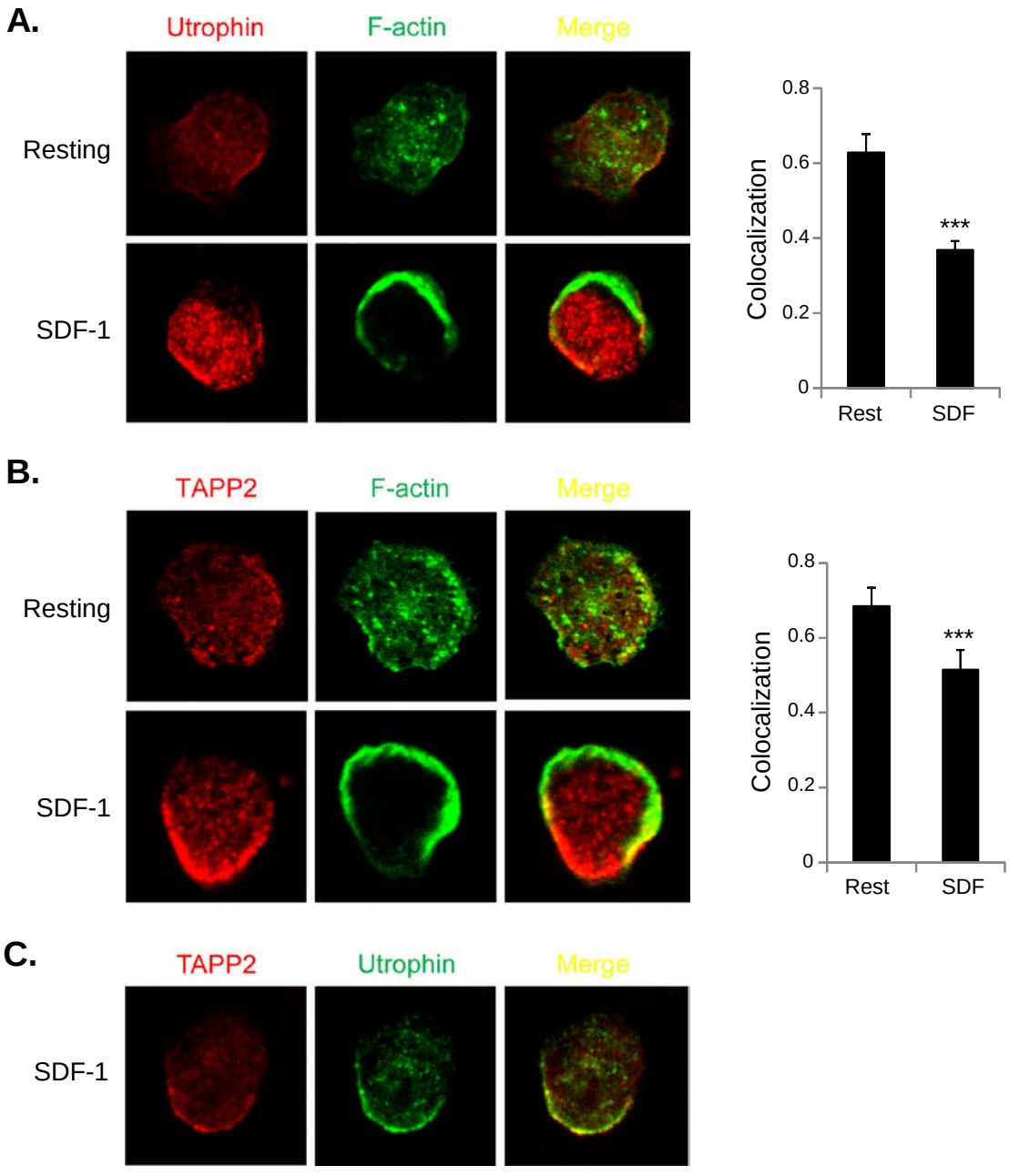
A.
Utrophin
F-actin
Merge
Resting
SDF-1
Colocalization
0.8
0.6
0.4
0.2
0
***
Rest
SDF
B.
TAPP2
F-actin
Merge
Resting
SDF-1
Colocalization
0.8
0.6
0.4
0.2
0
***
Rest
SDF
C.
TAPP2
Utrophin
Merge
SDF-1

Figure 4.7 Relative localization of TAPP2, utrophin and F-actin upon chemokine stimulation

A. Relative localization of utrophin versus F-actin. NALM-6 cells without or with 100 ng/ml SDF-1 stimulation for 1 minute were fixed, permeabilized and stained for utrophin and F-actin. Images shown are representative of five experiments. Right panel: Colocalization of utrophin and F-actin was calculated as the average Pearson's correlation coefficient of more than 100 cells from 5 experiments. With SDF-1 stimulation, the overall colocalization of utrophin and F-actin significantly decreased, as determined by Student *t* test: *** $p < 0.001$. **B.** Relative localization of TAPP2 versus F-actin was visualized and quantified using similar methods as in (5 experiments). A significant reduction in the overall colocalization of TAPP2 and F-actin was seen in SDF-1 stimulated cells (Student *t* test: *** $p < 0.001$). **C**. TAPP2 colocalizes with utrophin at the sides and rear of migrating cells. NALM-6 cells were stimulated, processed and visualized as in **A**. Images representing two experiments are shown.

4.2.7 TAPP2 KD led to dysregulation of Rac

Rho family GTPases are important mediators of cell polarization events underlying cell migration. Typically, Rac is activated in the front to generate protrusions, while Rho is active in the back to promote retraction of the cell rear. To determine whether TAPP2 impacts on the activity of Rho family GTPases we performed pull-down assays to measure active Rac and Rho in control and TAPP2 KD cells in response to SDF-1 stimulation. TAPP2 KD cells exhibited over-activation of Rac1 but showed no significant difference in activity of Rho (Figure 4.8A). In the same experiments, the pull-down assays failed to detect active Cdc42 signal comparable to that of Rac or Rho, presumably due to its low abundance in these cells (data not shown). In an attempt to visualize the distribution of Rac activity, we used GST-tagged p21-binding domain of p21-activated kinase (PAK PBD) to probe active Rac. Cells were co-stained with antibody against non-muscle myosin II heavy chain, a widely used marker to label the back of migrating cells. In control cells, a front-back polarity was seen, with myosin II and active Rac localizing reciprocally and accumulating towards the two opposing ends of the cell, whereas TAPP2 KD cells showed a multi-polar morphology where active Rac colocalized with myosin II in peripheral protruding structures (Figure 4.8B). The frequency of this multi-polar pattern was significantly higher in TAPP2 KD cells than in control cells (Figure 4.8B right panel). These results further supported a role of TAPP2 in cell polarity and suggested that TAPP2 is required to restrict localization of active Rac to the front of the cell. Collectively, our observations suggest that TAPP2 may act as part of a complex with utrophin and stable F-actin to spatially restrict Rac activation and reduce excessive formation of membrane protrusions (Figure 4.9).

Figure 4.8

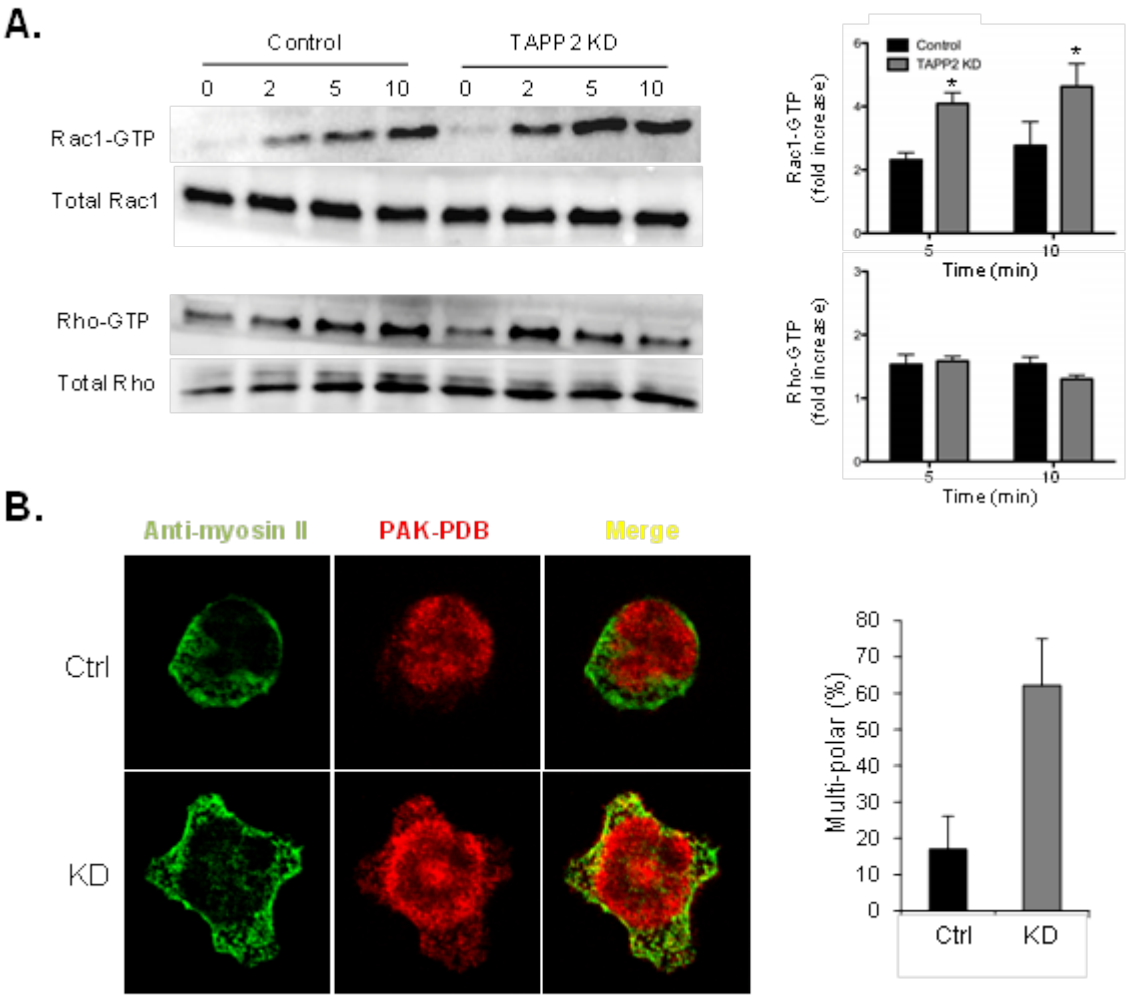
A.
Control
TAPP2 KD
0 2 5 10 0 2 5 10
Rac1-GTP
Total Rac1
Rho-GTP
Total Rho
Control
TAPP2 KD
Rac1-GTP (fold increase)
Time (min)
Rho-GTP (fold increase)
Time (min)
B.
Anti-myosin II
PAK-PDB
Merge
Ctrl
KD
Multi-polar (%)
Ctrl
KD

Figure 4.8 TAPP2 KD leads to dysregulation of Rac

A. TAPP2 KD cells increased activation of Rac, but not Rho. Control or TAPP2 KD NALM-6 cells without stimulation (time point 0) or stimulated with 100 ng/ml SDF-1 for 2, 5 or 10 minutes were lysed. Total protein extracts, Rac-GTP pulldowns or Rho-GTP pulldowns were Western blotted and probed for Rac or Rho. Blots shown represent three independent experiments that all demonstrated a general pattern of Rac overactivation. Activity was quantified as the ratio of active to total Rac or Rho and normalized relative to time point 0. Bar graph on the right indicates the mean and SEM of three independent determinations. * indicates $p < 0.05$ by paired T test. The Rho GTPase activity assays were performed in collaboration with Sen Hou. **B.** TAPP2 KD leads to mislocalization of Rac. Cells were stimulated with SDF-1, fixed and stained with antibody against non-muscle myosin II heavy chain, and with PAK PBD to probe active Rac. Representative images show reciprocally polarized distribution of Rac activity versus myosin II in control cells. In contrast, a multipolar distribution pattern was more often seen in TAPP2 KD cells, where active Rac colocalizes with myosin II in peripheral protrusions. The bar graph compares frequencies of the multipolar pattern (with more than two protrusions) in control and TAPP2 KD cells based on four experiments. For each group more than 100 cells were analyzed. The frequency is significantly higher in TAPP2 KD cells than in control cells, as indicated by Student's *t* test: ** $p < 0.01$.

Figure 4.9

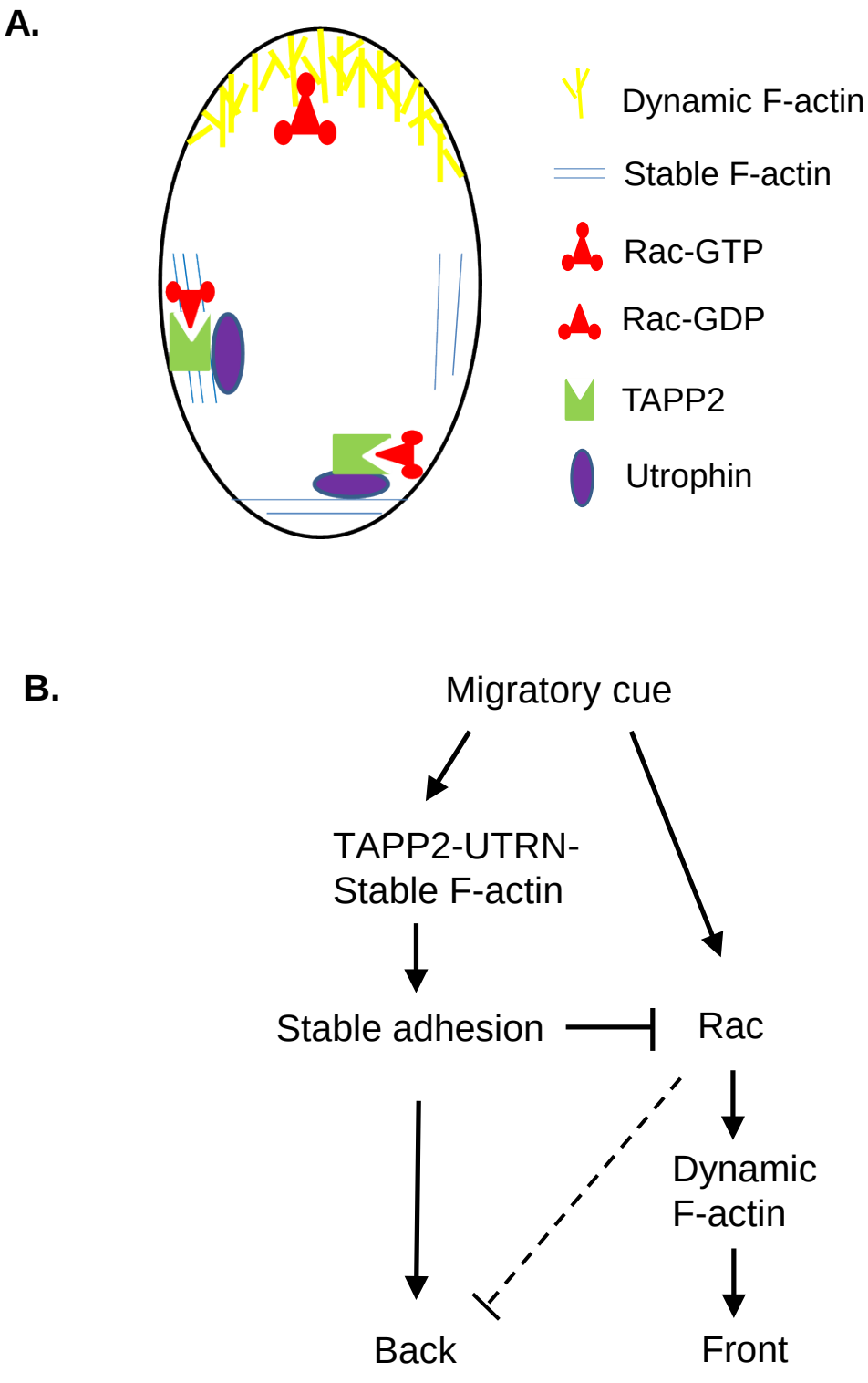
A.
Dynamic F-actin
Stable F-actin
Rac-GTP
Rac-GDP
TAPP2
Utrophin
B.
Migratory cue
TAPP2-UTRN-
Stable F-actin
Stable adhesion
Rac
Dynamic
F-actin
Back
Front

Figure 4.9 Proposed model of TAPP2 signaling in a migrating human malignant B cell

A. Schematic representation of molecular localization in a migrating cell under the control of TAPP2. **B.** Signal pathways involved in TAPP2-mediated migration. In response to a migratory cue, such as SDF-1 induction, activated Rac produces dynamic F-actin-based protrusion in the front (leading edge) and TAPP2, distributed away from the destined front and colocalized with utrophin and stable F-actin, promotes the formation or maintenance of the cell back (including lateral sides and trailing edge) through mediating stable adhesions whereby Rac activation is inhibited. The restriction of Rac activity by TAPP2 signaling prevents uncontrolled or mislocated protrusions from being generated, and may potentially relieve the suppressive effect of otherwise misactivated Rac on proper signaling at the back. Thus, TAPP2 contributes to balanced “frontness” versus “backness” signaling required by effective cell migration.

4.2.8 TAPP2 KD impairs migration of malignant B cells into bone marrow stromal cell layers

Human malignant B cells are capable of migrating into layers of bone marrow stromal cells in a process also termed pseudoemperipolesis [302]. This chemokine-dependent process is thought to reflect a homing mechanism by which malignant B cells find favorable niches that promote their survival. To examine whether TAPP2 regulates this process we set up a co-culture system where NALM-6 cells migrated into layers of bone marrow stromal cells. We found that migration was inhibited by pertussis toxin, a GPCR inhibitor and to a lesser extent by PI3K inhibitor GDC-094 (Figure 4.10A), consistent with a chemokine receptor dependent event. Under-stroma migration was also partially inhibited by AMD3100, an antagonist of the SDF1 receptor CXCR4, or by pretreatment with SDF-1 to downregulate CXCR4 surface expression (Figure 4.10B). Consistent with the role of TAPP2 in SDF-1-dependent migration in transwell and microfluidic migration assays, TAPP2 KD also inhibited the under-stroma migration (Figure 4.10C and D). These data suggested that disruption of TAPP2 function can impair malignant B cell migration in the context of interaction with chemokine-producing stromal cells. We further examined the impact of TAPP2 KD on stromal cell-dependent drug resistance of leukemic cells. Compared to suspension culture without stromal cells, co-culture with stromal cells led to significantly enhanced survival of in the presence of fludarabine, a chemotherapy drug (Figure 4.11A). However, consistent with the impaired under-stroma migration, the drug resistance of Nalm-6 cells in the coculture was significantly inhibited by TAPP2 KD (Figure 4.11B). Collectively, these data suggest that TAPP2 may be a

potential therapeutic intervention target to be used for disrupting malignant B cell migration and resistance to chemotherapy.

Figure 4.10

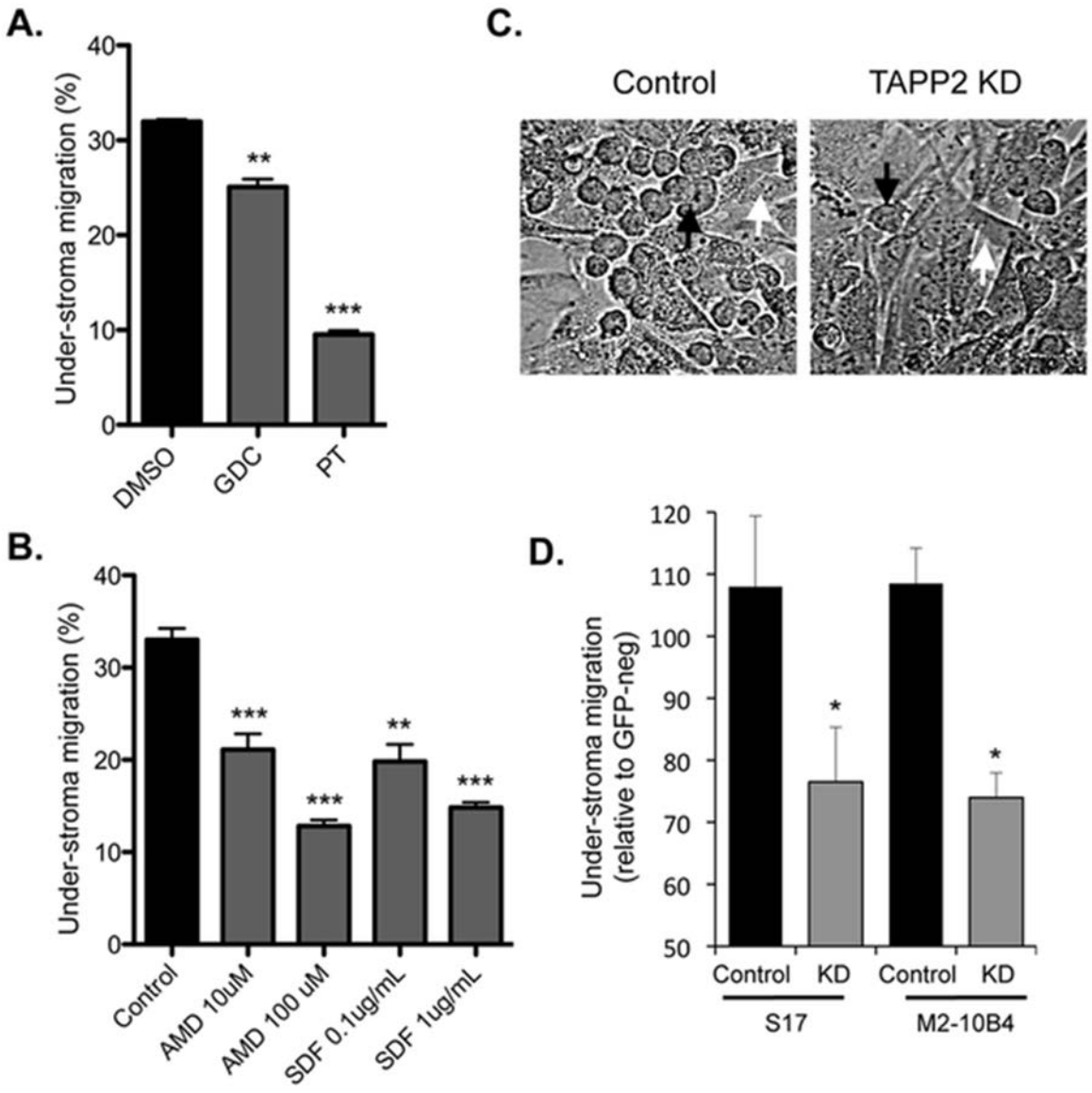

Figure 4.10 TAPP2 KD impairs leukemic cell migration into bone marrow stromal cell layers

NALM-6 cells were added to a confluent layer of S17 stromal cells and allowed to migrate for 10 hours. Under-stroma migration was quantified as percentage of total input cells as described in Methods. **A.** Under-stroma migration is pertussis toxin sensitive and partially blocked by PI3K inhibtion. PT: addition of 0.1 μg/ml pertussis toxin (GPCR inhibitor); GDC: addition of 2 μM GDC-0941 (pan PI3K inhibitor); DMSO, vehicle control for GDC-0941. **B.** Under-stroma migration is partially dependent on the SDF-1 receptor CXCR4. NT, not treated; AMD, 10 or 100 μM AMD3100 (CXCR4 inhibitor); SDF, 0.1 or 1 μg/ml SDF-1 (to desensitize CXCR4). Results are mean ± SD of three independent experiments. Significant difference in leukemic migration into the stromal layer was determined by Student's *t* test: ** $p < 0.01$ or *** $p < 0.001$. **C.** Phase contrast imaging of the under-stroma migration of control or TAPP2 KD NALM-6 cells into S17 stromal cells. Migrated cells, indicated by black arrows, are characterized by the dark round appearance in contrast to the stromal cells, indicated by white arrows. Images represent two independent experiments. **D.** Quantification of TAPP2 KD inhibition of under-stroma migration. NALM-6 cells were partially transduced with GFP-expressing pSIH1-H1-copGFP control lentivirus or TAPP2 KD lentivirus. Migration into S17 or M2-10B4 stromal layers was normalized as the migration of GFP+ (transduced) cells relative to that of GFP- cells (internal control) in the same sample. Results from one experiment performed in replicates were shown as mean ± SD, representing two independent experiments confirming migration inhibition by TAPP2 KD. Significant difference between control and KD cells based on each stromal type was calculated with

Student *t* test: * $p < 0.05$.

Figure 4.11

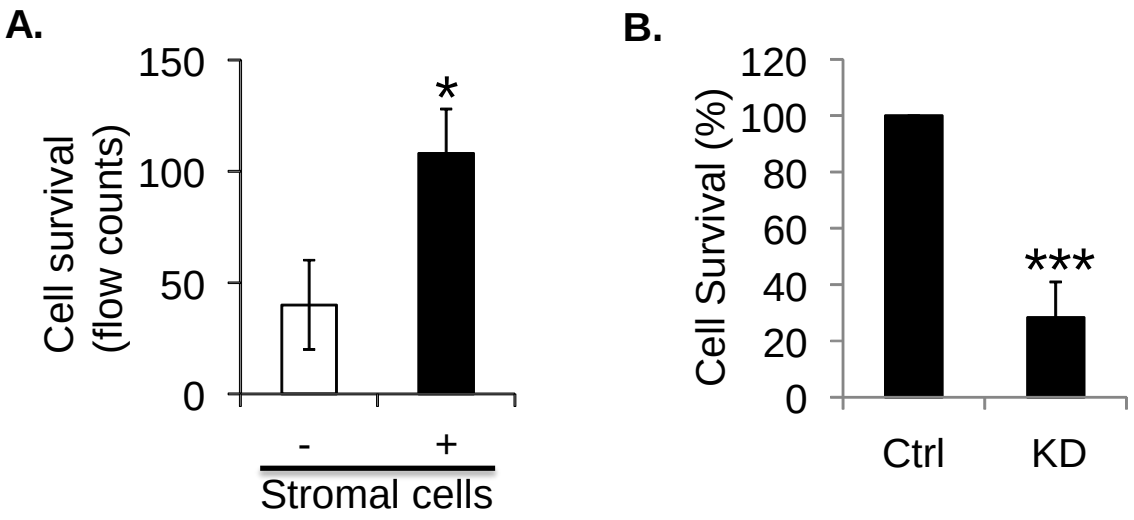

Figure 4.11 TAPP2 KD results in reduced resistance of leukemic cells to Fludarabine treatment in coculture with bone marrow stromal cells.

A. NALM-6 cells were cultured in suspension or cocultured with S17 stromal cells for 3 days in the presence of 50 μM fludarabine, a concentration pre-tested to result in massive cell death in suspension culture (data not shown). Survived leukemic cell numbers were counted by flow cytometry. Coculture with stromal cells significantly enhanced cell survival as determined by Student's *t* test: * $p < 0.05$. **B.** NALM-6 cells were transduced as in Figure 4.9, and were cocultured with S17 stromal cells in the presence of 50 μM fludarabine for 3 days. Survived leukemic cell numbers were counted by flow cytometry. Results are normalized as percentage relative to Control cells and represent mean ± SD of two independent experiments. Significance of difference in leukemic cell survival in stromal coculture was assessed with Student's *t* test: *** $p < 0.001$.

4.3 Discussion

In this study TAPP2 is identified as a novel regulator of human malignant B cell migration in different contexts, including crawling on 2D substrates and passing through 3D micropores of the Transwell membrane. Migration into a bone marrow stromal cell layer, a process that depends on SDF-1 gradient, was also repressed in TAPP2 KD cells.

Our results provide initial insights into the mechanisms by which TAPP2 performs this function. TAPP2 was found to be directly implicated in chemokine-responsive changes in the actin cytoskeleton, a central machinery driving cell migration. Loss of TAPP2 dramatically altered the pattern of F-actin-based cellular protrusions induced by SDF-1, leading to loss of normal cellular polarity. Associated with this alteration was the over-activation and mislocalization of active Rac, a master regulator of plasma membrane protrusion [44, 297]. These data suggested that TAPP2 is important for cell polarity and restricts local Rac activity that may underlie F-actin dependent membrane protrusion.

Cell migration relies on the precise front-back coordination of cellular events in order to establish functional migratory polarity. The current dominant model proposes that “frontness” signaling, controlled by Rac, promote membrane protrusion in the front but inhibit the formation of the back [108, 303]. Conversely, “backness” signaling pathways promote the formation of the back but inhibit that of the front [108, 303]. Consistent with this polarity model, the overactivation of Rac inhibits backness signaling in T lymphocytes, leading to multiple protrusions and loss of uropod (structure of migratory

back in T cells) [304]. TAPP2 KD cells stimulated with SDF-1 showed mislocalized and increased activity of Rac and formation of multiple protrusions, consistent with failure to control “frontness” signaling and establish polarized “backness” necessary for effective migration.

Our Lab previously found that TAPP2, in association with the F-actin-binding proteins utrophin and syntrophin [229, 230], functions in the firm adhesion of BCR- or SDF-1-activated cancer B cells to extracellular matrix proteins [225]. Since control of adhesion and de-adhesion between a migrating cell and the substrate on which it moves is part of the known migration mechanisms, the TAPP2/utrophin complex may act at the level of adhesion to regulate Rac, membrane protrusion and migration. A recent study indicated that the rear formation of a migrating cell was characterized by the generation of stable adhesions that do not signal to Rac [305]. It is possible that TAPP2 KD disrupts adhesion-associated signaling pathways that restrict local Rac activity in regions that should form the rear of a polarized migratory cell, leading to frequent mislocalized membrane protrusions. More complete understanding of how TAPP2 executes such controls with relevance to the proper front-back polarity critical for migration will require future investigations.

While restricting multiple random or mislocated protrusions, TAPP2 appears to also promote “healthy” protrusion formation. The protrusions in TAPP2 KD cells displayed less organized morphology, with less intensive accumulation of F-actin. The mechanism(s) remain to be elucidated that explain how TAPP2, distributed away from the front

protrusions and towards the back, where backness activators accumulate according to the current polarity model, contributes positively to normal frontness. Meanwhile, it is worth mentioning that the discrepancy between the “weak” protrusions with less F-actin and enhanced activity of Rac, normally a positive regulator of F-actin dynamics driving protrusions, may seem surprising. An interesting clue comes from an emerging concept of how Rac function is precisely performed in the context of a migratory front. According to the canonical migratory polarity model, whereas Rac GEFs, which activate Rac, need to accumulate to the front, inhibitory Rac GAPs should be excluded from the front and localize to the back. However, a Rac GAP, SH3BP1, was found to be present in the migrating front, where it worked towards inactivating Rac [306]. SH3BP1 silenced cells also showed overactivation of Rac, defective protrusions and migration. This striking finding, together with other previous data, led to the proposed model that Rac function requires a dynamic cycling between its GTP-bound active form and GDP-bound inactive form, under the coordinated control by GEFs and GAPs, probably occurring in subdomains of the front. The new concept strongly indicates that the proper function of Rac depends not solely on the amount of its active form but also on its dynamic GTP/GDP switch. Perturbing the dynamics of Rac will thus disrupt its normal function. It is tempting to speculate that cellular availability of TAPP2 may be critical for Rac dynamics, or the function of SH3BP1, as this would explain the otherwise contradictory observations in TAPP2 KD cells – increased Rac activity but defective protrusions with inhibited dynamic F-actin accumulation. In other words, lack of TAPP2 would inactivate SH3BP1 or mislocalize it away from Rac, leading to overactivation of Rac due to decreased GAP activity, whereas on the other hand, the switch from Rac-GTP to

Rac-GDP inhibited. In turn, the disrupted activation-inactivation cycling of Rac, regardless of its increased activity, results in F-actin and protrusion defects.

A subsequent question of interest is what pathways link TAPP2 to its target signaling events in the front, such as, as hypothesized, SH3BP1 activation or localization. Previous work from our lab indicated that TAPP2 co-precipitated with endocytic transporter proteins. It is likely that TAPP2 connect frontness and backness signaling through directing the transportation and thereby the redistribution of migration regulators/effectors. For example, TAPP2 may co-transport away from the front with frontness inhibitory proteins, such as an SH3BP1 suppressor, along its relocalization during cellular polarization. Or alternatively, TAPP2 may exclude frontness activators, such as SH3BP1, from the back and facilitate its re-localization to the front.

To summarize, the data from this study, combined with our and others' previous findings, tempt to propose a two tiered regulation of cell migration by TAPP2. TAPP2 promotes stable adhesions at the back, where Rac activity is inhibited, and suppresses multiple random or mislocated protrusions from being generated. On the other hand, TAPP2 promotes the formation of dynamic F-actin-rich, healthy protrusion in the front, with the possibility of TAPP2 contributing to the dynamic cycling of Rac worth testing.

The detailed signaling pathways upstream of TAPP2 during cell migration remain elusive. TAPP2 is best known as a PI(3,4)P2 binding protein [70, 220, 236], and it would be expected that the localization and function of TAPP2 depend on PI3K and PI(3,4)P2.

However, the localization of TAPP2 at the sides and rear of migrating cells does not seem to be consistent with that of PI(3,4)P2, which is extensively present at the membrane with more enrichment at the front. Instead, TAPP2 well colocalizes with utrophin. It is possible that the interaction between TAPP2 and utrophin may primarily drive the localization of TAPP2 in migrating cells. However, the possibility is not ruled out that the presence of PI(3,4)P2 at the back of the cell may contribute to the function of TAPP2. This is supported by the previous finding from our lab that the regulation of adhesion by TAPP2 depends on its PI(3,4)P2-binding PH domain [225].

In the presence of Class I PI3K inhibitors, TAPP2 KD further inhibits the chemotaxis to SDF-1 but not random motility. It is likely that upon SDF-1 stimulation, PI(3,4)P2 could be generated from two sources: Conversion of PIP3 produced by class I PI3K into PI(3,4)P2 by SHIP, or phosphorylation of PI(4)P into PI(3,4)P2 by class II PI3K. Class I PI3K inhibitors do not eliminate PI(3,4)P2 from the latter source, which may act to support TAPP2 function and thus in this scenario TAPP2 KD demonstrates impact on migration. During random motility without SDF-1 stimulation, PI(3,4)P2 may be produced only from the class I PI3K-SHIP source. Therefore class I PI3K inhibitors would completely shut off PI(3,4)P2 production. Under this condition, no PI(3,4)P2 would support TAPP2 function, leading to no effect of TAPP2 KD on migration.

A class I PI3K-independent role of TAPP2 in chemokine-induced migration may represent new therapeutic opportunity. While class I PI3K inhibitor drugs have been demonstrated to strongly reduce malignant B cell chemotaxis in general [58, 307],

complete inhibition remains to be accomplished [54], indicating the existence of alternative/redundant signaling mechanisms, such as those potentially through class II PI3K. In the context of class I PI3K-dependent migration, I found here that targeting TAPP2 in combination with PI3K inhibitors achieved greater inhibition, which seems to reflect the shutting down of two independent components of migratory pathways. TAPP2 expression is largely restricted to hematopoietic cells with overexpression observed in more migratory CLL B cells [70, 220, 225]. Therefore, combining TAPP2 silencing and isoform-selective PI3K inhibitors could offer a relatively specific and more effective treatment targeting malignant B cell migration.

Chapter 5 Lamellipodin and Akt mediate malignant B cell migration

This chapter is partly based on of a submitted paper:

Li H, Wu X, Hou S, Noh E, Makondo KJ, Du Q, Wilkins JA, Johnston JB, Gibson SB, Lin F and Marshall AJ. Phosphatidylinositol-3,4-bisphosphate and its binding protein lamellipodin regulate chemotaxis of malignant B lymphocytes. Proc Natl Acad Sci U S A. Status: Reviewed by Editorial Board on 2014-10-08 and by Editor on 2014-10-10, and being reviewed by reviewers since 2014-10-10.

5.1 Introduction

Lamellipodin/RAPH1 (Lpd) is believed to be another specific PI(3,4)P2-binding protein based on direct evidence from in vitro lipid overlay assays [71]. This view remains to be confirmed by live cell data and has been challenged by a recent study proposing that the PH domain of Lpd is not functional in binding phosphoinositides based on crystal structures and in vitro fluorescence-polarization assay [247]. Lpd interacts with actin remodeling proteins and mediates the migration of several cell types but its expression and function in lymphocytes has not been studied. Here, we provide evidence that further supports Lpd as a PI(3,4)P2-binding protein in live cell setting and that Lpd serves as a PI(3,4)P2 effector mediating the directionality of malignant B cell chemotaxis depending on PH domain binding to PI(3,4)P2.

The protein kinase Akt is considered another potential effector of PI(3,4)P2 in mediating

malignant B cell migration. Akt has a PH domain with dual capacity to bind PI(3,4)P2 and PIP3 [293, 294]. The current model is that both PIP3 and PI(3,4)P2 can promote Akt phosphorylation (at conserved sites Thr308 and Ser473) and subsequent activation [127]. However the relative importance of PIP3 and PI(3,4)P2 in different cell signaling systems may be variable. Akt phosphorylation normally correlates with activation and is widely used as a readout of Akt activation. However, exceptions have also been reported [308-310].

As reviewed in Chapter 1, Akt is a known regulator of cell migration, with multiple Akt isoforms showing differential stimulatory or inhibitory functions depending on the cellular contexts. The effect of PI(3,4)P2 depletion on Akt phosphorylation and activity as well as the role of Akt in cell migration in malignant B cells have not been previously determined. The observations described below may serve to provide some initial insights towards addressing these issues.

5.2 Results

5.2.1 Lamellipodin (Lpd) colocalizes with PI(3,4)P2 in migrating B cells in a PH domain-dependent fashion

We examined expression of the putative PI(3,4)P2 binding protein Lpd in human B cells and found that Lpd is expressed in a variety of malignant B cell lines and primary CLL B cells (Figure 5.1). We were interested to provide additional experimental evidence to help clarify if Lpd is indeed a PI(3,4)P2 binding protein in live cell scenarios as well as to determine the potential function of Lpd linking PI(3,4)P2 signaling to B cell migration. To visualize the respective subcellular localization of PI(3,4)P2 and Lpd, EGFP-tagged wild type Lpd protein (Lpd-GFP WT) or PH domain deleted mutant (Lpd-GFP ΔPH) were overexpressed in RAJI cells (Figure 5.2A), subjected to an SDF-1 gradient, and then fixed, stained for PI(3,4)P2 and analyzed by confocal microscopy. Images from individual Z-positions (Fig. 5.2B and C) as well as 3D image reconstructions (Videos 5.1-5.6) demonstrated a co-enrichment of PI(3,4)P2 and Lpd-GFP WT at the cell membrane, whereas Lpd-GFP ΔPH was not membrane - accumulated, but uniformly distributed inside the cell. Image analysis confirmed that Lpd-GFP WT more strongly co-localized with PI(3,4)P2 than Lpd-GFP ΔPH (Fig. 5.2C, D and E). The PH domain-dependent co-localization of Lpd with PI(3,4)P2 in live cells provides strong support for Lpd as a PI(3,4)P2 binding protein.

Figure 5.1

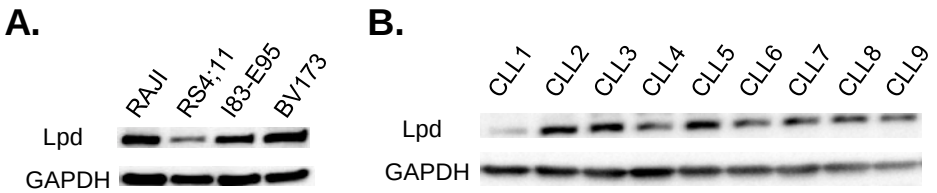

Figure 5.1 Lpd is endogenously expressed in malignant B cells

A. Western blot showing Lpd expression in B cell lines. Data were acquired by Sen Hou.

B. Western blot showing Lpd expression in primary CLL B cells. Data were acquired by Edward Noh.

Figure 5.2

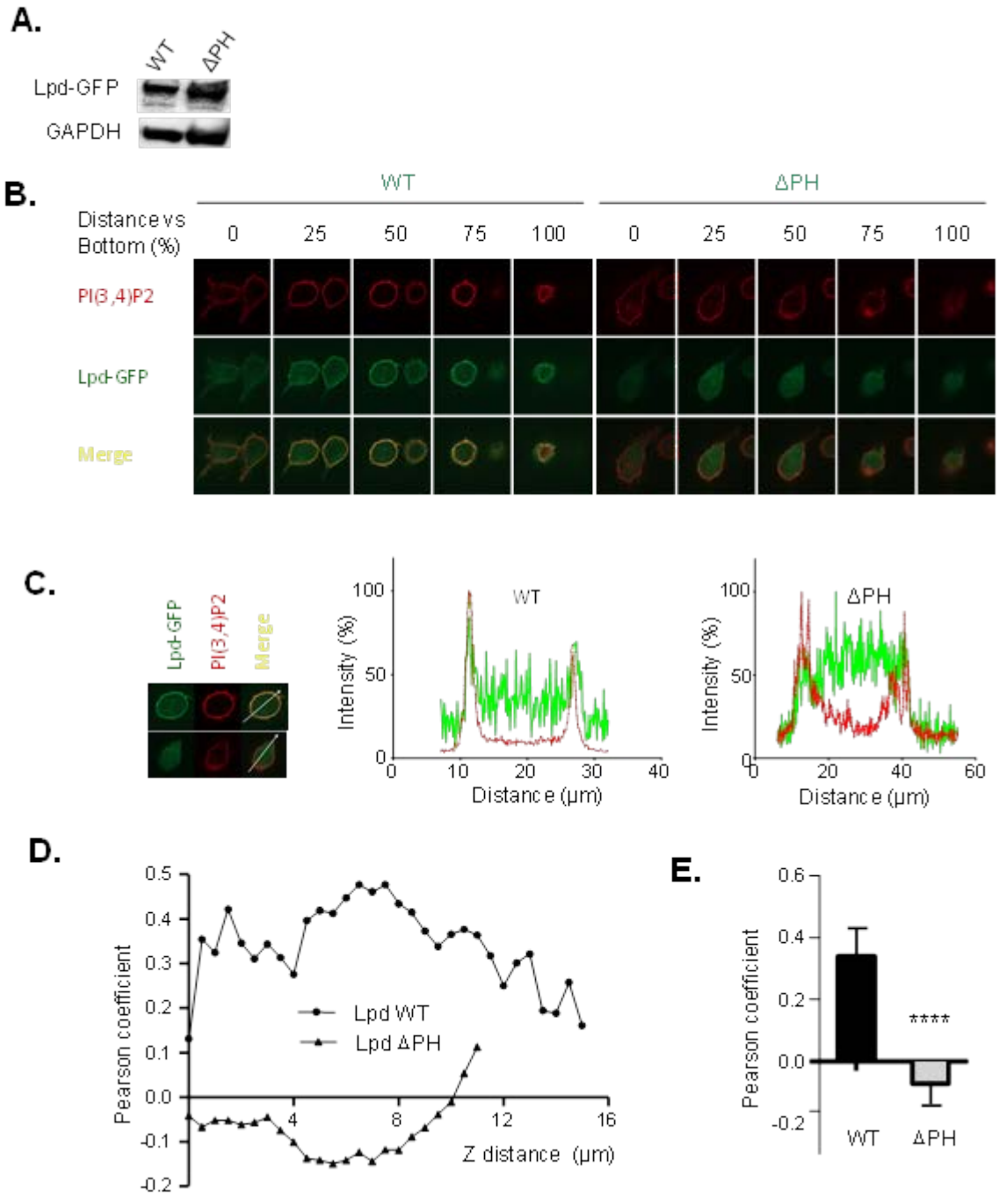
A.
WT
ΔPH
Lpd-GFP
GAPDH
B.
WT
ΔPH
Distance vs Bottom (%)
0
25
50
75
100
PI(3,4)P2
Lpd-GFP
Merge
C.
Lpd-GFP
PI(3,4)P2
Merge
WT
ΔPH
Intensity (%)
Distance (μm)
D.
Pearson coefficient
Lpd WT
Lpd ΔPH
Z distance (μm)
E.
Pearson coefficient
****
WT
ΔPH

Figure 5.2 Lpd colocalizes with PI(3,4)P2 in migrating B cells in a PH domain-dependent fashion

A. Western blot of RAJI cells transfected to overexpress EGFP-tagged full-length Lpd (WT) or PH domain-deleted Lpd (ΔPH). Note lower bands below Lpd-GFPs represent endogenous Lpd. **B.** Cells were allowed to migrate on fibronectin coated surface in a microfluidic chemotaxis device under a SDF-1 gradient. Migrating cells were fixed, intracellularly stained for PI(3,4)P2 and visualized by confocal microscopy (63X). Representative Z stack images demonstrate co-enrichment of Lpd-GFP WT, but not ΔPH, with PI(3,4)P2. See also Videos 5.1-5.6 for 3D localizations re-constructed based on Z-stacks. **C.** Representative images from experiments in B are shown. Fluorescence intensities along the lines drawn across the cell sections were plotted by ZEN2012 software, and show that intensity peaks of Lpd-GFP WT matched those of PI(3,4)P2. In contrast, the intensity of Lpd-GFP ΔPH showed no peak at the cell periphery but uniform distribution. **D.** Migrating cells expressing Lpd-GFP WT or ΔPH were quantified for localization correlation between Lpd and PI(3,4)P2 (Pearson's correlation coefficients) at multiple Z positions. Results from one representative cell are shown for each transfectant indicating an overall higher colocalization of Lpd-GFP WT with PI(3,4)P2 than ΔPH. **E.** Statistical analysis of the results from D. Pearson's correlation coefficients for Lpd and PI(3,4)P2 were quantified in 10 Lpd-GFP WT and 10 ΔPH cells, respectively, based on one median Z-position per cell. Significant difference was determined by Student's *t* test: *** $p < 0.001$. Western blot and imaging were performed in collaboration with Sen Hou and Xun Wu, respectively.

Videos 5.1-5.6 Lpd colocalizes with PI(3,4)P2 in migrating B cells in a PH domain-dependent fashion

Video 5.1 3D reconstruction of PI(3,4)P2 distribution in migrating Lpd-GFP WT cells

RAJI cells were transfected to express Lpd-GFP WT and allowed to migrate on fibronectin coated surface in a microfluidic chemotaxis device that maintains a 100 nM SDF-1 gradient with higher SDF-1 concentration at the top. Cells were fixed, intracellularly stained for PI(3,4)P2 and analyzed by confocal microscopy to acquire Z image stacks. 3D reconstruction of PI(3,4)P2 distribution was performed using ZEN2012 software. Video demonstrates accumulation of PI(3,4)P2 at the cell membrane.

Video 5.2 3D reconstruction of Lpd-GFP WT distribution in migrating cells

Lpd-GFP WT images from the same cells as in Video 3 were 3D-reconstructed. Video demonstrates accumulation of Lpd-GFP WT at the cell membrane.

Video 5.3 3D distribution of PI(3,4)P2 versus Lpd-GFP WT (merged)

Z-stack images of PI(3,4)P2 and Lpd-GFP WT for Videos 5.1 and 5.2 were merged and 3D reconstructed. Video indicates colocalization of PI(3,4)P2 and Lpd-GFP WT at the cell membrane.

Video 5.4 3D reconstruction of PI(3,4)P2 distribution in a migrating Lpd-GFP ΔPH cell

3D distribution of PI(3,4)P2 in a Lpd-GFP ΔPH cell was visualized using the same method as in Video 5.1. Video demonstrates accumulation of PI(3,4)P2 at the cell membrane.

Video 5.5 3D reconstruction of Lpd-GFP ΔPH distribution in a migrating cell

Lpd-GFP ΔPH images from the same cells as in Video 5.4 were 3D-reconstructed. Video indicates uniform distribution of Lpd-GFP ΔPH protein inside the cell without membrane accumulation.

Video 5.6 3D distribution of PI(3,4)P2 versus Lpd-GFP ΔPH (merged)

Z-stack images of PI(3,4)P2 and Lpd-GFP ΔPH for Videos 5.4 and 5.5 were merged and 3D reconstructed. Video indicates that Lpd-GFP ΔPH largely localizes away from PI(3,4)P2 through uniform distribution inside the cell. Experiments for Videos 5.1-5.6 were performed in collaboration with Xun Wu.

5.2.2 Enrichment of Lpd in the migrating front

As described in Chapter 3, PI(3,4)P2 showed a unique localization pattern, with a local enrichment at the cell front and detectable levels throughout the cell membrane (Figure 3.3). Consistent with the interaction of Lpd with PI(3,4)P2, 3D cellular anatomy analysis (methods explained in Figure 3.3 legends) indicated that, like PI(3,4)P2, Lpd WT was enriched towards the cellular front facing the direction of cell movement, while Lpd ΔPH was uniformly distributed throughout the cell (Figure 5.3A). In addition to imaging fixed cells, the temporal dynamics of Lpd localization during chemotaxis was also tracked by time series live cell imaging (10X DIC and confocal) in RAJI cells expressing Lpd-GFP WT or ΔPH (Fig. 5.3B, Videos 5.7 and 5.8). Lpd-GFP WT appears to be enriched towards the front during chemotaxis up SDF-1 gradient, however this enriched pattern was lost at the end of active chemotactic movement. In contrast, Lpd-GFP ΔPH did not accumulate towards the direction of cell movement (Figure 5.3B), which was associated with the failure of these transfectants cell to maintain consistent directional migration. Collectively, the localization patterns of PI(3,4)P2 and Lpd seemed to be consistent with potential function in mediating migration directionality.

Figure 5.3

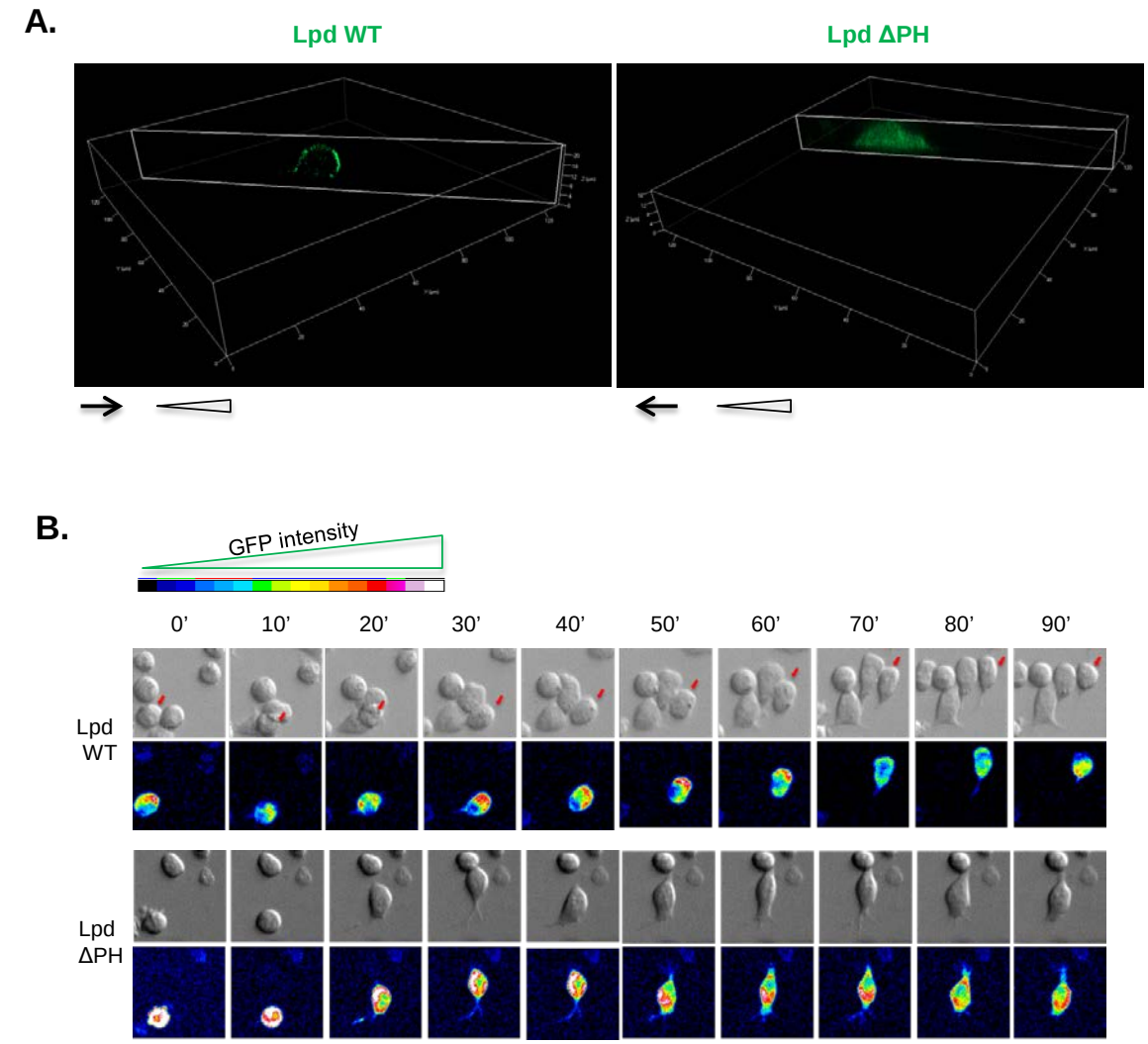
A.
Lpd WT
Lpd ΔPH
B.
GFP intensity
0’
10’
20’
30’
40’
50’
60’
70’
80’
90’
Lpd WT
Lpd ΔPH

Figure 5.3 Spatiotemporal organization of Lpd in migrating B cells. **A.** The enrichment of Lpd at the front of migrating cells visualized by 3D analysis of fixed cells. Lpd-GFP WT or ΔPH cells chemotaxing under a SDF-1 gradient were fixed and analyzed by 63X confocal microscopy. Z-stack images were 3D-reconstructed and subject to cellular anatomy using similar methods as described in Figure 3.3 legends. Arrow and triangle indicate directions of cell movement and SDF-1 gradient, respectively. Localization patterns were consistently observed in 10 out of 10 cells randomly examined for each cell type. **B.** Time lapse imaging of live migrating B cells indicates enrichment of Lpd towards the migrating front in a PH domain dependent manner. Intensities of Lpd GFP fusions in migrating RAJI cells were pseudo color-coded according to the standard Image J color coding system, with white color representing the highest intensity. 10x magnification DIC images of the same cells are also shown. See also Videos 5.7 and 5.8 for dynamic patterns in live moving cells.

Videos 5.7 and 5.8 Lpd was enriched towards the front in a PH domain dependent manner during live cell chemotaxis

Video 5.7 Localization of Lpd-GFP WT in a live migrating cell

Lpd-GFP WT cells were loaded onto a microfluidic chemotaxis device that maintains a 100 nM SDF-1 gradient with higher SDF-1 concentration at the top. Time lapse images (10X confocal) were converted to video using Image J. Note that GFP signal was enriched towards the front during active migration and the pattern discontinued at the end of active migration.

Video 5.8 Localization of Lpd-GFP ΔPH in a live migrating cell

Video was generated for Lpd-GFP ΔPH cells under the same condition as in Video 5.7. Note that GFP signal does not follow the typical pattern of enrichment to the migrating front as in Lpd-GFP WT. Experiments for Videos 5.7 and 5.8 were performed in collaboration with Xun Wu.

5.2.3 Lpd mediates malignant B cell migration in a PH domain-dependent manner

The function of Lpd in cell migration was assessed by overexpression of Lpd-GFP or knock-down (KD) of endogenous Lpd. Lpd-GFP overexpression led to increased migration of RAJI cells to SDF-1 in Transwell assays (Figure 5.4A), while migration was significantly inhibited by Lpd KD using shRNAs targeting either Lpd coding sequence (KD-CDS) or 3' UTR (KD-UTR) (Figure 5.4B and C). Lpd KD did not affect cell surface expression of CXCR4 (Figure 5.5). To dissect the role of the Lpd PH domain in controlling motility and directionality, KD rescue experiments were performed by adding back Lpd-GFP WT or ΔPH to KD-UTR cells and tracking the cells in microfluidic chemotaxis assays (Figure 5.4D-F). Under these conditions, Lpd KD cells were severely impaired in motility (Figure 5.4D and E). Expression of Lpd-GFP WT but not ΔPH in KD-UTR cells restored a similar pattern of cell tracks compared to control cells (Figure 5.4D). Quantitative analysis indicated that both Lpd-GFP WT and ΔPH restored migration speed (Figure 5.4E), suggesting that Lpd controls motility independently of PH domain binding to PI(3,4)P2. Interestingly, however, Lpd-GFP ΔPH was strongly impaired in maintaining cellular directionality (Figure 5.4F). These results indicate that Lpd serves as a PI(3,4)P2 effector, controlling the directionality of malignant B cell chemotaxis through PH domain binding to PI(3,4)P2.

Figure 5.4

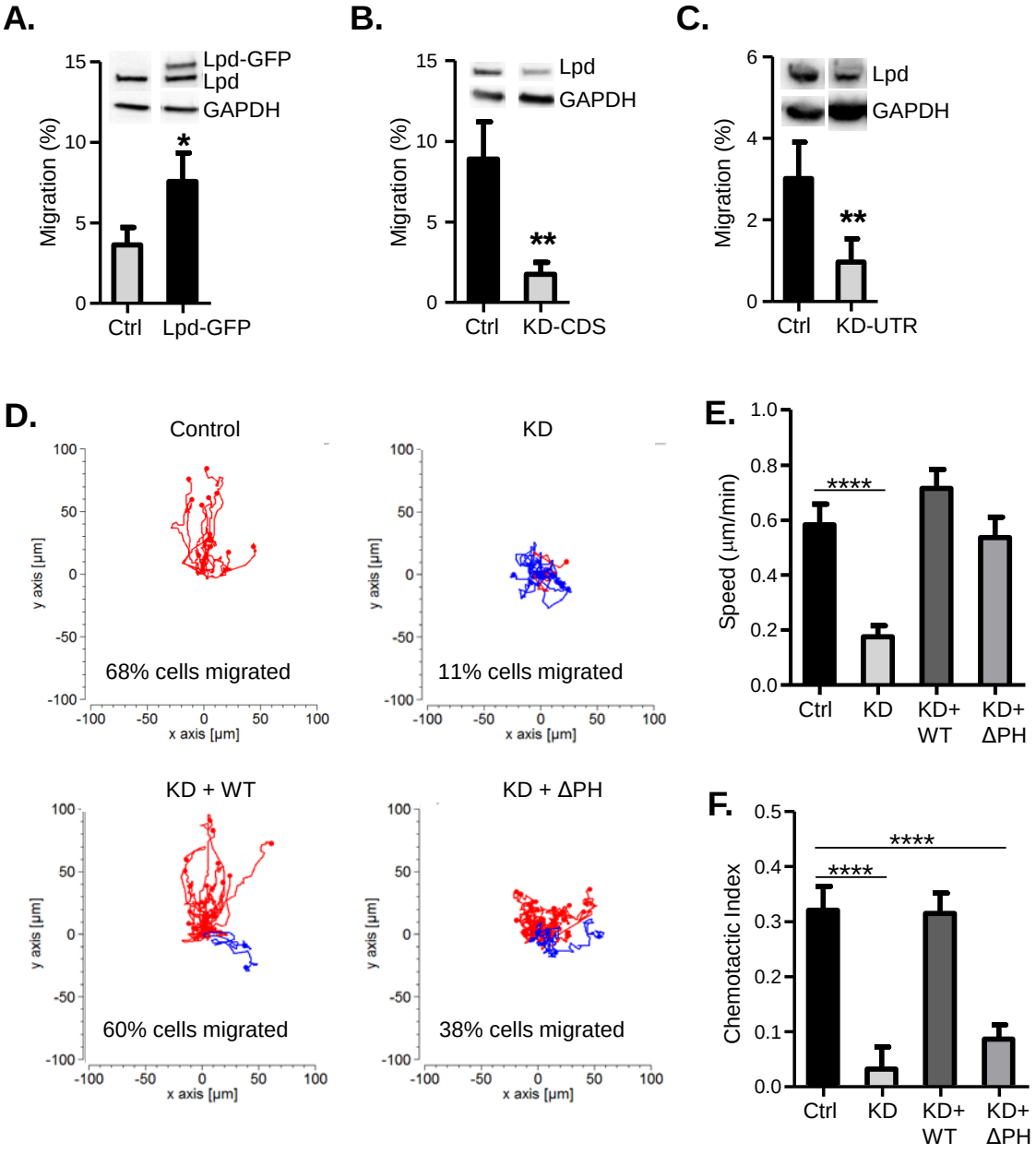
A.
Lpd-GFP
Lpd
GAPDH
Migration (%)
Ctrl
Lpd-GFP
B.
Lpd
GAPDH
Migration (%)
Ctrl
KD-CDS
C.
Lpd
GAPDH
Migration (%)
Ctrl
KD-UTR
D.
Control
68% cells migrated
KD
11% cells migrated
KD + WT
60% cells migrated
KD + ΔPH
38% cells migrated
x axis [μm]
y axis [μm]
E.
Speed (μm/min)
Ctrl
KD
KD+ WT
KD+ ΔPH
F.
Chemotactic Index
Ctrl
KD
KD+ WT
KD+ ΔPH

Figure 5.4 Lpd mediates malignant B cell migration in a PH domain-dependent manner. A. Lpd overexpression promotes migration. RAJI cells were mock transfected (Ctrl) or transfected with Lpd-GFP vector and protein expression was confirmed by Western blot. Cells were assayed for migration toward SDF-1 using transwell chamber assays. Bars represent mean ± SD of six experiments, including one that was done by Edward Noh. A significant difference in cell migration was confirmed by Student's paired t test: * $p < 0.05$. **B and C.** Lpd knock down (KD) inhibits migration. RAJI cells were transduced with control lentivirus or lentivirus expressing shRNA that targets endogenous Lpd coding sequence (KD-CDS in B) or 3' UTR (KD-UTR in C). Lpd protein KD was confirmed by three Western blots for each of the shRNAs. Western blots were performed by Sen Hou and Edward Noh. Cells were assayed for migration toward SDF-1 using transwell chamber assays. Results (mean ± SD) in B are from one experiment performed in replicates representing two independent experiments and in C are based on four independent experiments. Significant differences were determined by Student's unpaired (B) and paired (C) *t* tests, respectively: ** $p < 0.01$. **D.** Visualization of Lpd KD and rescue effects on chemotaxis. RAJI cells transfected with control vector, KD-UTR, KD-UTR + Lpd-GFP WT or KD-UTR + Lpd-GFP ΔPH were assayed for microfluidic chemotaxis to SDF-1. Cell migration tracks were normalized to a common origin (0,0) in 2D plots. **E and F.** Migration speed and chemotactic index were calculated as described in Methods. Bars represent the mean ± SEM based on 77, 98, 81 and 77 cells for the four above-mentioned groups, respectively, from two independent experiments. Statistical significance was calculated by Student's *t* test: **** $p < 0.0001$. The Lpd KD rescue experiments were carried out in collaboration with Xun Wu.

Figure 5.5

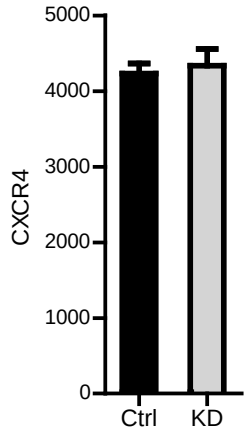

Figure 5.5 Lpd KD does not affect cell surface expression of CXCR4

Control or Lpd KD cells were stained for cell surface CXCR4 and analyzed by flow cytometry. MFIs from three independent experiments were shown as mean ± SD. No significant difference in CXCR4 expression was found by Student's paired *t* test.

5.2.4 Effect of PI(3,4)P2 depletion on Akt phosphorylation and activity

To examine the role of PI(3,4)P2 in controlling Akt phosphorylation, PI(3,4)P2 - depleted (INPP4A WT) or control (INPP4A Mut) RAJI cells were stimulated with SDF-1 or B cell antigen receptor (BCR) activating antibody and analyzed for Akt phosphorylation at Ser308 and Thr473 using a Western blot-based method (Figure 5.6A, B). According to the majority of the previous observations in other cell types, PI(3,4)P2 depletion should have led to the inhibition of Akt phosphorylation. However, in the context of RAJI cells, Akt phosphorylation did not show any reduction as a result of PI(3,4)P2 depletion, but instead suggested a trend of enhancement at multiple time points and for both phosphorylation sites (Figure 5.6A,B). This effect was further confirmed by an alternative quantification method based on ELISA assay of Ser473 -phosphorylated Akt (Figure 5.6C). Notably, an enhancing effect of PI(3,4)P2 depletion on Akt phosphorylation was once reported in 293T cells, a human kidney epithelial cell line [311].

Concerning the direct effect of PI(3,4)P2 depletion on Akt enzymatic activity, our preliminary data obtained so far seemingly suggest that PI(3,4)P2 depletion in RAJI cells is associated with reduced phosphorylation of Akt substrates p70SK, GSK-3 and 4E-BP1 (Figure 5.7). This would agree with the previous finding that, although only seen in rare cases, Akt phosphorylation may not necessarily correlate with activity [308-310].

Figure 5.6

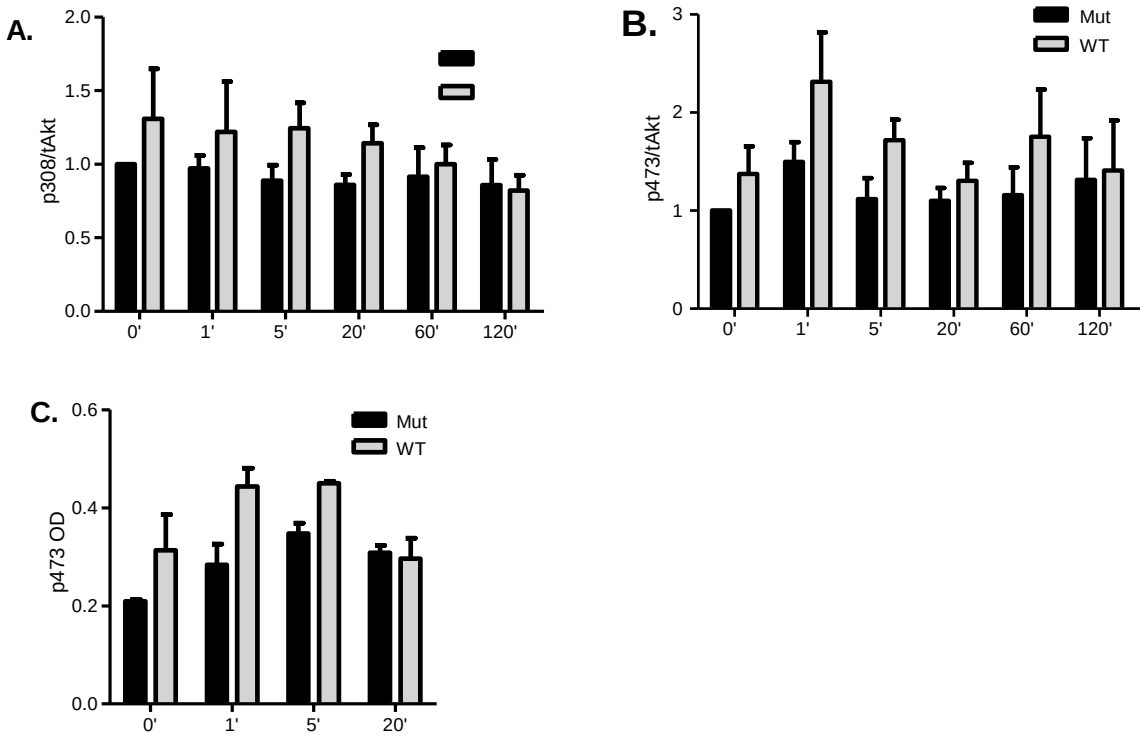

Figure 5.6 Effect of PI(3,4)P2 depletion on Akt phosphorylation

INPP4A Mut or WT cells were serum-starved, stimulated with SDF-1 for a series of time points or not ("time point 0"), lysed and analyzed by Western blot or ELISA for Ser473-phosphorylated (p473), Thr308-phosphorylated (p308) or total (t) Akt. **A.** The ratio of p473 to tAkt was quantified by densitometry and normalized to Mut cells at time point 0. Data are mean ± SEM from seven blots based on three independent batches of SDF-1 stimulation. No inhibition of Akt Ser473 phosphorylation in WT cells vs Mut cells was observed. **B.** Akt Thr308 phosphorylation was quantified similarly to A, and was not found to be inhibited in WT vs Mut cells. **C.** Cellular p473 levels were quantified as OD values in ELISA. Results are mean ± SEM from two experiments. p473 levels was not found to be reduced in WT vs Mut cells. The use of an alternative stimulus, a BCR

activating antibody led to similar patterns as in A-C (data not shown for simplicity). Results were obtained in collaboration with Sen Hou and Nipun Jayachandran.

Figure 5.7

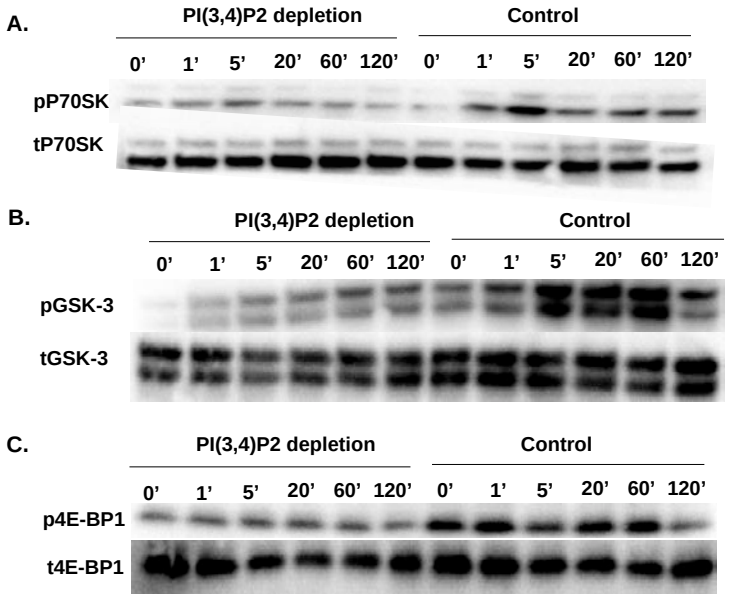

Figure 5.7 PI(3,4)P2 depletion may lead to reduced Akt activity.

PI(3,4)P2-depleted (INPP4A WT) and control (INPP4A Mut) RAJI cells as in Figure 6.1 were stimulated with SDF-1 or a BCR activating antibody and analyzed by Western blot for phospho- (P) and total (t) p70SK, GSK-3 and 4E-BP1 proteins, substrates of Akt. Blots shown represent two batches of experiments, together suggesting a trend of reduced phosphorylation of these Akt substrates.

5.2.5 Akt positively regulates malignant B cell migration

To investigate the role of Akt in malignant B cell migration, Akt inhibitors MK-2206 (100 nM), Perifosine (1 μM) or Triciribine (1 μM) were applied to RAJI cells and migration to SDF-1 was assessed by transwell chamber assay. All three inhibitors led to reduced migration, indicating a positive role of Akt in this cellular context (Figure 5.8). These data, together with the observations that PI(3,4)P2 depletion may inhibit Akt activity, suggest that PI(3,4)P2 may mediate malignant B cell migration partly through promoting Akt activity.

Figure 5.8

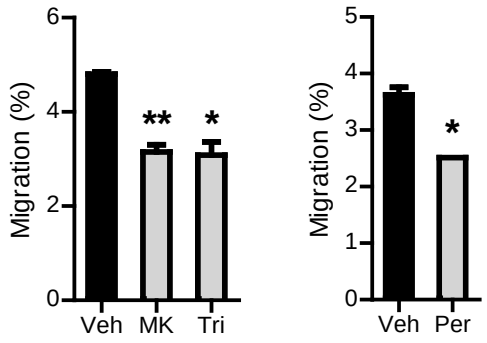

Figure 5.8 Akt promotes malignant B cell migration

RAJI cells were assayed for Transwell migration to SDF-1 in the presence of Akt inhibitors MK-2206 (100 nM), Triciribine (1 uM) or Perifosine, or their vehicles DMSO (for MK-2206 and Triciribine) or H2O (for Perifosine). Results from three independent experiments were graphed as mean ± SD. Significant difference in cell migration was determined by Student's *t* test: * $p < 0.05$ and ** $p < 0.01$.

5.3 Discussion

In this study Lpd is found to be endogenously expressed in malignant B cells. Stringent confocal microscopy experiments here indicate that the localization pattern of Lpd in live chemotaxing B cells highly matches that of PI(3,4)P2, and this colocalization depends on its PH domain. Our results strongly support the current belief that Lpd is a PI(3,4)P2-binding protein. In other cell types, Lpd is known to interact with Ena/VASP and Scar/WAVE, protein complexes that regulate F-actin and lamellipodia dynamics. Lpd (or its orthologue Pico in Drosophila) was recently found to mediate the migration of mouse embryonic fibroblasts, mouse and Xenopus neural crest cells and Drosophila epithelial border cells by promoting random motility [260]. The role of Lpd in mediating directional migration (chemotaxis) has not been investigated. In this study, we have observed that Lpd controls both the speed and directionality of chemotaxis in the context of human B cells.

We have further dissected Lpd functions in migration concerning their dependence on the PH domain. Both wild type Lpd (Lpd-GFP WT) and PH domain-deleted mutant (Lpd-GFP ΔPH) rescued the motility defect in Lpd KD cells. However, compared to Lpd-GFP WT, Lpd-GFP ΔPH was strongly impaired in the ability to maintain directionality in Lpd KD cells. In addition, when expressed in cells without endogenous Lpd depletion, Lpd-GFP ΔPH appeared to disrupt migration, perhaps by interfering with endogenous Lpd signaling. In both cases, the Lpd-GFP ΔPH-expressing cells failed to migrate persistently at the direction of attractant gradient (SDF-1). These data indicate that Lpd serves as an effector of PI(3,4)P2 signaling in controlling migration

directionality, whereas Lpd function in promoting motility is independent of PI(3,4)P2. Since PI(3,4)P2 also controls motility (not through Lpd), this function must be through other PI(3,4)P2 effectors.

Akt is the most widely known effector of PI3K signaling, and a large body of literature has established that the Akt kinase isoforms are involved in diverse cellular functions. Among these, cell migration was found to be differentially regulated by both stimulatory and inhibitory Akt isoforms. In the context of RAJI lymphoma B cell migration, inhibition of Akt activity leads to reduced migration, suggesting that Akt activity is needed for optimal migration. It remains to be determined whether different Akt isoforms are expressed and what role each individual isoform plays in regulating migration in B cells.

Regarding a potential role of Akt as a PI(3,4)P2 effector in controlling migration, it is currently dominant belief that PI(3,4)P2 can promote Akt phosphorylation and activation; However, the opposite effect was also reported [311]. Akt phosphorylation is generally required for its full activation and these two events are often found to be correlated. However, it is also been observed that the level of phosphorylation does not necessarily indicate that of activity [308-310]. This suggests that Akt phosphorylation may not on its own be sufficient to determine activity and other regulatory steps may modulate Akt activity as well. Overall, the literature seems to suggest that Akt is subject to complex regulation, which may depend on cellular contexts.

In RAJI cells treated with SDF-1 or BCR activating antibody, PI(3,4)P2 depletion largely does not significantly affect Akt phosphorylation. However, Akt activity appears to be inhibited as suggested by reduced phosphorylation of Akt substrates. The mechanisms are unknown by which PI(3,4)P2 modulates the activity of Akt, especially at the level of specific isoforms in the B cell context. Collectively, the results here suggest that PI(3,4)P2 control of migration may be in part by promoting Akt activity. A number of downstream targets of Akt are known to mediate migration of other cell types, such as GSK-3, which promotes integrin recycling (See Introduction section 1.13). In the context of malignant B cell migration, their potential involvement may be tested. Taking together the present and previous studies, it will be significant future work and require major undertaking to understand the mechanisms by which PI(3,4)P2 differentially regulate Akt phosphorylation and activity, and how different Akt isoforms impact on cell migration, in different cellular contexts including in B cells.

Chapter 6 General discussion and summary of findings, significance and future directions

6.1 Technical challenges facing B cell migration study and methodological advancements accomplished in this thesis

The study of molecular mechanisms of B cell migration has remained largely an untouched area of research and has been hindered by technical challenges. Primary B cells and B cell-derived cancer cells such as CLL B cells are highly sensitive to in vitro culture conditions. These cells, together with cell lines derived from them, are known to be difficult-to-transfect using traditional methods of gene transfer such as lipid- or electroporation-based methods, placing a major obstacle to gene function studies. Particularly, transfections often lead to significant reduction in cell viability, which is critical for cell migration experiments. In addition, in-depth insights into cell migration require high resolution imaging of intracellular molecular dynamics and distribution. This has been achievable in studies of random migration; however in the case of chemotaxis, high resolution imaging needs to be coupled with chemoattractant gradient control system. To induce Dictyostelium chemotaxis, chemoattractant can be simply applied by a glass pipette, since monitoring the fast migration of Dictyostelium needs only a transient gradient profile. However, in the slower chemotaxing B cells, a stable gradient has to be maintained over time by better controlled system, such as the microfluidic technology that is becoming more widely used in the recent years. Visualization of intracellular

molecules during chemotaxis is often facilitated by using fluorescent fusion bioprobes in live cells. However, in many more scenarios, cells have to be fixed and further processed. For example, the bioprobes can themselves interfere with the cellular function of interest. It has been noticed that RFP-tagged TAPP PH domains intended to probe PI(3,4)P2 distribution in chemotaxing RAJI cells appear to inhibit migration, making it not possible to track PI(3,4)P2 in "migrating" cells using this method (Data not shown). Alternatively intracellular molecules can be stained by antibodies, which requires cell fixation, permeabilization and other steps before the imaging.

Intensive efforts have been made towards overcoming the challenge of gene transfer into B cells. While the set-up of materials and methods consumed particularly significant part of time available to advance the projects, encouraging success has been achieved to establish the prerequisite methods. Taking advantage of the capability of lentivirus to transduce most, if not all, mammalian cell types, including both dividing and non-dividing cells, I have established and optimized the production protocols of VSV-G pseudotyped lentivirus and transduction of a variety of leukemia or lymphoma B cell lines for gene overexpression or knock-down. To transduce primary CLL B cells, I have obtained preliminary success by optimizing the protocols for production and use of measles virus glycoprotein-pseudotyped lentivirus (M-LV) in collaboration with Drs. Cosset and Verhoeyen from France [312]. This method in my hands showed high transduction efficiency in primary CLL B cells (Figure 6.1).

Figure 6.1

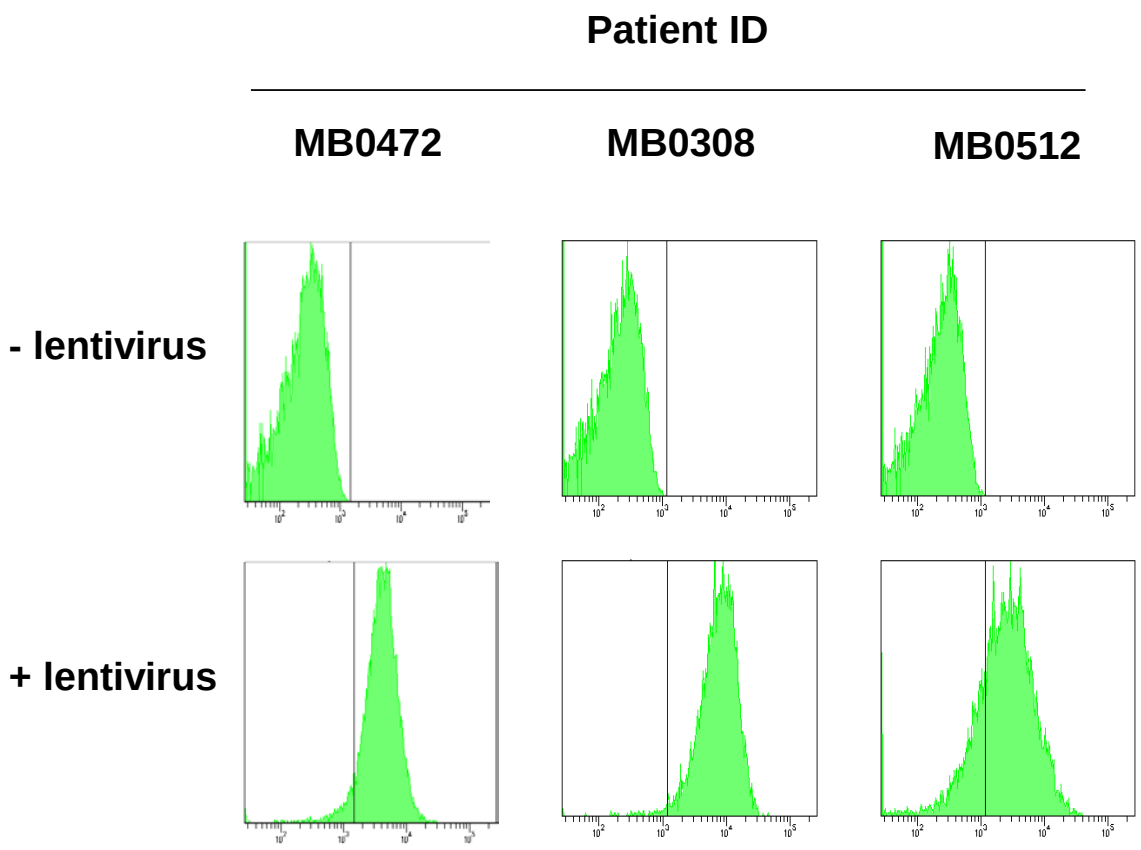

Figure 6.1 High efficiency transduction of primary CLL B cells by M-LV

CLL B cells were transduced with M-LV expressing a GFP co-reporter at MOI = 100 and analyzed by flow cytometry. Intracellular expression of GFP was confirmed by confocal microscopy (data not shown).

However, the method for generation of M-LV requires further optimization to overcome low and variable viral packaging efficiency. An alternative method for gene transfer into primary B cells has been developed and used, based on the Neon Transfection System, new generation of electroporation-based technology. I have established Neon transfection protocols in RAJI cells and primary CLL B cells. Additional protocols have also been established for a series of other B cell lines by Edward Noh, a former colleague in our lab under my training.

Despite the B cell sensitivity to in vitro conditions of culture, transfection/transduction and other manipulations, I have established procedures to quantify effects of single gene knock-down or overexpression on migration in transwell chambers, which can sometimes be at minor magnitudes. Thanks to the collaborative work between our and Dr. Francis Lin's laboratories, new methods have been established to characterize and quantify the chemotactic behaviors of individual B cells using the microfluidic chemotaxis system, which provides controlled chemokine profile coupled to confocal microscopy. Particularly, optimization of the assay conditions for B cells and establishment of methods of fixing and further processing chemotaxing cells within the microfluidic device now makes possible the staining of intracellular molecules in cells chemotaxing under controlled chemoattractant gradient for high resolution imaging. To the best of my knowledge, high resolution imaging based on real time fixation of chemotaxing cells in the microfluidic device (to maintain the chemotaxis status of cells) has not been reported.

6.2 The migration of malignant B cells are controlled by multiple chemokines and possibly multiple PI3K isoforms

In this thesis, the roles of PI3K-PI(3,4)P2 signaling axis and its regulators have been studied using SDF-1-induced chemotaxis as a model system, because SDF-1 has been the best studied and perhaps the most important chemoattractant of malignant B cells. However, these cells were also reported to express other functional chemokine receptors such as CXCR5 and CCR7, and are attracted by CXCL13 (ligand for CXCR5) as well as CCL19 and CCL21 (ligands for CCR7). Chemotaxis of malignant B cells driven by these latter chemokines are also dependent on PI3K [291, 292]. It will be interesting to test if PI(3,4)P2-related signaling is also implicated in malignant B cell migration induced by chemoattractants other than SDF-1, to determine a general versus SDF-1-specific role.

PI3K isoforms appear to play differential roles in mediating the chemotaxis and homing of lymphocytes in mice, with p110γ and p110δ specifically required in T cells and B cells, respectively [313]. However, my data here suggest that the migration of multiple human malignant B cell lines is inhibited by all tested Class I PI3K inhibitors including pan isoform inhibitor GDC-0941, β isoform inhibitor TGX-221, γ isoform inhibitor AS-605240, and δ isoform inhibitor CAL-101, except that an α isoform inhibitor PI-103 inhibits migration in some but not other cell lines (data not shown). These previous and present observations suggest that in different cellular contexts, cells may use different PI3K isoforms to migrate. The mechanisms underlying the differential dependence on PI3K isoforms are currently unknown. It is also a remaining question whether the

activities of multiple PI3K isoforms add up to contribute to an overall cellular PI3K activity required for optimal chemotaxis, or the different isoforms may play unique non-redundant functions.

It should be mentioned that the use of pharmacological inhibitors always concerns potential off-target effects as in other ways to inhibit signaling proteins. The PI3K inhibitor study here was based on a single concentration of 2 uM, which was much higher than the IC50 of these inhibitors (http://www.selleckchem.com/), intended to maximize PI3K inhibition: The IC50 values GDC-0941 are 3 nM for p110α and δ, 33 nM for p110β and 75 nM for p110γ. The IC50s of TGX-221, AS-605240 and CAL-101 for p110β, γ and δ, respectively, are 5 nM, 8 nM and 2.5 nM. To reduce potential off-target effects, optimization of the experimental conditions would be to titrate down the concentrations of these inhibitors to nearer their IC50s. In addition, to better confirm the effects of PI3K inhibition on malignant B cell migration, several alternative methods may be applied, including using multiple inhibitors targeting the same PI3K isoform, genetic knock-down of specific PI3K isoforms of interest and knock-in of their kinase-dead mutants.

Additional insight remaining to be obtained in these PI3K inhibitor experiments is whether the inhibition of PI3K activity is complete. A traditional way to test this is based on the quantification of the phosphorylation and activity of Akt, a major target of PI3K signaling. Alternatively, it is expected that PI3Ks may be pulled-down from the lysates of the B cells and assayed for in vitro kinase activity directly. As discussed before in Chapter 4, a possible (Class I) PI3K-independent role of TAPP2 was mentioned based on

the assumption that ideally a complete inhibition of PI3K activity might have been achieved. However, I would tempt to speculate that very possibly the inhibition of (class I PI3K) activity was incomplete. In addition, the activity of Class II PI3Ks, which is not inhibitable by the Class I inhibitors used in this study, may serve to provide significant source of PI(3,4)P2. As a result, under these conditions, PI(3,4)P2 may be still available to promote TAPP2 function in cell migration. Therefore, these possibilities are worth addressing in future investigations towards more in-depth understanding of the PI3K-PI(3,4)P2-TAPP2 pathway in cell migraton.

6.3 PI3K in cell migration: Not just PIP3

The PI3K signaling network generates 3-phosphoinositide messengers, including PIP3, PI(3,4)P2 and PI(3)P (Figure 1.1). PIP3 is known to regulate cell migration. Some Rho GTPases regulate migration depending on their PIP3-specific PH domains (See Chapter section 1.10). It remains as a key question in the field of cell migration research whether PI(3,4)P2 and PI(3)P function in cell migration. The findings described in this thesis indicate that PI(3,4)P2 depletion by its specific phosphatase INPP4A or INPP4B, relative to their phosphatase-dead mutants, inhibits malignant B cell chemotaxis, indicating an essential role of PI(3,4)P2 in mediating both the speed and directionality. In the attempts to identify signaling effectors downstream of PI(3,4)P2, the authenticated PI(3,4)P2-specific binding protein TAPP2 is found to phenocopy the functions of PI(3,4)P2 in malignant B cell chemotaxis. Concerning Lpd, another possible signaling effector of PI(3,4)P2, strong evidence is provided here in favor of the idea that Lpd binds to PI(3,4)P2 via its PH domain in live cells. Interestingly, Lpd mediates the directionality

of malignant B cell chemotaxis depending on its PH domain, whereas it also functions to promote migration speed in a PH domain-independent fashion. Lpd is known to bind WAVE complex to promote F-actin based protrusion, a major known driving force of cell motility [260]. It also limits G-actin level to maintain the activity of serum response factor and consequently the transcription of cytoskeleton – regulatory genes [270]. It is worth testing if Lpd performs these functions to promote migration speed independently of PH domain binding to PI(3,4)P2. Lastly, another PI(3,4)P2-binding protein Akt (which also binds to PIP3), plays a positive role in the context of malignant B cell migration. These studies indicate that PI(3,4)P2 leads a new branch of PI3K signaling in regulating cell migration and identify PI(3,4)P2-specific phosphatase INPP4 and binding proteins TAPP2, Lpd and Akt as important regulators of malignant B cell migration, which may potentially serve as therapeutic intervention targets.

A potential caveat of using INPP4 to deplete PI(3,4)P2 is that as a result of PI(3,4)P2 degradation, another lipid messenger of PI3K signaling, PI(3)P, is produced. As mentioned in the Introduction, the cellular level of PI(3)P is much greater than that of PI(3,4)P2 and hence it is the current belief that the effect of INPP4 phosphatase activity is by turning off signaling through PI(3,4)P2, but not the resulting production of PI(3)P, which has negligible contribution to the cellular pool of PI(3)P [62, 63, 65, 66]. The clear role of PI(3,4)P2 signaling here is further supported by the evidence that the specific PI(3,4)P2-binding protein Lpd, which does not bind to PIP3 or PI(3)P, mediates the directionality of chemotaxis depending on its PH domain.

PI(3)P as a functional signaling molecule has been considerably well studied in recent years. It is predominantly generated by Class II and III PI3Ks on endosomes, multivesicular bodies and phagosomes [63, 65]. PI(3)P recruits FYVE or PX domain-containing proteins and mediates endosomal trafficking, cargo sorting to lysosomes, autophagy and cytokinesis [314-316]. So far PI(3)P has not been reported to regulate cell migration, however it remains possible that localized production of PI(3)P may enhance endocytosis of chemokine receptor at the migrating front, contributing to the effect we observe. Several PI(3)P phosphatases have been identified [317]. To best confirm that INPP4 phosphatase activity inhibits migration through PI(3,4)P2 degradation but not PI(3)P production, one of the future experiments of interest would be to test the effects of hybrid molecules of INPP4 tethered to PI(3)P phosphatases, which removes PI(3)P generated along with PI(3,4)P2 degradation.

It is noteworthy that based on the experimental system of this work, an apparently small percent increase of PI(3,4)P2 accumulation is induced by SDF-1 stimulation in RAJI cells (up to approximately 20% relative to its cellular levels at “basal” state). The magnitude of PI(3,4)P2 reduction by INPP4 expression was comparable to that of the chemokine-induced increase in PI(3,4)P2. This magnitude of PI(3,4)P2 changes were similarly observed in leukemic B cells from CLL patients (data not shown). The failure of INPP4 expression to eliminate all basal level of cellular PI(3,4)P2 signal may be explained by the following possibilities. Since quantification of PI(3,4)P2 in malignant B cells has not been reported, my data suggest that PI(3,4)P2 may be present at significant levels in these cells even at their resting state. INPP4 protein and some of the cellular

PI(3,4)P2 pools may localize to distinct cellular microdomains, which renders INPP4 inaccessible to these PI(3,4)P2 pools. Distinguishing such microdomains would need imaging methods with higher resolution than those used in this work. In addition, although the PI(3,4)P2 antibody was reported to be specific for PI(3,4)P2 (see below), potential non-specific binding may add to the apparent basal PI(3,4)P2 signal. Alternative methods, such as the traditional chromatography may provide additional insights into the cellular levels of PI(3,4)P2 in malignant B cells under basal condition, and the effect of chemokine stimulation and INPP4 expression. Despite the apparently "small" percentage of reduction in cellular PI(3,4)P2 levels resulting from INPP4 expression, this did lead to significant migration inhibition in RAJI cells and some of the CLL patient cells, suggesting that the migration of these cells is highly sensitive to perturbation of PI(3,4)P2 signaling. In some other CLL patients, PI(3,4)P2 inhibition seemed to affect migration at relatively lower magnitude. It is likely that the migration of these cells is relatively less strongly dependent on the maintenance of high PI(3,4)P2 level or a lower level of PI(3,4)P2 depletion was achieved in these patient samples.

6.4 Localization of PI(3,4)P2 in migrating cells

In general, cell migration regulatory molecules are characterized by special, often asymmetric or polarized, subcellular distribution patterns. PI3K products were generally believed to be highly enriched at the front of a migrating cell. However, most previous work used the PH domain of Akt to probe PI3K activity, which does not distinguish between PIP3 and PI(3,4)P2 [293, 294]. A few studies applied GFP fusions or FRET biosensors based on the PI(3,4)P2-specific PH domain of TAPP1 to investigate the

localization of PI(3,4)P2 in migrating cells. The zebrafish primordial germ cells (PGCs) directionally migrate to the region of gonad. GFP-TAPP1 PH transfected into these cells did not show any preferential local enrichment [318]. During random migration of zebrafish neutrophils, GFP-TAPP1 PH was enriched at the front, and (seemingly to a lesser extent) at the tail [55]. In motile Madin-Darby canine kidney (MDCK) cells, FRET experiments indicated that PI(3,4)P2 signal was the most accumulated at the leading edge, while the enrichment was also seen on the membrane of the other parts of the cell [319]. In this thesis work, a PI(3,4)P2-specific antibody [62, 248] was used to stain PI(3,4)P2 in migrating B cells. We extended previous studies by visualizing the localization in 3D. PI(3,4)P2 is extensively present on the cell membrane, but more enriched at the front. The PI(3,4)P2 distribution pattern was faithfully matched by that of its binding protein and signaling effector, Lpd. These distribution patterns appear consistent with the function of PI(3,4)P2-Lpd signaling in maintaining persistent migration directionality.

Notably, the colocalization of PI(3,4)P2 and Lpd was determined within the capacity of the current confocal microscopy technology. While potentially these molecules could localize to separate microdomains of the cell membrane, this possibility can only be addressed with higher resolution imaging methods. Nevertheless, these live cell – based data are consistent with the classical in vitro lipid overlay experiments showing specific direct binding of Lpd to PI(3,4)P2 [71], both cases together supporting Lpd as a PI(3,4)P2-binding protein. A third way to further support this argument is to assess the effect of INPP4 expression on Lpd localization, with expectation that INPP4 WT, but not Mut control, reduces the membrane accumulation of Lpd.

The variation in PI(3,4)P2 localization patterns from different reports may be explained or consolidated as follows. Different cell types and/or migration contexts (random motility or chemotaxis) may differentially depend on variant versions of distribution patterns of PI(3,4)P2 as part of the migration machinery that suits that specific context. Note that depending on cellular contexts, PI3K is known to differentially regulate multiple aspects of cell migration, such as motility versus directionality. In addition, variables may potentially arise from different detection methods. GFP-TAPP PH has been an useful tool traditionally to probe PI(3,4)P2. Theoretically, however, the GFP fusion is constitutively fluorescent whether or not binding to PI(3,4)P2, which raises the potential concern that the fluorescent signal may not faithfully represent PI(3,4)P2 or reflect its differential localization if the GFP-TAPP PH molecules overwhelmingly outnumber PI(3,4)P2. Thus, the expression level of the probe may preferably be controlled. Presumably, a FRET biosensor or antibody may have the advantage of giving signal only when binding to PI(3,4)P2. In our work, the PI(3,4)P2 staining pattern was further supported by strong consistency with the localization pattern of its binding protein and effector Lpd.

As above mentioned, previous studies extensively used Akt PH domain to probe PI3K products in migrating cells. However, this probe does not distinguish between PIP3 and PI(3,4)P2. Apart from this work, where PI(3,4)P2 localization was visualized by using its specific antibody, no report has indeed been made regarding the localization of PIP3 in chemotaxing B cells. This will be one of the major future insights remaining to be

obtained in understanding phosphoinoside regulation of B cell chemotaxis. PIP3-specific antibodies and PH domain probes such as that from Btk are expected to be useful tools. Another interesting issue is that PI(3,4)P2 did not seem to be present at significant level at the cellular contact with the substratum, fibronectin – coated surface. However, it is possible that technically this contact plane, expected to be very thin, is hard to catch by regular confocal Z stack imaging method as used in this study. Higher resolution method, such as total internal reflection fluorescence microscopy (TIRF), should be applied to image PI(3,4)P2 and PIP3 localization proximal to the cell – matrix interface.

6.5 Implication of the PI(3,4)P2 pathway in component processes of malignant B cell chemotaxis

6.5.1 Regulation of cell surface expression of CXCR4

PI(3,4)P2 depletion reduces cell surface CXCR4 by approximately 20%, which may contribute to impaired chemotaxis, potentially affecting both directionality and motility, as the sensing of SDF-1 by CXCR4 is the first step of cellular activation leading to directional migration. One possible future experiment to confirm this might be to knock down CXCR4 expression to such extent that the surface level of CXCR4 is similar to that of PI(3,4)P2-depleted cells, and test effect on chemotaxis.

The mechanism(s) by which cell surface CXCR4 is downregulated in PI(3,4)P2-depleted cells are not known. The effect does not appear to arise from the disruption of TAPP2 or

Lpd signaling, since the knock-down of either molecule does not affect the surface level of CXCR4. The potential involvement of other PI(3,4)P2 effectors such as Akt and SNX9 may be worth testing. CXCR4 is known to be internalized from cell surface through clathrin-mediated endocytosis [320]. It is recently reported that PI(3,4)P2-depletion by INPP4B inhibits clathrin-mediated endocytosis [62]. According to this study, a reduced endocytosis would have led to increased retention of CXCR4 on the surface and thereby higher level of surface CXCR4. However, other cellular processes may contribute to the net outcome. PI(3,4)P2 depletion may lead to reduced synthesis of CXCR4 or its trafficking to the surface, or increased degradation, by unknown mechanisms. It will be interesting to examine the intracellular level and distribution of CXCR4 in PI(3,4)P2-depleted cells versus control cells.

6.5.2 Regulation of the actin cytoskeleton

All the three PI(3,4)P2-binding proteins investigated in this thesis, TAPP2, Lpd and Akt, have been shown elsewhere or in studies here to regulate the actin cytoskeleton. TAPP2 KD in malignant B cells leads to impaired F-actin accumulation in response to chemokine stimulation and aberrant actin cytoskeleton structure forming multi-protrusions. In other cell types studied previously, Lpd is known to interact with actin regulatory protein complex WAVE to promote highly branched F-actin structure and lamellipodia formation required for cell migration [260]. By converting G-actin to F-actin, Lpd also maintains the activity of SRF, a transcription factor that regulates the expression of cytoskeleton-regulatory genes [270-272]. In other cell types, Akt is found to directly bind to and phosphorylate actin [139-141]. It also phosphorylates the actin binding

protein girdin/APE to promote integrity of actin structures and migration [129]. It will be essential future work to test if INPP4, Lpd and Akt, in the context of malignant B cell migration, also impact on these downstream targets described above to modulate actin dynamics critical for migration.

6.5.3 Adhesion

A previous study of our lab indicated that TAPP2 promotes the adhesion of malignant B cells to matrix proteins fibronectin and laminin through interacting with utrophin. This function appears to depend on the binding of TAPP2 to PI(3,4)P2, as PH domain-mutant TAPP2 inhibits adhesion [225]. It is likely that PI(3,4)P2 controls malignant B cell migration in part by modulating the adhesion to matrix proteins.

6.5.4 Cell body contraction and rear retraction

As revealed in this thesis and some other recent studies, PI(3,4)P2 is present not only at the front but also other parts of a migrating cell. It is worth testing if PI(3,4)P2 signaling and its regulators are implicated in signaling events contributing to cell body contraction and rear retraction, such as rear definition, actomyosin contractility and adhesion molecule recycling. As discussed in Chapter 3, TAPP2, colocalized with utrophin and stable F-actin, known rear markers of migrating cells, may act to promote backness signaling by inhibiting Rac. Akt is known to regulate myosin II assembly and integrin recycling, which can also be tested in the context of B cell migration.

6.6 Other potential PI(3,4)P2 effectors in cell migration

In addition to Akt, some other signaling proteins have been found to bind both PI(3,4)P2 and PIP3 [66], such as SWAP-70 [321, 322], PDK1 [207], PLCγ1 [293], ARNO [222] and Bam32 [69]. Recent data indicate (potential) involvements of these molecules in the migration of various cell types, to be detailed later. Among these, SWAP-70 is already known to control B cell migration, but the roles of the other four remain to be assessed in this cellular context. It will be interesting future work to address the relative contribution of PI(3,4)P2 versus PIP3 to the migration-regulatory functions of these molecules.

In switch-associated protein-70 (SWAP-70), the PH domain is required for PI3K-dependent translocation of SWAP-70 from the cytoplasm to membrane [322]. SWAP-70 possesses a PH domain-dependent Rac GEF function and was proposed to regulate F-actin dynamics [321-325]. It also directly binds to non-muscle F-actin [323] and interacts with cofilin, to regulate the bundling and stability of F-actin [326]. In addition, SWAP-70 is implicated in RhoA activation and retraction of the trailing edge in migrating bone marrow-derived dendritic cells (BMDCs) stimulated with sphingosine 1-phosphate (S1P) [327]. In B cells, eosinophils and mast cells, SWAP-70 deficiency leads to impaired adhesion and migration [324, 325, 328, 329]. The migration phenotype is typically characterized by inefficient polarization to form the leading edge and uropod [324, 328, 329].

PDK1 has been reported to promote the migration of endothelial cells, melanoma cells, T cells, neutrophils and epithelial cells [330-334]. PDK1 was proposed to regulate cell migration via phosphorylating Akt [332-334]. However, the effects of PDK1 on cell migration turn out to be independent of its kinase activity [330, 331]. PDK1 promotes myosin light chain (MLC) phosphorylation and actomyosin contractility by two mechanisms so far identified. It directly binds to ROCK1 and promotes its localization to the cell membrane. This interaction keeps ROCK1 from being bound by RhoE/Rnd3, a negative regulator of ROCK1. In turn, ROCK1 increases MLC phosphorylation and actomyosin contractility [331]. Similarly, PDK1 interacts with and positively modulates the activity of myotonic dystrophy kinase-related Cdc42-binding kinase α (MRCKα), another MLC kinase [330].

PLCγ1 localizes at the leading edge of migrating MDA-MB-231 breast cancer cells in a PI3K-dependent manner based on its PH domain. Stable expression of the PH domain fragment blocks migration [335]. PLCγ1 mediates CCL21-induced T cell migration on fibronectin through cross-talk with ERK1/2 [336]. It also promotes Rac activation, invasion and metastasis in breast cancer cells [337].

Regarding ARNO/cytohesin2, it mediates the migration of Madin-Darby canine kidney (MDCK) cells and mouse preadipocyte 3T3-L1 cells by acting as a GEF for Arf (ADP ribosylation factor) family small GTPase Arf6, which cross-talks with and activates Rac [338, 339].

Bam32/DAPP1 is found by our lab to mediate Rac activation, F-actin remodeling and adhesion function in B cells [290, 340], implying a potential function in B cell migration that is worth testing.

6.7 The PI(3,4)P2 pathway may serve as potential therapeutic intervention targets: Possible implication in the migration, localization and drug resistance of malignant B cells in vivo

Malignant B cells can sense chemokine attractants, including SDF-1, CXCL13, CCL19 and CCL21, which are believed to drive the spread of these cells into destination organs such as bone marrow and lymph nodes, where they localize to supportive microenvironments, form proliferation centers and acquire drug resistance. Encouragingly, TAPP2 KD in NALM-6 leukemic cells disrupts SDF-1-induced chemotaxis and migration under co-cultured bone marrow-derived stromal cells. While stromal cells are found to enhance drug resistance of the leukemic cells to a chemotherapy drug, fludarabine, TAPP2 KD sensitizes the leukemic cells to drug killing in the stromal coculture context. Similar experiments may be carried out to assess the roles of INPP4, Lpd and Akt in this system. Lastly, the effects of targeting PI(3,4)P2 signaling and its regulators on malignant B cell dissemination, localization, expansion and drug sensitivity may be evaluated in vivo using xenograft models based on immunodeficient mice inoculated with malignant B cell lines or primary CLL B cells expressing different levels of INPP4, TAPP2, Lpd or Akt in combination with inhibitor or drug treatments.

6.8 Summary of major findings, significance and future directions

6.8.1 Major findings

In malignant B cells:

- Depletion of the lipid messenger PI(3,4)P2 by its specific phosphatase INPP4 inhibits chemotaxis, reducing both directionality and speed.
- PI(3,4)P2-binding protein TAPP2 mediates both directionality and speed of chemotaxis
- PI(3,4)P2-binding protein Lpd mediates the directionality of chemotaxis depending on its PI(3,4)P2-binding PH domain, while it promotes speed independently of its PH domain.

6.8.2 Significance

Cell migration is critical to a wide range of physiological and pathological events and is central to disease progression of B cell-derived leukemia and lymphoma and many other types of cancer. However, signaling pathways controlling cell migration remain to be better understood. The projects described in this thesis have provided novel findings indicating that PI(3,4)P2 signaling plays an important role in cell migration in the context of malignant B cell chemotaxis. This work has also made substantial progress towards the identification and characterization of signaling regulators or (potential) effectors of the

PI(3,4)P2 pathway that impact on cell migration. These contributions are expected to kindle new research efforts to advance our understanding of the biology of cell migration. The insights into PI(3,4)P2-related signaling regulators or effectors presented here also suggest the potential of these molecules to serve as therapeutic intervention targets for disrupting malignant B cell dissemination, expansion and drug resistance, which encourages future investigation.

6.8.3 Future directions

PI3K is known to control migration function at multiple levels depending on cellular contexts, dictating speed or/and directionality [25, 27, 29, 56, 57]. The present and previous studies indicate that PI3K is essential to malignant B cell migration to chemokine attractants based on Transwell assay. However, this traditional method quantifies only the net percentage of cells that migrate from the upper chamber to the chemokine-containing lower chamber, providing no information distinguishing speed versus directionality. Also, the detailed migration behaviors of individual cell movements and migratory cell morphology cannot be visualized. It will be interesting future experiments to observe malignant B cell chemotaxis in the microfluidic chemotaxis system where cells are treated with PI3K inhibitors (or Akt inhibitors as well).

While the role of PI(3,4)P2 signaling in cell migration was investigated here in the context of malignant B cells, it remains an interesting question whether this is generalizable to normal B cells or other cells types or it is specific for malignant B cells. Several lines of hints imply that the former possibility may be true. As described in

Chapter 2, loss of PI(3,4)P2-specific phosphatase INPP4B leads to enhanced wound healing response in breast cancer and melanoma cells and the PI(3,4)P2 binding protein Lpd mediates random motility in multiple cell types. These data imply that PI(3,4)P2 may play a general role in cell migration including in normal B cells. It is open possibility as well that some specific cellular contexts may not or less depend on PI(3,4)P2 pathway, since variations in the cellular machinery can sometimes arise from diverse signaling contexts, as exemplified by the recent findings that Dictyostelium and neutrophil use different phosphoinositide phosphatases, PTEN and SHIP, respectively, to migrate (See Chapter 1 Introduction). Therefore, the role of PI(3,4)P2 signaling is anticipated to be further examined in the future in normal B cells as well as other cell types in general.

Regarding part of the signaling mechanism downstream of PI(3,4)P2, stringent imaging analysis in this thesis work suggests co-enrichment of Lpd with PI(3,4)P2 at the cell membrane in a PH domain – dependent manner. This live cell – based observation and previously identified specific binding of Lpd to PI(3,4)P2, supporting each other, suggest that Lpd is a PI(3,4)P2 binding protein. This view may be further strengthened by a third method examining the effect of INPP4 overexpression on Lpd re-localization. In this scenario, Lpd-GFP will be co-transfected with mKate-tagged membrane marker into RAJI cells stably expressing INPP4A Mut or WT (based on the lentiviral vectors from pLenti4/v5 DEST as described in Chapter 2 Materials and Methods). It is also necessary to test the alternative combination, where Lpd-GFP will be co-transfected with cell membrane - targeted mCherry-INPP4B Mut or WT. It is anticipated that in INPP4 Mut cells, Lpd-GFP will be cell membrane - accumulated, whereas in INPP4 WT cells,

Lpd-GFP will be less membrane - accumulated, or largely show uniform distribution inside the cell, due to the lack of PI(3,4)P2 for targeting Lpd to the membrane. Imaging analysis can be performed first in chambered coverglass without or with uniform stimulation of the cells by SDF-1 (100 ng/ml) for a series of time points including 1, 5 and 20 minutes. Cells will then be fixed with 2% PFA, nuclear stained with DAPI for distinguishing healthy cells (with intact nucleus) from dead cells (with broken nucleus), and analyzed by confocal microscopy for Lpd-GFP localization relative to the membrane – localized proteins. Following this, cells may also be subjected to a stable SDF-1 gradient in the microfluidic chemotaxis system, and then fixed, stained with DAPI and analyzed by confocal microscopy.

Based on the above discussed potential cellular components that may be regulated by PI(3,4)P2 signaling as well as its multiple potential effector proteins , several other future tasks are anticipated to further understand the biology of PI(3,4)P2 - regulated malignant B cell migration. These may include examining the effects of PI(3,4)P2 depletion on F-actin dynamics, polarity, adhesion, cell body translocation and rear retraction; Further investigating whether TAPP2 function in chemotaxis and random motility requires PI(3,4)P2 binding by way of TAPP2 KD rescue with intact versus PH domain mutant TAPP2; Further confirming the effect of PI(3,4)P2 depletion on Akt phosphorylation and activity; Identifying signaling components linking TAPP2, Lpd and Akt to migration phenotypes; And identifying other PI(3,4)P2 effectors in cell migration.

Extending the pioneering efforts of this work based on in vitro systems, a major future

direction is to examine the function of PI(3,4)P2 signaling in cell migration in vivo and evaluate the effect of targeting PI(3,4)P2 signaling on malignant B cell dissemination, expansion and drug resistance in vivo. There are currently several mouse models available with INPP4A or B gene deficient in PI(3,4)P2 phosphatase activity, TAPP proteins deficient in PI(3,4)P2 binding, or Lpd gene knocked-out (See Chapter 1 Introduction). Our lab is also currently developing complete TAPP knock-out mice. B cells from these mice can be adoptively transferred into B cell deficient mice and the in vivo homing and trafficking of PI(3,4)P2 signaling – modified B cells can be analyzed by quantifying migrated cells into different organs/tissues or by real time in vivo imaging. In the cancer setting, genetically manipulation will be performed (for example overexpressing INPP4 or knocking down Lpd based on vectors with a GFP reporter gene) in malignant B cell lines or primary malignant B cells from patients. The GFP+ transduced cells will be mixed at 1:1 ratio with normalizer cells transduced with lentivirus expressing RFP, and injected via tail vein into interleukin common γ chain deficient mice (immunodeficient) in collaboration with Dr. Sam Kung's Lab. At a series of time points, 1, 2, 3 or 4 weeks, mice will be sacrificed, single cell suspensions will be made from bone marrow, lymph nodes, spleen, liver and lung, and the disseminated human cancer B cells will be quantified by flow cytometry based on FSC/SSC, human CD19 staining and GFP or RFP. The GFP+ control, INPP4A or Lpd KD cell numbers will be compared after their normalization to RFP+ cells from the same mouse. A reduced dissemination will be expected in GFP+ INPP4A overexpressing and Lpd KD cells compared to GFP+ empty vector control cells. In vivo cell movements can be real-time analyzed by two photon microscopy. Furthermore, these cell migration experiments can

be combined with the use of therapeutic drugs such as chemotherapy agents. It is anticipated that inhibiting PI(3,4)P2 signaling will block the infiltration and localization of malignant B cells in supportive microenvironments and facilitate the elimination (or improved killing) of these cells by therapeutic drugs.

PI3K inhibitor drugs currently tested in clinical trials target Class I PI3Ks, which are expected to block all PIP3-mediated migratory pathways. However, PI(3,4)P2 can be generated by PI3Ks other than Class I (See Figure 1.1). Therefore, to achieve more effective inhibition of malignant B cell migration, future drugs aimed at fully shutting off PI(3,4)P2 signaling are anticipated to be developed and applied in combinatorial therapy with current class I PI3K inhibitor drugs.

References

1. Schneider, I.C. and J.M. Haugh, *Mechanisms of gradient sensing and chemotaxis: conserved pathways, diverse regulation.* Cell Cycle, 2006. **5**(11): p. 1130-4.
2. Uriu, K., L.G. Morelli, and A.C. Oates, *Interplay between intercellular signaling and cell movement in development.* Semin Cell Dev Biol, 2014.
3. Reig, G., E. Pulgar, and M.L. Concha, *Cell migration: from tissue culture to embryos.* Development, 2014. **141**(10): p. 1999-2013.
4. Trepat, X., Z. Chen, and K. Jacobson, *Cell migration.* Compr Physiol, 2012. **2**(4): p. 2369-92.
5. Oak, J.S., et al., *Lymphocyte cell motility: the twisting, turning tale of phosphoinositide 3-kinase.* Biochem Soc Trans, 2007. **35**(Pt 5): p. 1109-13.
6. Turner, M.D., et al., *Cytokines and chemokines: At the crossroads of cell signalling and inflammatory disease.* Biochim Biophys Acta, 2014. **1843**(11): p. 2563-2582.
7. Reymond, N., B.B. d'Agua, and A.J. Ridley, *Crossing the endothelial barrier during metastasis.* Nat Rev Cancer, 2013. **13**(12): p. 858-70.
8. *Cell Migration Gateway.* Migration 101 - An Introduction to Cell Migration. https://www.cellmigration.org/science/.
9. Ten Hacken, E. and J.A. Burger, *Microenvironment dependency in Chronic Lymphocytic Leukemia: The basis for new targeted therapies.* Pharmacol Ther, 2014.
10. Zuckerman, T. and J.M. Rowe, *Pathogenesis and prognostication in acute lymphoblastic leukemia.* F1000Prime Rep, 2014. **6**: p. 59.
11. Colosia, A., et al., *Clinical Efficacy and Safety in Relapsed/Refractory Diffuse Large B-Cell Lymphoma: A Systematic Literature Review.* Clin Lymphoma Myeloma Leuk, 2014. **14**(5): p. 343-355 e6.
12. Kuruvilla, J., et al., *A Canadian Evidence-Based Guideline for the First-Line Treatment of Follicular Lymphoma: Joint Consensus of the Lymphoma Canada Scientific Advisory Board.* Clin Lymphoma Myeloma Leuk, 2014.
13. Zullo, A., et al., *Gastric MALT lymphoma: old and new insights.* Ann Gastroenterol, 2014. **27**(1): p. 27-33.
14. Zucca, E., A. Stathis, and F. Bertoni, *The management of nongastric MALT lymphomas.* Oncology (Williston Park), 2014. **28**(1): p. 86-93.
15. Pejcic, I., et al., *Mantle cell lymphoma-current literature overview.* J BUON, 2014. **19**(2): p. 342-9.
16. Schmitz, R., et al., *Oncogenic mechanisms in Burkitt lymphoma.* Cold Spring Harb Perspect Med, 2014. **4**(2).
17. Mehta, G.R., et al., *Multiple myeloma.* Dis Mon, 2014.
18. Burger, J.A. and A. Burkle, *The CXCR4 chemokine receptor in acute and chronic leukaemia: a marrow homing receptor and potential therapeutic target.* Br J Haematol, 2007. **137**(4): p. 288-96.
19. Burger, J.A., et al., *The microenvironment in mature B-cell malignancies: a target for new treatment strategies.* Blood, 2009. **114**(16): p. 3367-75.
20. Wong, D. and W. Korz, *Translating an Antagonist of Chemokine Receptor CXCR4: from bench to bedside.* Clin Cancer Res, 2008. **14**(24): p. 7975-80.
21. Teicher, B.A. and S.P. Fricker, *CXCL12 (SDF-1)/CXCR4 pathway in cancer.* Clin Cancer Res, 2010. **16**(11): p. 2927-31.
22. Busillo, J.M. and J.L. Benovic, *Regulation of CXCR4 signaling.* Biochim Biophys Acta, 2007. **1768**(4): p. 952-63.
23. Kucia, M., et al., *CXCR4-SDF-1 signalling, locomotion, chemotaxis and adhesion.* J Mol Histol, 2004. **35**(3): p. 233-45.
24. Konopleva, M., et al., *Therapeutic targeting of microenvironmental interactions in leukemia: mechanisms and approaches.* Drug Resist Updat, 2009. **12**(4-5): p. 103-13.
25. Cain, R.J. and A.J. Ridley, *Phosphoinositide 3-kinases in cell migration.* Biol Cell, 2009. **101**(1): p. 13-29.
26. Yamazaki, D., S. Kurisu, and T. Takenawa, *Regulation of cancer cell motility through actin*

reorganization. Cancer Sci, 2005. **96**(7): p. 379-86.
27. Jin, T., *Gradient sensing during chemotaxis.* Curr Opin Cell Biol, 2013. **25**(5): p. 532-7.
28. Sadik, C.D. and A.D. Luster, *Lipid-cytokine-chemokine cascades orchestrate leukocyte recruitment in inflammation.* J Leukoc Biol, 2012. **91**(2): p. 207-15.
29. Weiger, M.C. and C.A. Parent, *Phosphoinositides in chemotaxis.* Subcell Biochem, 2012. **59**: p. 217-54.
30. Murphy, P.M., *International Union of Pharmacology. XXX. Update on chemokine receptor nomenclature.* Pharmacol Rev, 2002. **54**(2): p. 227-9.
31. McDonald, B., et al., *Intravascular danger signals guide neutrophils to sites of sterile inflammation.* Science, 2010. **330**(6002): p. 362-6.
32. Iijima, M., Y.E. Huang, and P. Devreotes, *Temporal and spatial regulation of chemotaxis.* Dev Cell, 2002. **3**(4): p. 469-78.
33. Janetopoulos, C., T. Jin, and P. Devreotes, *Receptor-mediated activation of heterotrimeric G-proteins in living cells.* Science, 2001. **291**(5512): p. 2408-11.
34. Xu, X., et al., *Coupling mechanism of a GPCR and a heterotrimeric G protein during chemoattractant gradient sensing in Dictyostelium.* Sci Signal, 2010. **3**(141): p. ra71.
35. Germena, G. and E. Hirsch, *PI3Ks and small GTPases in neutrophil migration: two sides of the same coin.* Mol Immunol, 2013. **55**(1): p. 83-6.
36. Neer, E.J., *Heterotrimeric G proteins: organizers of transmembrane signals.* Cell, 1995. **80**(2): p. 249-57.
37. Jin, T., et al., *Localization of the G protein betagamma complex in living cells during chemotaxis.* Science, 2000. **287**(5455): p. 1034-6.
38. Xiao, Z., et al., *Dynamic distribution of chemoattractant receptors in living cells during chemotaxis and persistent stimulation.* J Cell Biol, 1997. **139**(2): p. 365-74.
39. Servant, G., et al., *Polarization of chemoattractant receptor signaling during neutrophil chemotaxis.* Science, 2000. **287**(5455): p. 1037-40.
40. Xu, X., et al., *Quantitative imaging of single live cells reveals spatiotemporal dynamics of multistep signaling events of chemoattractant gradient sensing in Dictyostelium.* Mol Biol Cell, 2005. **16**(2): p. 676-88.
41. Iglesias, P.A., *Spatial regulation of PI3K signaling during chemotaxis.* Wiley Interdiscip Rev Syst Biol Med, 2009. **1**(2): p. 247-53.
42. Janetopoulos, C., et al., *Chemoattractant-induced phosphatidylinositol 3,4,5-trisphosphate accumulation is spatially amplified and adapts, independent of the actin cytoskeleton.* Proc Natl Acad Sci U S A, 2004. **101**(24): p. 8951-6.
43. Senoo, H. and M. Iijima, *Rho GTPase: A molecular compass for directional cell migration.* Commun Integr Biol, 2013. **6**(6): p. e27681.
44. Yoo, S.K., et al., *Differential regulation of protrusion and polarity by PI3K during neutrophil motility in live zebrafish.* Dev Cell, 2010. **18**(2): p. 226-36.
45. Lauffenburger, D.A. and A.F. Horwitz, *Cell migration: a physically integrated molecular process.* Cell, 1996. **84**(3): p. 359-69.
46. Alberts B, J.A., Lewis J, Raff M, Roberts K, Walter P, *The cytoskeleton.* Molecular Biology of the Cell 5th edition, 2007: p. 1036-1046.
47. Takenawa, T. and S. Suetsugu, *The WASP-WAVE protein network: connecting the membrane to the cytoskeleton.* Nat Rev Mol Cell Biol, 2007. **8**(1): p. 37-48.
48. Funamoto, S., et al., *Spatial and temporal regulation of 3-phosphoinositides by PI 3-kinase and PTEN mediates chemotaxis.* Cell, 2002. **109**(5): p. 611-23.
49. Iijima, M. and P. Devreotes, *Tumor suppressor PTEN mediates sensing of chemoattractant gradients.* Cell, 2002. **109**(5): p. 599-610.
50. Knall, C., G.S. Worthen, and G.L. Johnson, *Interleukin 8-stimulated phosphatidylinositol-3-kinase activity regulates the migration of human neutrophils independent of extracellular signal-regulated kinase and p38 mitogen-activated protein kinases.* Proc Natl Acad Sci U S A, 1997. **94**(7): p. 3052-7.
51. Sadhu, C., et al., *Essential role of phosphoinositide 3-kinase delta in neutrophil directional movement.* J Immunol, 2003. **170**(5): p. 2647-54.

52. Hannigan, M., et al., *Neutrophils lacking phosphoinositide 3-kinase gamma show loss of directionality during N-formyl-Met-Leu-Phe-induced chemotaxis.* Proc Natl Acad Sci U S A, 2002. **99**(6): p. 3603-8.
53. Hirsch, E., et al., *Central role for G protein-coupled phosphoinositide 3-kinase gamma in inflammation.* Science, 2000. **287**(5455): p. 1049-53.
54. Afonso, P.V. and C.A. Parent, *PI3K and chemotaxis: a priming issue?* Sci Signal, 2011. **4**(170): p. pe22.
55. Lam, P.Y., et al., *The SH2-domain-containing inositol 5-phosphatase (SHIP) limits the motility of neutrophils and their recruitment to wounds in zebrafish.* J Cell Sci, 2012. **125**(Pt 21): p. 4973-8.
56. Falke, J.J. and B.P. Ziemba, *Interplay between phosphoinositide lipids and calcium signals at the leading edge of chemotaxing ameboid cells.* Chem Phys Lipids, 2014. **182**: p. 73-9.
57. Ward, S.G., *Do phosphoinositide 3-kinases direct lymphocyte navigation?* Trends Immunol, 2004. **25**(2): p. 67-74.
58. Pauls, S.D., et al., *The phosphoinositide 3-kinase signaling pathway in normal and malignant B cells: activation mechanisms, regulation and impact on cellular functions.* Front Immunol, 2012. **3**: p. 224.
59. Balla, T., *Phosphoinositides: tiny lipids with giant impact on cell regulation.* Physiol Rev, 2013. **93**(3): p. 1019-137.
60. Deane, J.A. and D.A. Fruman, *Phosphoinositide 3-kinase: diverse roles in immune cell activation.* Annu Rev Immunol, 2004. **22**: p. 563-98.
61. Li, H., et al., *The tandem PH domain-containing protein 2 (TAPP2) regulates chemokine-induced cytoskeletal reorganization and malignant B cell migration.* PLoS One, 2013. **8**(2): p. e57809.
62. Posor, Y., et al., *Spatiotemporal control of endocytosis by phosphatidylinositol-3,4-bisphosphate.* Nature, 2013. **499**(7457): p. 233-7.
63. Vanhaesebroeck, B., et al., *The emerging mechanisms of isoform-specific PI3K signalling.* Nat Rev Mol Cell Biol, 2010. **11**(5): p. 329-41.
64. Backer, J.M., *The regulation and function of Class III PI3Ks: novel roles for Vps34.* Biochem J, 2008. **410**(1): p. 1-17.
65. Agoulnik, I.U., et al., *INPP4B: the new kid on the PI3K block.* Oncotarget, 2011. **2**(4): p. 321-8.
66. Xie, J., C. Erneux, and I. Pirson, *How does SHIP1/2 balance PtdIns(3,4)P2 and does it signal independently of its phosphatase activity?* Bioessays, 2013. **35**(8): p. 733-43.
67. Balla, T., *Inositol-lipid binding motifs: signal integrators through protein-lipid and protein-protein interactions.* J Cell Sci, 2005. **118**(Pt 10): p. 2093-104.
68. Damen, J.E., et al., *The 145-kDa protein induced to associate with Shc by multiple cytokines is an inositol tetraphosphate and phosphatidylinositol 3,4,5-triphosphate 5-phosphatase.* Proc Natl Acad Sci U S A, 1996. **93**(4): p. 1689-93.
69. Zhang, T.T., et al., *Phosphoinositide 3-kinase-regulated adapters in lymphocyte activation.* Immunol Rev, 2009. **232**(1): p. 255-72.
70. Marshall, A.J., et al., *TAPP1 and TAPP2 are targets of phosphatidylinositol 3-kinase signaling in B cells: sustained plasma membrane recruitment triggered by the B-cell antigen receptor.* Mol Cell Biol, 2002. **22**(15): p. 5479-91.
71. Krause, M., et al., *Lamellipodin, an Ena/VASP ligand, is implicated in the regulation of lamellipodial dynamics.* Dev Cell, 2004. **7**(4): p. 571-83.
72. Thomas, C.C., et al., *Crystal structure of the phosphatidylinositol 3,4-bisphosphate-binding pleckstrin homology (PH) domain of tandem PH-domain-containing protein 1 (TAPP1): molecular basis of lipid specificity.* Biochem J, 2001. **358**(Pt 2): p. 287-94.
73. Lietzke, S.E., et al., *Structural basis of 3-phosphoinositide recognition by pleckstrin homology domains.* Mol Cell, 2000. **6**(2): p. 385-94.
74. Baraldi, E., et al., *Structure of the PH domain from Bruton's tyrosine kinase in complex with inositol 1,3,4,5-tetrakisphosphate.* Structure, 1999. **7**(4): p. 449-60.
75. Etienne-Manneville, S. and A. Hall, *Rho GTPases in cell biology.* Nature, 2002. **420**(6916): p. 629-35.
76. Hanna, S. and M. El-Sibai, *Signaling networks of Rho GTPases in cell motility.* Cell Signal, 2013. **25**(10): p. 1955-61.

77. Gambardella, L. and S. Vermeren, *Molecular players in neutrophil chemotaxis--focus on PI3K and small GTPases.* J Leukoc Biol, 2013. **94**(4): p. 603-12.
78. DerMardirossian, C. and G.M. Bokoch, *GDIs: central regulatory molecules in Rho GTPase activation.* Trends Cell Biol, 2005. **15**(7): p. 356-63.
79. Garcia-Mata, R., E. Boulter, and K. Burridge, *The 'invisible hand': regulation of RHO GTPases by RHOGDIs.* Nat Rev Mol Cell Biol, 2011. **12**(8): p. 493-504.
80. Pollitt, A.Y. and R.H. Insall, *WASP and SCAR/WAVE proteins: the drivers of actin assembly.* J Cell Sci, 2009. **122**(Pt 15): p. 2575-8.
81. Symons, M., et al., *Wiskott-Aldrich syndrome protein, a novel effector for the GTPase CDC42Hs, is implicated in actin polymerization.* Cell, 1996. **84**(5): p. 723-34.
82. Miki, H., et al., *Induction of filopodium formation by a WASP-related actin-depolymerizing protein N-WASP.* Nature, 1998. **391**(6662): p. 93-6.
83. Suetsugu, S., et al., *Differential roles of WAVE1 and WAVE2 in dorsal and peripheral ruffle formation for fibroblast cell migration.* Dev Cell, 2003. **5**(4): p. 595-609.
84. Yamazaki, D., et al., *WAVE2 is required for directed cell migration and cardiovascular development.* Nature, 2003. **424**(6947): p. 452-6.
85. Matsui, T., et al., *Rho-associated kinase, a novel serine/threonine kinase, as a putative target for small GTP binding protein Rho.* EMBO J, 1996. **15**(9): p. 2208-16.
86. Narumiya, S., M. Tanji, and T. Ishizaki, *Rho signaling, ROCK and mDia1, in transformation, metastasis and invasion.* Cancer Metastasis Rev, 2009. **28**(1-2): p. 65-76.
87. Aoki, K., et al., *Local phosphatidylinositol 3,4,5-trisphosphate accumulation recruits Vav2 and Vav3 to activate Rac1/Cdc42 and initiate neurite outgrowth in nerve growth factor-stimulated PC12 cells.* Mol Biol Cell, 2005. **16**(5): p. 2207-17.
88. Weiner, O.D., et al., *A PtdInsP(3)- and Rho GTPase-mediated positive feedback loop regulates neutrophil polarity.* Nat Cell Biol, 2002. **4**(7): p. 509-13.
89. Park, K.C., et al., *Rac regulation of chemotaxis and morphogenesis in Dictyostelium.* EMBO J, 2004. **23**(21): p. 4177-89.
90. Smerling, C., et al., *Role of the alpha(1) integrin cytoplasmic tail in the formation of focal complexes, actin organization, and in the control of cell migration.* Exp Cell Res, 2007. **313**(14): p. 3153-65.
91. Yoshii, S., et al., *alphaPIX nucleotide exchange factor is activated by interaction with phosphatidylinositol 3-kinase.* Oncogene, 1999. **18**(41): p. 5680-90.
92. Keely, P.J., et al., *Cdc42 and Rac1 induce integrin-mediated cell motility and invasiveness through PI(3)K.* Nature, 1997. **390**(6660): p. 632-6.
93. Welch, H.C., et al., *P-Rex1, a PtdIns(3,4,5)P3- and Gbetagamma-regulated guanine-nucleotide exchange factor for Rac.* Cell, 2002. **108**(6): p. 809-21.
94. Costa, C., et al., *Negative feedback regulation of Rac in leukocytes from mice expressing a constitutively active phosphatidylinositol 3-kinase gamma.* Proc Natl Acad Sci U S A, 2007. **104**(36): p. 14354-9.
95. Papakonstanti, E.A., A.J. Ridley, and B. Vanhaesebroeck, *The p110delta isoform of PI 3-kinase negatively controls RhoA and PTEN.* EMBO J, 2007. **26**(13): p. 3050-61.
96. Merlot, S. and R.A. Firtel, *Leading the way: Directional sensing through phosphatidylinositol 3-kinase and other signaling pathways.* J Cell Sci, 2003. **116**(Pt 17): p. 3471-8.
97. Funamoto, S., et al., *Role of phosphatidylinositol 3' kinase and a downstream pleckstrin homology domain-containing protein in controlling chemotaxis in dictyostelium.* J Cell Biol, 2001. **153**(4): p. 795-810.
98. Rameh, L.E. and L.C. Cantley, *The role of phosphoinositide 3-kinase lipid products in cell function.* J Biol Chem, 1999. **274**(13): p. 8347-50.
99. Vanhaesebroeck, B., et al., *Synthesis and function of 3-phosphorylated inositol lipids.* Annu Rev Biochem, 2001. **70**: p. 535-602.
100. Nishio, M., et al., *Control of cell polarity and motility by the PtdIns(3,4,5)P3 phosphatase SHIP1.* Nat Cell Biol, 2007. **9**(1): p. 36-44.
101. Ward, S.G., J. Westwick, and S. Harris, *Sat-Nav for T cells: Role of PI3K isoforms and lipid phosphatases in migration of T lymphocytes.* Immunol Lett, 2011. **138**(1): p. 15-8.

102. Burridge, K. and R. Doughman, *Front and back by Rho and Rac.* Nat Cell Biol, 2006. **8**(8): p. 781-2.
103. Khalil, B.D. and M. El-Sibai, *Rho GTPases in primary brain tumor malignancy and invasion.* J Neurooncol, 2012. **108**(3): p. 333-9.
104. Guilluy, C., R. Garcia-Mata, and K. Burridge, *Rho protein crosstalk: another social network?* Trends Cell Biol, 2011. **21**(12): p. 718-26.
105. Pertz, O., et al., *Spatiotemporal dynamics of RhoA activity in migrating cells.* Nature, 2006. **440**(7087): p. 1069-72.
106. Wong, K., et al., *Neutrophil polarization: spatiotemporal dynamics of RhoA activity support a self-organizing mechanism.* Proc Natl Acad Sci U S A, 2006. **103**(10): p. 3639-44.
107. Kurokawa, K. and M. Matsuda, *Localized RhoA activation as a requirement for the induction of membrane ruffling.* Mol Biol Cell, 2005. **16**(9): p. 4294-303.
108. Xu, J., et al., *Divergent signals and cytoskeletal assemblies regulate self-organizing polarity in neutrophils.* Cell, 2003. **114**(2): p. 201-14.
109. Li, Z., et al., *Regulation of PTEN by Rho small GTPases.* Nat Cell Biol, 2005. **7**(4): p. 399-404.
110. El-Sibai, M., et al., *RhoA/ROCK-mediated switching between Cdc42- and Rac1-dependent protrusion in MTLn3 carcinoma cells.* Exp Cell Res, 2008. **314**(7): p. 1540-52.
111. Ginsberg, M.H., A. Partridge, and S.J. Shattil, *Integrin regulation.* Curr Opin Cell Biol, 2005. **17**(5): p. 509-16.
112. Cote, J.F. and K. Vuori, *GEF what? Dock180 and related proteins help Rac to polarize cells in new ways.* Trends Cell Biol, 2007. **17**(8): p. 383-93.
113. Han, J., et al., *Role of substrates and products of PI 3-kinase in regulating activation of Rac-related guanosine triphosphatases by Vav.* Science, 1998. **279**(5350): p. 558-60.
114. Welch, H.C., et al., *Phosphoinositide 3-kinase-dependent activation of Rac.* FEBS Lett, 2003. **546**(1): p. 93-7.
115. Kiosses, W.B., et al., *Rac recruits high-affinity integrin alphavbeta3 to lamellipodia in endothelial cell migration.* Nat Cell Biol, 2001. **3**(3): p. 316-20.
116. Cox, E.A. and A. Huttenlocher, *Regulation of integrin-mediated adhesion during cell migration.* Microsc Res Tech, 1998. **43**(5): p. 412-9.
117. Kwiatkowska, A. and M. Symons, *Signaling determinants of glioma cell invasion.* Adv Exp Med Biol, 2013. **986**: p. 121-41.
118. Sanders, L.C., et al., *Inhibition of myosin light chain kinase by p21-activated kinase.* Science, 1999. **283**(5410): p. 2083-5.
119. Mizutani, T., et al., *Regulation of cellular contractile force in response to mechanical stretch by diphosphorylation of myosin regulatory light chain via RhoA signaling cascade.* Cell Motil Cytoskeleton, 2009. **66**(7): p. 389-97.
120. Gardiner, E.M., et al., *Spatial and temporal analysis of Rac activation during live neutrophil chemotaxis.* Curr Biol, 2002. **12**(23): p. 2029-34.
121. Ohta, Y., J.H. Hartwig, and T.P. Stossel, *FilGAP, a Rho- and ROCK-regulated GAP for Rac binds filamin A to control actin remodelling.* Nat Cell Biol, 2006. **8**(8): p. 803-14.
122. Ghosh, M., et al., *Cofilin promotes actin polymerization and defines the direction of cell motility.* Science, 2004. **304**(5671): p. 743-6.
123. Worthylake, R.A. and K. Burridge, *RhoA and ROCK promote migration by limiting membrane protrusions.* J Biol Chem, 2003. **278**(15): p. 13578-84.
124. Graupera, M., et al., *Angiogenesis selectively requires the p110alpha isoform of PI3K to control endothelial cell migration.* Nature, 2008. **453**(7195): p. 662-6.
125. Wang, Y., et al., *Rho GTPases orient directional sensing in chemotaxis.* Proc Natl Acad Sci U S A, 2013. **110**(49): p. E4723-32.
126. Roberts, M.S., et al., *Protein kinase B/Akt acts via glycogen synthase kinase 3 to regulate recycling of alpha v beta 3 and alpha 5 beta 1 integrins.* Mol Cell Biol, 2004. **24**(4): p. 1505-15.
127. Toker, A. and S. Marmiroli, *Signaling specificity in the Akt pathway in biology and disease.* Adv Biol Regul, 2014. **55**: p. 28-38.
128. Kim, D., et al., *Akt/PKB promotes cancer cell invasion via increased motility and metalloproteinase production.* FASEB J, 2001. **15**(11): p. 1953-62.

129. Enomoto, A., et al., *Akt/PKB regulates actin organization and cell motility via Girdin/APE.* Dev Cell, 2005. **9**(3): p. 389-402.
130. Stambolic, V. and J.R. Woodgett, *Functional distinctions of protein kinase B/Akt isoforms defined by their influence on cell migration.* Trends Cell Biol, 2006. **16**(9): p. 461-6.
131. Li, J., et al., *Phosphorylation of ACAP1 by Akt regulates the stimulation-dependent recycling of integrin beta1 to control cell migration.* Dev Cell, 2005. **9**(5): p. 663-73.
132. Cross, D.A., et al., *Inhibition of glycogen synthase kinase-3 by insulin mediated by protein kinase B.* Nature, 1995. **378**(6559): p. 785-9.
133. Kobayashi, T., et al., *Glycogen synthase kinase 3 and h-prune regulate cell migration by modulating focal adhesions.* Mol Cell Biol, 2006. **26**(3): p. 898-911.
134. Chung, C.Y., G. Potikyan, and R.A. Firtel, *Control of cell polarity and chemotaxis by Akt/PKB and PI3 kinase through the regulation of PAKa.* Mol Cell, 2001. **7**(5): p. 937-47.
135. Higuchi, M., et al., *Akt mediates Rac/Cdc42-regulated cell motility in growth factor-stimulated cells and in invasive PTEN knockout cells.* Curr Biol, 2001. **11**(24): p. 1958-62.
136. Morales-Ruiz, M., et al., *Vascular endothelial growth factor-stimulated actin reorganization and migration of endothelial cells is regulated via the serine/threonine kinase Akt.* Circ Res, 2000. **86**(8): p. 892-6.
137. Meili, R., C. Ellsworth, and R.A. Firtel, *A novel Akt/PKB-related kinase is essential for morphogenesis in Dictyostelium.* Curr Biol, 2000. **10**(12): p. 708-17.
138. Meili, R., et al., *Chemoattractant-mediated transient activation and membrane localization of Akt/PKB is required for efficient chemotaxis to cAMP in Dictyostelium.* EMBO J, 1999. **18**(8): p. 2092-105.
139. Cenni, V., et al., *Targeting of the Akt/PKB kinase to the actin skeleton.* Cell Mol Life Sci, 2003. **60**(12): p. 2710-20.
140. Vandermoere, F., et al., *Proteomics exploration reveals that actin is a signaling target of the kinase Akt.* Mol Cell Proteomics, 2007. **6**(1): p. 114-24.
141. Ho, Y.P., et al., *beta-Actin is a downstream effector of the PI3K/AKT signaling pathway in myeloma cells.* Mol Cell Biochem, 2011. **348**(1-2): p. 129-39.
142. Manning, B.D. and L.C. Cantley, *AKT/PKB signaling: navigating downstream.* Cell, 2007. **129**(7): p. 1261-74.
143. Bae, S.S., et al., *Isoform-specific regulation of insulin-dependent glucose uptake by Akt/protein kinase B.* J Biol Chem, 2003. **278**(49): p. 49530-6.
144. Cho, H., et al., *Akt1/PKBalpha is required for normal growth but dispensable for maintenance of glucose homeostasis in mice.* J Biol Chem, 2001. **276**(42): p. 38349-52.
145. Cho, H., et al., *Insulin resistance and a diabetes mellitus-like syndrome in mice lacking the protein kinase Akt2 (PKB beta).* Science, 2001. **292**(5522): p. 1728-31.
146. Chen, W.S., et al., *Growth retardation and increased apoptosis in mice with homozygous disruption of the Akt1 gene.* Genes Dev, 2001. **15**(17): p. 2203-8.
147. Garofalo, R.S., et al., *Severe diabetes, age-dependent loss of adipose tissue, and mild growth deficiency in mice lacking Akt2/PKB beta.* J Clin Invest, 2003. **112**(2): p. 197-208.
148. Tschopp, O., et al., *Essential role of protein kinase B gamma (PKB gamma/Akt3) in postnatal brain development but not in glucose homeostasis.* Development, 2005. **132**(13): p. 2943-54.
149. Dummler, B., et al., *Life with a single isoform of Akt: mice lacking Akt2 and Akt3 are viable but display impaired glucose homeostasis and growth deficiencies.* Mol Cell Biol, 2006. **26**(21): p. 8042-51.
150. Irie, H.Y., et al., *Distinct roles of Akt1 and Akt2 in regulating cell migration and epithelial-mesenchymal transition.* J Cell Biol, 2005. **171**(6): p. 1023-34.
151. Liu, H., et al., *Mechanism of Akt1 inhibition of breast cancer cell invasion reveals a protumorigenic role for TSC2.* Proc Natl Acad Sci U S A, 2006. **103**(11): p. 4134-9.
152. Yoeli-Lerner, M., et al., *Akt blocks breast cancer cell motility and invasion through the transcription factor NFAT.* Mol Cell, 2005. **20**(4): p. 539-50.
153. Yiu, G.K. and A. Toker, *NFAT induces breast cancer cell invasion by promoting the induction of cyclooxygenase-2.* J Biol Chem, 2006. **281**(18): p. 12210-7.
154. Yazawa, K., et al., *Selective inhibition of cyclooxygenase-2 inhibits colon cancer cell adhesion to*

extracellular matrix by decreased expression of beta1 integrin. Cancer Sci, 2005. **96**(2): p. 93-9.
155. Dormond, O., et al., *NSAIDs inhibit alpha V beta 3 integrin-mediated and Cdc42/Rac-dependent endothelial-cell spreading, migration and angiogenesis.* Nat Med, 2001. **7**(9): p. 1041-7.
156. Dormond, O., et al., *Prostaglandin E2 promotes integrin alpha Vbeta 3-dependent endothelial cell adhesion, rac-activation, and spreading through cAMP/PKA-dependent signaling.* J Biol Chem, 2002. **277**(48): p. 45838-46.
157. Chin, Y.R. and A. Toker, *The actin-bundling protein palladin is an Akt1-specific substrate that regulates breast cancer cell migration.* Mol Cell, 2010. **38**(3): p. 333-44.
158. Arboleda, M.J., et al., *Overexpression of AKT2/protein kinase Bbeta leads to up-regulation of beta1 integrins, increased invasion, and metastasis of human breast and ovarian cancer cells.* Cancer Res, 2003. **63**(1): p. 196-206.
159. Chin, Y.R., et al., *Targeting Akt3 signaling in triple-negative breast cancer.* Cancer Res, 2014. **74**(3): p. 964-73.
160. Chung, S., et al., *N-cadherin regulates mammary tumor cell migration through Akt3 suppression.* Oncogene, 2013. **32**(4): p. 422-30.
161. Zhou, G.L., et al., *Opposing roles for Akt1 and Akt2 in Rac/Pak signaling and cell migration.* J Biol Chem, 2006. **281**(47): p. 36443-53.
162. Cariaga-Martinez, A.E., et al., *Distinct and specific roles of AKT1 and AKT2 in androgen-sensitive and androgen-independent prostate cancer cells.* Cell Signal, 2013. **25**(7): p. 1586-97.
163. Haslinger, P., et al., *AKT isoforms 1 and 3 regulate basal and epidermal growth factor-stimulated SGHPL-5 trophoblast cell migration in humans.* Biol Reprod, 2013. **88**(3): p. 54.
164. Liu, G., et al., *Kinase AKT1 negatively controls neutrophil recruitment and function in mice.* J Immunol, 2013. **191**(5): p. 2680-90.
165. Tsen, F., et al., *Extracellular heat shock protein 90 signals through subdomain II and the NPVY motif of LRP-1 receptor to Akt1 and Akt2: a circuit essential for promoting skin cell migration in vitro and wound healing in vivo.* Mol Cell Biol, 2013. **33**(24): p. 4947-59.
166. Wang, S. and M.D. Basson, *Identification of functional domains in AKT responsible for distinct roles of AKT isoforms in pressure-stimulated cancer cell adhesion.* Exp Cell Res, 2008. **314**(2): p. 286-96.
167. Brognard, J., et al., *PHLPP and a second isoform, PHLPP2, differentially attenuate the amplitude of Akt signaling by regulating distinct Akt isoforms.* Mol Cell, 2007. **25**(6): p. 917-31.
168. Chin, Y.R. and A. Toker, *Akt isoform-specific signaling in breast cancer: uncovering an anti-migratory role for palladin.* Cell Adh Migr, 2011. **5**(3): p. 211-4.
169. Chin, Y.R. and A. Toker, *Function of Akt/PKB signaling to cell motility, invasion and the tumor stroma in cancer.* Cell Signal, 2009. **21**(4): p. 470-6.
170. Bansal, V.S., R.C. Inhorn, and P.W. Majerus, *The metabolism of inositol 1,3,4-trisphosphate to inositol 1,3-bisphosphate.* J Biol Chem, 1987. **262**(20): p. 9444-7.
171. Bansal, V.S., K.K. Caldwell, and P.W. Majerus, *The isolation and characterization of inositol polyphosphate 4-phosphatase.* J Biol Chem, 1990. **265**(3): p. 1806-11.
172. Norris, F.A. and P.W. Majerus, *Hydrolysis of phosphatidylinositol 3,4-bisphosphate by inositol polyphosphate 4-phosphatase isolated by affinity elution chromatography.* J Biol Chem, 1994. **269**(12): p. 8716-20.
173. Norris, F.A., R.C. Atkins, and P.W. Majerus, *The cDNA cloning and characterization of inositol polyphosphate 4-phosphatase type II. Evidence for conserved alternative splicing in the 4-phosphatase family.* J Biol Chem, 1997. **272**(38): p. 23859-64.
174. Gewinner, C., et al., *Evidence that inositol polyphosphate 4-phosphatase type II is a tumor suppressor that inhibits PI3K signaling.* Cancer Cell, 2009. **16**(2): p. 115-25.
175. Ivetac, I., et al., *Regulation of PI(3)K/Akt signalling and cellular transformation by inositol polyphosphate 4-phosphatase-1.* EMBO Rep, 2009. **10**(5): p. 487-93.
176. Ivetac, I., et al., *The type Ialpha inositol polyphosphate 4-phosphatase generates and terminates phosphoinositide 3-kinase signals on endosomes and the plasma membrane.* Mol Biol Cell, 2005. **16**(5): p. 2218-33.
177. Shin, H.W., et al., *An enzymatic cascade of Rab5 effectors regulates phosphoinositide turnover in the endocytic pathway.* J Cell Biol, 2005. **170**(4): p. 607-18.

178. Ferron, M. and J. Vacher, *Characterization of the murine Inpp4b gene and identification of a novel isoform.* Gene, 2006. **376**(1): p. 152-61.
179. Rogers, S., R. Wells, and M. Rechsteiner, *Amino acid sequences common to rapidly degraded proteins: the PEST hypothesis.* Science, 1986. **234**(4774): p. 364-8.
180. Wang, K.K., A. Villalobo, and B.D. Roufogalis, *Calmodulin-binding proteins as calpain substrates.* Biochem J, 1989. **262**(3): p. 693-706.
181. Nystuen, A., et al., *A null mutation in inositol polyphosphate 4-phosphatase type I causes selective neuronal loss in weeble mutant mice.* Neuron, 2001. **32**(2): p. 203-12.
182. Sasaki, J., et al., *The PtdIns(3,4)P(2) phosphatase INPP4A is a suppressor of excitotoxic neuronal death.* Nature, 2010. **465**(7297): p. 497-501.
183. Sachs, A.J., et al., *Patterned neuroprotection in the Inpp4a(wbl) mutant mouse cerebellum correlates with the expression of Eaat4.* PLoS One, 2009. **4**(12): p. e8270.
184. Sharma, M., et al., *A genetic variation in inositol polyphosphate 4 phosphatase a enhances susceptibility to asthma.* Am J Respir Crit Care Med, 2008. **177**(7): p. 712-9.
185. Aich, J., et al., *Loss-of-function of inositol polyphosphate-4-phosphatase reversibly increases the severity of allergic airway inflammation.* Nat Commun, 2012. **3**: p. 877.
186. Henricks, P.A. and F.P. Nijkamp, *Reactive oxygen species as mediators in asthma.* Pulm Pharmacol Ther, 2001. **14**(6): p. 409-20.
187. Van der Kaay, J., et al., *Distinct phosphatidylinositol 3-kinase lipid products accumulate upon oxidative and osmotic stress and lead to different cellular responses.* J Biol Chem, 1999. **274**(50): p. 35963-8.
188. Marjanovic, J., et al., *The role of inositol polyphosphate 4-phosphatase 1 in platelet function using a weeble mouse model.* Adv Enzyme Regul, 2011. **51**(1): p. 101-5.
189. Page, C. and S. Pitchford, *Platelets and allergic inflammation.* Clin Exp Allergy, 2014. **44**(7): p. 901-13.
190. Aich, J., et al., *Resveratrol attenuates experimental allergic asthma in mice by restoring inositol polyphosphate 4 phosphatase (INPP4A).* Int Immunopharmacol, 2012. **14**(4): p. 438-43.
191. Ferron, M., et al., *Inositol polyphosphate 4-phosphatase B as a regulator of bone mass in mice and humans.* Cell Metab, 2011. **14**(4): p. 466-77.
192. Fedele, C.G., et al., *Inositol polyphosphate 4-phosphatase II regulates PI3K/Akt signaling and is lost in human basal-like breast cancers.* Proc Natl Acad Sci U S A, 2010. **107**(51): p. 22231-6.
193. Weigman, V.J., et al., *Basal-like Breast cancer DNA copy number losses identify genes involved in genomic instability, response to therapy, and patient survival.* Breast Cancer Res Treat, 2012. **133**(3): p. 865-80.
194. Won, J.R., et al., *A survey of immunohistochemical biomarkers for basal-like breast cancer against a gene expression profile gold standard.* Mod Pathol, 2013. **26**(11): p. 1438-50.
195. Hodgson, M.C., et al., *Decreased expression and androgen regulation of the tumor suppressor gene INPP4B in prostate cancer.* Cancer Res, 2011. **71**(2): p. 572-82.
196. Balakrishnan, A. and J.R. Chaillet, *Role of the inositol polyphosphate-4-phosphatase type II Inpp4b in the generation of ovarian teratomas.* Dev Biol, 2013. **373**(1): p. 118-29.
197. Perez-Lorenzo, R., et al., *A tumor suppressor function for the lipid phosphatase INPP4B in melanocytic neoplasms.* J Invest Dermatol, 2014. **134**(5): p. 1359-68.
198. Lundin, C., et al., *High frequency of BTG1 deletions in acute lymphoblastic leukemia in children with down syndrome.* Genes Chromosomes Cancer, 2012. **51**(2): p. 196-206.
199. Ross, M.E., et al., *Classification of pediatric acute lymphoblastic leukemia by gene expression profiling.* Blood, 2003. **102**(8): p. 2951-9.
200. LaTulippe, E., et al., *Comprehensive gene expression analysis of prostate cancer reveals distinct transcriptional programs associated with metastatic disease.* Cancer Res, 2002. **62**(15): p. 4499-506.
201. Erkeland, S.J., et al., *Large-scale identification of disease genes involved in acute myeloid leukemia.* J Virol, 2004. **78**(4): p. 1971-80.
202. Helgason, C.D., et al., *Targeted disruption of SHIP leads to hemopoietic perturbations, lung pathology, and a shortened life span.* Genes Dev, 1998. **12**(11): p. 1610-20.
203. Liu, Q., et al., *The inositol polyphosphate 5-phosphatase ship is a crucial negative regulator of B*

cell antigen receptor signaling. J Exp Med, 1998. **188**(7): p. 1333-42.
204. Suzuki, A., et al., *High cancer susceptibility and embryonic lethality associated with mutation of the PTEN tumor suppressor gene in mice.* Curr Biol, 1998. **8**(21): p. 1169-78.
205. Bertucci, M.C. and C.A. Mitchell, *Phosphoinositide 3-kinase and INPP4B in human breast cancer.* Ann N Y Acad Sci, 2013. **1280**: p. 1-5.
206. Stokoe, D., et al., *Dual role of phosphatidylinositol-3,4,5-trisphosphate in the activation of protein kinase B.* Science, 1997. **277**(5325): p. 567-70.
207. Alessi, D.R., et al., *Characterization of a 3-phosphoinositide-dependent protein kinase which phosphorylates and activates protein kinase Balpha.* Curr Biol, 1997. **7**(4): p. 261-9.
208. Franke, T.F., et al., *Direct regulation of the Akt proto-oncogene product by phosphatidylinositol-3,4-bisphosphate.* Science, 1997. **275**(5300): p. 665-8.
209. Frech, M., et al., *High affinity binding of inositol phosphates and phosphoinositides to the pleckstrin homology domain of RAC/protein kinase B and their influence on kinase activity.* J Biol Chem, 1997. **272**(13): p. 8474-81.
210. Klippel, A., et al., *A specific product of phosphatidylinositol 3-kinase directly activates the protein kinase Akt through its pleckstrin homology domain.* Mol Cell Biol, 1997. **17**(1): p. 338-44.
211. Thomas, C.C., et al., *High-resolution structure of the pleckstrin homology domain of protein kinase b/akt bound to phosphatidylinositol (3,4,5)-trisphosphate.* Curr Biol, 2002. **12**(14): p. 1256-62.
212. Salsman, S., et al., *Induction of Akt phosphorylation in rat primary astrocytes by H2O2 occurs upstream of phosphatidylinositol 3-kinase: no evidence for oxidative inhibition of PTEN.* Arch Biochem Biophys, 2001. **386**(2): p. 275-80.
213. Scheid, M.P., et al., *Phosphatidylinositol (3,4,5)P3 is essential but not sufficient for protein kinase B (PKB) activation; phosphatidylinositol (3,4)P2 is required for PKB phosphorylation at Ser-473: studies using cells from SH2-containing inositol-5-phosphatase knockout mice.* J Biol Chem, 2002. **277**(11): p. 9027-35.
214. Sarbassov, D.D., et al., *Phosphorylation and regulation of Akt/PKB by the rictor-mTOR complex.* Science, 2005. **307**(5712): p. 1098-101.
215. Aman, M.J., et al., *The inositol phosphatase SHIP inhibits Akt/PKB activation in B cells.* J Biol Chem, 1998. **273**(51): p. 33922-8.
216. Taylor, V., et al., *5' phospholipid phosphatase SHIP-2 causes protein kinase B inactivation and cell cycle arrest in glioblastoma cells.* Mol Cell Biol, 2000. **20**(18): p. 6860-71.
217. Ott, V.L., et al., *Downstream of kinase, p62(dok), is a mediator of Fc gamma IIB inhibition of Fc epsilon RI signaling.* J Immunol, 2002. **168**(9): p. 4430-9.
218. Ma, K., et al., *PI(3,4,5)P3 and PI(3,4)P2 levels correlate with PKB/akt phosphorylation at Thr308 and Ser473, respectively; PI(3,4)P2 levels determine PKB activity.* Cell Signal, 2008. **20**(4): p. 684-94.
219. Schmid, S.L. and M. Mettlen, *Cell biology: Lipid switches and traffic control.* Nature, 2013. **499**(7457): p. 161-2.
220. Dowler, S., et al., *Identification of pleckstrin-homology-domain-containing proteins with novel phosphoinositide-binding specificities.* Biochem J, 2000. **351**(Pt 1): p. 19-31.
221. Allam, A. and A.J. Marshall, *Role of the adaptor proteins Bam32, TAPP1 and TAPP2 in lymphocyte activation.* Immunol Lett, 2005. **97**(1): p. 7-17.
222. Manna, D., et al., *Mechanistic basis of differential cellular responses of phosphatidylinositol 3,4-bisphosphate- and phosphatidylinositol 3,4,5-trisphosphate-binding pleckstrin homology domains.* J Biol Chem, 2007. **282**(44): p. 32093-105.
223. Yokogawa, T., et al., *Evidence that 3'-phosphorylated polyphosphoinositides are generated at the nuclear surface: use of immunostaining technique with monoclonal antibodies specific for PI 3,4-P(2).* FEBS Lett, 2000. **473**(2): p. 222-6.
224. Watt, S.A., et al., *Detection of novel intracellular agonist responsive pools of phosphatidylinositol 3,4-bisphosphate using the TAPP1 pleckstrin homology domain in immunoelectron microscopy.* Biochem J, 2004. **377**(Pt 3): p. 653-63.
225. Costantini, J.L., et al., *TAPP2 links phosphoinositide 3-kinase signaling to B cell adhesion through interaction with the cytoskeletal protein utrophin: expression of a novel cell adhesion-promoting*

complex in B cell leukemia. Blood, 2009.
226. Kimber, W.A., et al., *Evidence that the tandem-pleckstrin-homology-domain-containing protein TAPP1 interacts with Ptd(3,4)P2 and the multi-PDZ-domain-containing protein MUPP1 in vivo.* Biochem J, 2002. **361**(Pt 3): p. 525-36.
227. Kimber, W.A., et al., *Interaction of the protein tyrosine phosphatase PTPL1 with the PtdIns(3,4)P2-binding adaptor protein TAPP1.* Biochem J, 2003. **376**(Pt 2): p. 525-35.
228. Hogan, A., et al., *The phosphoinositol 3,4-bisphosphate-binding protein TAPP1 interacts with syntrophins and regulates actin cytoskeletal organization.* J Biol Chem, 2004. **279**(51): p. 53717-24.
229. Haenggi, T. and J.M. Fritschy, *Role of dystrophin and utrophin for assembly and function of the dystrophin glycoprotein complex in non-muscle tissue.* Cell Mol Life Sci, 2006. **63**(14): p. 1614-31.
230. Allikian, M.J. and E.M. McNally, *Processing and assembly of the dystrophin glycoprotein complex.* Traffic, 2007. **8**(3): p. 177-83.
231. Wiestner, A., et al., *ZAP-70 expression identifies a chronic lymphocytic leukemia subtype with unmutated immunoglobulin genes, inferior clinical outcome, and distinct gene expression profile.* Blood, 2003. **101**(12): p. 4944-51.
232. Szabo, M.C., T.K. Teague, and B.W. McIntyre, *Regulation of lymphocyte pseudopodia formation by triggering the integrin alpha 4/beta 1.* J Immunol, 1995. **154**(5): p. 2112-24.
233. Hangan, D., et al., *An epitope on VLA-6 (alpha6beta1) integrin involved in migration but not adhesion is required for extravasation of murine melanoma B16F1 cells in liver.* Cancer Res, 1997. **57**(17): p. 3812-7.
234. Mehes, E., et al., *Dystroglycan is involved in laminin-1-stimulated motility of Muller glial cells: combined velocity and directionality analysis.* Glia, 2005. **49**(4): p. 492-500.
235. Shaw, A.R., et al., *Ectopic expression of human and feline CD9 in a human B cell line confers beta 1 integrin-dependent motility on fibronectin and laminin substrates and enhanced tyrosine phosphorylation.* J Biol Chem, 1995. **270**(41): p. 24092-9.
236. Landego, I., et al., *Interaction of TAPP adapter proteins with phosphatidylinositol (3,4)-bisphosphate regulates B-cell activation and autoantibody production.* Eur J Immunol, 2012.
237. Wullschleger, S., et al., *Role of TAPP1 and TAPP2 adaptor binding to PtdIns(3,4)P2 in regulating insulin sensitivity defined by knock-in analysis.* Biochem J, 2011. **434**(2): p. 265-74.
238. Colo, G.P., E.M. Lafuente, and J. Teixido, *The MRL proteins: adapting cell adhesion, migration and growth.* Eur J Cell Biol, 2012. **91**(11-12): p. 861-8.
239. Manser, J., C. Roonprapunt, and B. Margolis, *C. elegans cell migration gene mig-10 shares similarities with a family of SH2 domain proteins and acts cell nonautonomously in excretory canal development.* Dev Biol, 1997. **184**(1): p. 150-64.
240. Jenzora, A., et al., *PREL1 provides a link from Ras signalling to the actin cytoskeleton via Ena/VASP proteins.* FEBS Lett, 2005. **579**(2): p. 455-63.
241. Lafuente, E.M., et al., *RIAM, an Ena/VASP and Profilin ligand, interacts with Rap1-GTP and mediates Rap1-induced adhesion.* Dev Cell, 2004. **7**(4): p. 585-95.
242. Lyulcheva, E., et al., *Drosophila pico and its mammalian ortholog lamellipodin activate serum response factor and promote cell proliferation.* Dev Cell, 2008. **15**(5): p. 680-90.
243. Watanabe, N., et al., *Mechanisms and consequences of agonist-induced talin recruitment to platelet integrin alphaIIbbeta3.* J Cell Biol, 2008. **181**(7): p. 1211-22.
244. Lee, H.S., et al., *RIAM activates integrins by linking talin to ras GTPase membrane-targeting sequences.* J Biol Chem, 2009. **284**(8): p. 5119-27.
245. Rodriguez-Viciana, P., C. Sabatier, and F. McCormick, *Signaling specificity by Ras family GTPases is determined by the full spectrum of effectors they regulate.* Mol Cell Biol, 2004. **24**(11): p. 4943-54.
246. Tasaka, G., M. Negishi, and I. Oinuma, *Semaphorin 4D/Plexin-B1-mediated M-Ras GAP activity regulates actin-based dendrite remodeling through Lamellipodin.* J Neurosci, 2012. **32**(24): p. 8293-305.
247. Chang, Y.C., et al., *Crystal structure of Lamellipodin implicates diverse functions in actin polymerization and Ras signaling.* Protein Cell, 2013. **4**(3): p. 211-9.

248. Bae, Y.H., et al., *Profilin1 regulates PI(3,4)P2 and lamellipodin accumulation at the leading edge thus influencing motility of MDA-MB-231 cells.* Proc Natl Acad Sci U S A, 2010. **107**(50): p. 21547-52.
249. Smith, K., et al., *Enteropathogenic Escherichia coli recruits the cellular inositol phosphatase SHIP2 to regulate actin-pedestal formation.* Cell Host Microbe, 2010. **7**(1): p. 13-24.
250. Garg, P., et al., *Actin-depolymerizing factor cofilin-1 is necessary in maintaining mature podocyte architecture.* J Biol Chem, 2010. **285**(29): p. 22676-88.
251. Huber, T.B., et al., *Nephrin and CD2AP associate with phosphoinositide 3-OH kinase and stimulate AKT-dependent signaling.* Mol Cell Biol, 2003. **23**(14): p. 4917-28.
252. Zhu, J., et al., *Nephrin mediates actin reorganization via phosphoinositide 3-kinase in podocytes.* Kidney Int, 2008. **73**(5): p. 556-66.
253. Venkatareddy, M., et al., *Nephrin regulates lamellipodia formation by assembling a protein complex that includes Ship2, filamin and lamellipodin.* PLoS One, 2011. **6**(12): p. e28710.
254. Bear, J.E., M. Krause, and F.B. Gertler, *Regulating cellular actin assembly.* Curr Opin Cell Biol, 2001. **13**(2): p. 158-66.
255. Michael, M., et al., *c-Abl, Lamellipodin, and Ena/VASP proteins cooperate in dorsal ruffling of fibroblasts and axonal morphogenesis.* Curr Biol, 2010. **20**(9): p. 783-91.
256. Yoshinaga, S., et al., *A phosphatidylinositol lipids system, lamellipodin, and Ena/VASP regulate dynamic morphology of multipolar migrating cells in the developing cerebral cortex.* J Neurosci, 2012. **32**(34): p. 11643-56.
257. Vehlow, A., et al., *Endophilin, Lamellipodin, and Mena cooperate to regulate F-actin-dependent EGF-receptor endocytosis.* EMBO J, 2013. **32**(20): p. 2722-34.
258. Campellone, K.G. and M.D. Welch, *A nucleator arms race: cellular control of actin assembly.* Nat Rev Mol Cell Biol, 2010. **11**(4): p. 237-51.
259. Insall, R.H. and L.M. Machesky, *Actin dynamics at the leading edge: from simple machinery to complex networks.* Dev Cell, 2009. **17**(3): p. 310-22.
260. Law, A.L., et al., *Lamellipodin and the Scar/WAVE complex cooperate to promote cell migration in vivo.* J Cell Biol, 2013. **203**(4): p. 673-89.
261. Suraneni, P., et al., *The Arp2/3 complex is required for lamellipodia extension and directional fibroblast cell migration.* J Cell Biol, 2012. **197**(2): p. 239-51.
262. Wu, C., et al., *Arp2/3 is critical for lamellipodia and response to extracellular matrix cues but is dispensable for chemotaxis.* Cell, 2012. **148**(5): p. 973-87.
263. Yan, C., et al., *WAVE2 deficiency reveals distinct roles in embryogenesis and Rac-mediated actin-based motility.* EMBO J, 2003. **22**(14): p. 3602-12.
264. Endris, V., et al., *SrGAP3 interacts with lamellipodin at the cell membrane and regulates Rac-dependent cellular protrusions.* J Cell Sci, 2011. **124**(Pt 23): p. 3941-55.
265. Quinn, C.C., et al., *UNC-6/netrin and SLT-1/slit guidance cues orient axon outgrowth mediated by MIG-10/RIAM/lamellipodin.* Curr Biol, 2006. **16**(9): p. 845-53.
266. Innocenti, M., et al., *Abi1 is essential for the formation and activation of a WAVE2 signalling complex.* Nat Cell Biol, 2004. **6**(4): p. 319-27.
267. Machesky, L.M. and R.H. Insall, *Scar1 and the related Wiskott-Aldrich syndrome protein, WASP, regulate the actin cytoskeleton through the Arp2/3 complex.* Curr Biol, 1998. **8**(25): p. 1347-56.
268. Steffen, A., et al., *Sra-1 and Nap1 link Rac to actin assembly driving lamellipodia formation.* EMBO J, 2004. **23**(4): p. 749-59.
269. Bear, J.E., et al., *Antagonism between Ena/VASP proteins and actin filament capping regulates fibroblast motility.* Cell, 2002. **109**(4): p. 509-21.
270. Pinheiro, E.M., et al., *Lpd depletion reveals that SRF specifies radial versus tangential migration of pyramidal neurons.* Nat Cell Biol, 2011. **13**(8): p. 989-95.
271. Miralles, F., et al., *Actin dynamics control SRF activity by regulation of its coactivator MAL.* Cell, 2003. **113**(3): p. 329-42.
272. Posern, G. and R. Treisman, *Actin' together: serum response factor, its cofactors and the link to signal transduction.* Trends Cell Biol, 2006. **16**(11): p. 588-96.
273. Lane, J., et al., *Structure and role of WASP and WAVE in Rho GTPase signalling in cancer.* Cancer Genomics Proteomics, 2014. **11**(3): p. 155-65.

274. Bae, Y.H., et al., *A FAK-Cas-Rac-lamellipodin signaling module transduces extracellular matrix stiffness into mechanosensitive cell cycling.* Sci Signal, 2014. **7**(330): p. ra57.
275. Endris, V., et al., *The novel Rho-GTPase activating gene MEGAP/ srGAP3 has a putative role in severe mental retardation.* Proc Natl Acad Sci U S A, 2002. **99**(18): p. 11754-9.
276. Guerrier, S., et al., *The F-BAR domain of srGAP2 induces membrane protrusions required for neuronal migration and morphogenesis.* Cell, 2009. **138**(5): p. 990-1004.
277. Soderling, S.H., et al., *The WRP component of the WAVE-1 complex attenuates Rac-mediated signalling.* Nat Cell Biol, 2002. **4**(12): p. 970-5.
278. Wong, K., et al., *Signal transduction in neuronal migration: roles of GTPase activating proteins and the small GTPase Cdc42 in the Slit-Robo pathway.* Cell, 2001. **107**(2): p. 209-21.
279. Casey, P.J. and M.C. Seabra, *Protein prenyltransferases.* J Biol Chem, 1996. **271**(10): p. 5289-92.
280. Niwa, H., K. Yamamura, and J. Miyazaki, *Efficient selection for high-expression transfectants with a novel eukaryotic vector.* Gene, 1991. **108**(2): p. 193-9.
281. Bartis, D., et al., *Intermolecular relations between the glucocorticoid receptor, ZAP-70 kinase, and Hsp-90,* in *Biochem Biophys Res Commun*. 2007: United States. p. 253-8.
282. Szabo, M., et al., *Fine-tuning of proximal TCR signaling by ZAP-70 tyrosine residues in Jurkat cells,* in *Int Immunol*. 2011: England. p. 79-87.
283. Kung, S.K., D.S. An, and I.S. Chen, *A murine leukemia virus (MuLV) long terminal repeat derived from rhesus macaques in the context of a lentivirus vector and MuLV gag sequence results in high-level gene expression in human T lymphocytes.* J Virol, 2000. **74**(8): p. 3668-81.
284. Tran, J. and S.K. Kung, *Lentiviral vectors mediate stable and efficient gene delivery into primary murine natural killer cells.* Mol Ther, 2007. **15**(7): p. 1331-9.
285. QIAGEN, *Quick-StartProtocol QIAGEN® Plasmid Mini, Midi, and Maxi Kits.* 2011: p. 1-2.
286. Zhang, T.T., M. Al-Alwan, and A.J. Marshall, *The pleckstrin homology domain adaptor protein Bam32/DAPP1 is required for germinal center progression.* J Immunol, 2010. **184**(1): p. 164-72.
287. Burger, J.A., M. Burger, and T.J. Kipps, *Chronic lymphocytic leukemia B cells express functional CXCR4 chemokine receptors that mediate spontaneous migration beneath bone marrow stromal cells.* Blood, 1999. **94**(11): p. 3658-67.
288. Lin, F. and E.C. Butcher, *T cell chemotaxis in a simple microfluidic device.* Lab Chip, 2006. **6**(11): p. 1462-9.
289. Cheung, S.M., et al., *Regulation of phosphoinositide 3-kinase signaling by oxidants: hydrogen peroxide selectively enhances immunoreceptor-induced recruitment of phosphatidylinositol (3,4) bisphosphate-binding PH domain proteins.* Cell Signal, 2007. **19**(5): p. 902-12.
290. Allam, A., et al., *The adaptor protein Bam32 regulates Rac1 activation and actin remodeling through a phosphorylation-dependent mechanism.* J Biol Chem, 2004. **279**(38): p. 39775-82.
291. Cuesta-Mateos, C., et al., *Analysis of migratory and prosurvival pathways induced by the homeostatic chemokines CCL19 and CCL21 in B-cell chronic lymphocytic leukemia.* Exp Hematol, 2010. **38**(9): p. 756-64, 764 e1-4.
292. Hoellenriegel, J., et al., *The phosphoinositide 3'-kinase delta inhibitor, CAL-101, inhibits B-cell receptor signaling and chemokine networks in chronic lymphocytic leukemia.* Blood, 2011. **118**(13): p. 3603-12.
293. Kavran, J.M., et al., *Specificity and promiscuity in phosphoinositide binding by pleckstrin homology domains.* J Biol Chem, 1998. **273**(46): p. 30497-508.
294. Lemmon, M.A., *Pleckstrin homology (PH) domains and phosphoinositides.* Biochem Soc Symp, 2007(74): p. 81-93.
295. Del Principe, M.I., et al., *Clinical significance of ZAP-70 protein expression in B-cell chronic lymphocytic leukemia.* Blood, 2006. **108**(3): p. 853-61.
296. Richardson, S.J., et al., *ZAP-70 expression is associated with enhanced ability to respond to migratory and survival signals in B-cell chronic lymphocytic leukemia (B-CLL).* Blood, 2006. **107**(9): p. 3584-92.
297. Barber, M.A. and H.C. Welch, *PI3K and RAC signalling in leukocyte and cancer cell migration.* Bull Cancer, 2006. **93**(5): p. E44-52.
298. Burkel, B.M., G. von Dassow, and W.M. Bement, *Versatile fluorescent probes for actin filaments based on the actin-binding domain of utrophin.* Cell Motil Cytoskeleton, 2007. **64**(11): p. 822-32.

299. Cooper, K.M., D.A. Bennin, and A. Huttenlocher, *The PCH family member proline-serine-threonine phosphatase-interacting protein 1 targets to the leukocyte uropod and regulates directed cell migration.* Mol Biol Cell, 2008. **19**(8): p. 3180-91.
300. Small, J.V. and G.P. Resch, *The comings and goings of actin: coupling protrusion and retraction in cell motility.* Curr Opin Cell Biol, 2005. **17**(5): p. 517-23.
301. Stossel, T.P., *On the crawling of animal cells.* Science, 1993. **260**(5111): p. 1086-94.
302. Bradstock, K.F., et al., *Effects of the chemokine stromal cell-derived factor-1 on the migration and localization of precursor-B acute lymphoblastic leukemia cells within bone marrow stromal layers.* Leukemia, 2000. **14**(5): p. 882-8.
303. Narang, A., *Spontaneous polarization in eukaryotic gradient sensing: a mathematical model based on mutual inhibition of frontness and backness pathways.* J Theor Biol, 2006. **240**(4): p. 538-53.
304. Cernuda-Morollon, E., et al., *Rac activation by the T-cell receptor inhibits T cell migration.* PLoS One, 2010. **5**(8): p. e12393.
305. Vicente-Manzanares, M., et al., *Myosin IIA/IIB restrict adhesive and protrusive signaling to generate front-back polarity in migrating cells.* J Cell Biol, 2011. **193**(2): p. 381-96.
306. Parrini, M.C., et al., *SH3BP1, an exocyst-associated RhoGAP, inactivates Rac1 at the front to drive cell motility.* Mol Cell, 2011. **42**(5): p. 650-61.
307. Niedermeier, M., et al., *Isoform-selective phosphoinositide 3'-kinase inhibitors inhibit CXCR4 signaling and overcome stromal cell-mediated drug resistance in chronic lymphocytic leukemia: a novel therapeutic approach.* Blood, 2009. **113**(22): p. 5549-57.
308. Breuleux, M., et al., *Increased AKT S473 phosphorylation after mTORC1 inhibition is rictor dependent and does not predict tumor cell response to PI3K/mTOR inhibition.* Mol Cancer Ther, 2009. **8**(4): p. 742-53.
309. Moore, S.F., R.W. Hunter, and I. Hers, *mTORC2 protein complex-mediated Akt (Protein Kinase B) Serine 473 Phosphorylation is not required for Akt1 activity in human platelets [corrected]*. J Biol Chem, 2011. **286**(28): p. 24553-60.
310. Vincent, E.E., et al., *Akt phosphorylation on Thr308 but not on Ser473 correlates with Akt protein kinase activity in human non-small cell lung cancer.* Br J Cancer, 2011. **104**(11): p. 1755-61.
311. Kisseleva, M.V., L. Cao, and P.W. Majerus, *Phosphoinositide-specific inositol polyphosphate 5-phosphatase IV inhibits Akt/protein kinase B phosphorylation and leads to apoptotic cell death.* J Biol Chem, 2002. **277**(8): p. 6266-72.
312. Frecha, C., et al., *Efficient and stable transduction of resting B lymphocytes and primary chronic lymphocyte leukemia cells using measles virus gp displaying lentiviral vectors.* Blood, 2009. **114**(15): p. 3173-80.
313. Reif, K., et al., *Cutting edge: differential roles for phosphoinositide 3-kinases, p110gamma and p110delta, in lymphocyte chemotaxis and homing.* J Immunol, 2004. **173**(4): p. 2236-40.
314. Raiborg, C., K.O. Schink, and H. Stenmark, *Class III phosphatidylinositol 3-kinase and its catalytic product PtdIns3P in regulation of endocytic membrane traffic.* FEBS J, 2013. **280**(12): p. 2730-42.
315. Roberts, R. and N.T. Ktistakis, *Omegasomes: PI3P platforms that manufacture autophagosomes.* Essays Biochem, 2013. **55**: p. 17-27.
316. Stenmark, H., *The Sir Hans Krebs Lecture. How a lipid mediates tumour suppression. Delivered on 29 June 2010 at the 35th FEBS Congress in Gothenburg, Sweden.* FEBS J, 2010. **277**(23): p. 4837-48.
317. Vergne, I. and V. Deretic, *The role of PI3P phosphatases in the regulation of autophagy.* FEBS Lett, 2010. **584**(7): p. 1313-8.
318. Dumstrei, K., R. Mennecke, and E. Raz, *Signaling pathways controlling primordial germ cell migration in zebrafish.* J Cell Sci, 2004. **117**(Pt 20): p. 4787-95.
319. Nishioka, T., et al., *Rapid turnover rate of phosphoinositides at the front of migrating MDCK cells.* Mol Biol Cell, 2008. **19**(10): p. 4213-23.
320. Marchese, A. and J.L. Benovic, *Agonist-promoted ubiquitination of the G protein-coupled receptor CXCR4 mediates lysosomal sorting.* J Biol Chem, 2001. **276**(49): p. 45509-12.
321. Hilpela, P., et al., *SWAP-70 identifies a transitional subset of actin filaments in motile cells.* Mol Biol Cell, 2003. **14**(8): p. 3242-53.

322. Shinohara, M., et al., *SWAP-70 is a guanine-nucleotide-exchange factor that mediates signalling of membrane ruffling*. Nature, 2002. **416**(6882): p. 759-63.
323. Ihara, S., T. Oka, and Y. Fukui, *Direct binding of SWAP-70 to non-muscle actin is required for membrane ruffling.* J Cell Sci, 2006. **119**(Pt 3): p. 500-7.
324. Pearce, G., et al., *Signaling protein SWAP-70 is required for efficient B cell homing to lymphoid organs*. Nat Immunol, 2006. **7**(8): p. 827-34.
325. Sivalenka, R.R. and R. Jessberger, *SWAP-70 regulates c-kit-induced mast cell activation, cell-cell adhesion, and migration.* Mol Cell Biol, 2004. **24**(23): p. 10277-88.
326. Chacon-Martinez, C.A., et al., *The switch-associated protein 70 (SWAP-70) bundles actin filaments and contributes to the regulation of F-actin dynamics.* J Biol Chem, 2013. **288**(40): p. 28687-703.
327. Ocana-Morgner, C., et al., *Sphingosine 1-phosphate-induced motility and endocytosis of dendritic cells is regulated by SWAP-70 through RhoA.* J Immunol, 2011. **186**(9): p. 5345-55.
328. Bahaie, N.S., et al., *Regulation of eosinophil trafficking by SWAP-70 and its role in allergic airway inflammation.* J Immunol, 2012. **188**(3): p. 1479-90.
329. Pearce, G., T. Audzevich, and R. Jessberger, *SYK regulates B-cell migration by phosphorylation of the F-actin interacting protein SWAP-70.* Blood, 2011. **117**(5): p. 1574-84.
330. Gagliardi, P.A., et al., *PDK1-mediated activation of MRCKalpha regulates directional cell migration and lamellipodia retraction.* J Cell Biol, 2014. **206**(3): p. 415-34.
331. Pinner, S. and E. Sahai, *PDK1 regulates cancer cell motility by antagonising inhibition of ROCK1 by RhoE*. Nat Cell Biol, 2008. **10**(2): p. 127-37.
332. Primo, L., et al., *Essential role of PDK1 in regulating endothelial cell migration.* J Cell Biol, 2007. **176**(7): p. 1035-47.
333. Waugh, C., et al., *Phosphoinositide (3,4,5)-triphosphate binding to phosphoinositide-dependent kinase 1 regulates a protein kinase B/Akt signaling threshold that dictates T-cell migration, not proliferation.* Mol Cell Biol, 2009. **29**(21): p. 5952-62.
334. Yagi, M., et al., *PDK1 regulates chemotaxis in human neutrophils.* J Dent Res, 2009. **88**(12): p. 1119-24.
335. Piccolo, E., et al., *The mechanism involved in the regulation of phospholipase Cgamma1 activity in cell migration.* Oncogene, 2002. **21**(42): p. 6520-9.
336. Shannon, L.A., et al., *CCR7/CCL21 migration on fibronectin is mediated by phospholipase Cgamma1 and ERK1/2 in primary T lymphocytes.* J Biol Chem, 2010. **285**(50): p. 38781-7.
337. Sala, G., et al., *Phospholipase Cgamma1 is required for metastasis development and progression.* Cancer Res, 2008. **68**(24): p. 10187-96.
338. Torii, T., et al., *Cytohesin-2/ARNO, through its interaction with focal adhesion adaptor protein paxillin, regulates preadipocyte migration via the downstream activation of Arf6.* J Biol Chem, 2010. **285**(31): p. 24270-81.
339. White, D.T., et al., *GRASP and IPCEF promote ARF-to-Rac signaling and cell migration by coordinating the association of ARNO/cytohesin 2 with Dock180.* Mol Biol Cell, 2010. **21**(4): p. 562-71.
340. Al-Alwan, M., et al., *Bam32/DAPP1 promotes B cell adhesion and formation of polarized conjugates with T cells.* J Immunol, 2010. **184**(12): p. 6961-9.

Appendix The original QIAGEN® Plasmid Quick-Start Protocol

1). Harvest overnight bacterial culture by centrifuging at 6000 x *g* for 15 min at 4°C.
2). Resuspend the bacterial pellet in 10 ml Buffer P1.
3). Add 10 ml Buffer P2, mix thoroughly by vigorously inverting 4–6 times, and incubate at room temperature (15–25°C) for 5 min. If using LyseBlue reagent, the solution will turn blue.
4). Add 10 ml prechilled Buffer P3, mix thoroughly by vigorously inverting 4–6 times. Incubate on ice for 20 min. If using LyseBlue reagent, mix the solution until it is colorless.
5). Centrifuge at ≥20,000 x *g* for 30 min at 4°C. Re-centrifuge the supernatant at ≥20,000 x *g* for 15 min at 4°C.
6). Equilibrate a QIAGEN-tip 500 by applying 10 ml Buffer QBT, and allow column to empty by gravity flow.
7). Apply the supernatant from step 5 to the QIAGEN-tip and allow it to enter the resin by gravity flow.
8). Wash the QIAGEN-tip with 2 x 30 ml Buffer QC. Allow Buffer QC to move through the QIAGEN-tip by gravity flow.
9). Elute DNA with 15 ml Buffer QF into a clean 50 ml vessel. For constructs larger than 45 kb,prewarming the elution buffer to 65°C may help to increase the yield.
10). Precipitate DNA by adding 10.5 ml (0.7 volumes) room-temperature isopropanol to the eluted DNA and mix. Centrifuge at ≥15,000 x *g* for 30 min at 4°C. Carefully decant the supernatant.
11). Wash the DNA pellet with 5 ml room-temperature 70% ethanol and centrifuge at ≥15,000 x *g* for 10 min. Carefully decant supernatant.
12). Air-dry pellet for 5–10 min and redissolve DNA in a suitable volume of appropriate buffer (e.g., TE buffer, pH 8.0, or 10 mM Tris·Cl, pH 8.5).”